This is to certify that the

dissertation entitled

COMPRESSION OF THREE SOILS UNDER LONG-TERM
TILLAGE AND WHEEL TRAFFIC

presented by

Moacir de Souza Dias Junior

has been accepted towards fulfillment
of the requirements for

Ph.D. degree in Crop and Soil Sciences/
Soil Physics

Major professor

Date October 14, 1994

COMPRESSION OF THREE SOILS UNDER LONG-TERM TILLAGE AND WHEEL TRAFFIC

By

Moacir de Souza Dias Junior

A DISSERTATION

Submitted to
Michigan State University
in partial fulfillment of the requirements
for the degree of

DOCTOR OF PHILOSOPHY

Department of Crop and Soil Sciences

1994

ABSTRACT

COMPRESSION OF THREE SOILS UNDER LONG-TERM TILLAGE AND WHEEL TRAFFIC

By

Moacir de Souza Dias Junior

Extremes in weather during critical periods, together with a move to conservation tillage systems, has renewed concerns over soil compaction during field operations in agricultural soils. This study examined the compressive behavior of three Michigan soils in response to changes in soil properties induced by tillage and wheel traffic; proposed a two component model of soil compressibility that accounts for stress history, and presented a spreadsheet procedure for estimation of the preconsolidation pressure (σ_p). Intact soil cores were equilibrated at four soil water contents and subjected to uniaxial confined compression tests over the range 25-1600 kPa applied stress. Near-surface penetrometer measurements were made weekly in 1993 on the Capac soil. In general, no-tillage (NT) shifted the compression curves due to higher bulk densities (ρ_b), increased the preconsolidation pressure (σ_p) in the Capac and Kalamazoo soils but not in the Misteguay, and had little effect on the compression index (m) in any of the soils. The unconfined strength (US) of the Capac soil confirmed laboratory measurements of σ_p, with NT and wheel tracked soil having higher US than conventional plow. Wheel traffic also shifted the position of the compression curves, increased σ_p, and decreased m. No-tillage had some effect but wheel traffic did more to decrease the susceptibility of these soils to further compaction by decreasing m and increasing σ_p. The stress history model relates σ_p as

a function of water content (θ_m) as $\sigma_p = 10^{(a + b\theta m)}$. The virgin compression model takes the form $\rho_{bfinal} = \rho_b + m \log (\sigma_{final} / \sigma)$, where σ is applied stress, and m is the compression index modeled as a function of θ_m as $m = a + b\theta_m + c\theta_m^2$. The stress history model predicted reasonably well σ_p ($R^2 = 0.84$ and 0.86) and the $\log_{10} \sigma_c$ ($R^2 = 0.78$ and 0.89) for the data reported in the literature. Field unconfined stress (US) measurements followed the stress history model and were linearly related to σ_p ($R^2 > 0.98$). A combined spreadsheet procedure was proposed to estimate σ_p for unsaturated soil conditions that compared well to published results and provided a fast and reliable estimation of σ_p.

To Mônica, Neto and Rod

and

in memory of my mother Iracy.

ACKNOWLEDGMENTS

I give my sincerest appreciation and thanks to my advisor Dr. Francis Pierce, for his guidance, encouragement, assistance in the preparation of this manuscript and for his constant friendship. Appreciation is also extended to Dr. Thomas Wolff, Dr. James Crum and Dr. Alvin Smucker for serving on my guidance committee. I thank Dr. Thomas Wolff for his help and the use of laboratory. In addition, I would like to thank the Brazilian government through MEC - CAPES for the financial support and the DCS - ESAL for being part of the process.

Acknowledgment is also made to Luiz, Humberto, and Joana Dias, Gaye Burpee, Kathy Emmenecker, Jonathan Landeck, José Oswaldo, Marcos and Leadir Fries, Reimar Carlesso and Everson for my beginning. I thank Brian Long for his technical assistance on the research. Appreciation is also extend to Lima, Corá and Chuanguo.

Finally, I would like to thank my wife Mônica and my children Moacir and Rodrigo who have always supported and encouraged me to complete this degree and to whom I am grateful for their love and understanding.

TABLE OF CONTENTS

LIST OF TABLES viii

LIST OF FIGURES ix

LIST OF SYMBOLS xii

INTRODUCTION 1

List of References 3

LITERATURE REVIEW 5

Soil compaction process 5
Modeling soil compaction 8
Methods to determine the preconsolidation pressure 10
List of references 14

CHAPTER 1. Soil compressibility of three glacial soils in response to tillage and wheel traffic 27

Abstract 27
Introduction 29
Material and Methods 30
Soils 30
Soil sampling 31
Laboratory compression measurements 32
Field unconfined strength measurements 33
Statistics 34
Results and Discussion 34
Initial soil properties 34
Soil compression curves 36
Field measurements 39
Summary 40
List of References 42

CHAPTER 2. Accounting for stress history in modeling soil compaction 59

Abstract 59
Introduction 61
Material and Methods 63
Model development 63
Model validation 65
Results and Discussion 66
Model validation 66
Conclusions 68
List of References 70

CHAPTER 3. A spreadsheet procedure for estimating preconsolidation pressure from soil compression curves 83

Abstract 83
Introduction 85
Review of current methods 87
Material and Methods 89
Spreadsheet procedure 89
Results and Discussion 91
Spreadsheet procedure overview 94
Conclusions 94
List of References 96

SUMMARY AND CONCLUSIONS 108

APPENDIX 1. Cells of the suggested spreadsheet procedure for estimation of the preconsolidation pressure from soil compression curves 111

APPENDIX 2. Computer screen and cells of the free flow spreadsheet for computation of the compressibilty test 112

LIST OF TABLES

LITERATURE REVIEW

Table 1. Relationship between soil properties used to assess soil compaction . . . 22

CHAPTER 1

Table 1. Soil properties of the Capac loam, Kalamazoo loam and Misteguay silty clay soils averaged across treatments 46

Table 2. Bulk density prior to compression test for the Capac loam, Kalamazoo loam soils. 47

Table 3. Coefficients of the regression of bulk density (ρ_b) on soil water content (θ_m) prior to compression test for the Misteguay silty clay using the regression model (ρ_b = a + b θ_m) 48

Table 4. Comparison of regression equations of the form ($m = a + b\theta_m + c\theta_m^2$) for compression index (m) and soil water content (θ_m) for Capac loam, and Misteguay silty clay 49

Table 5. Comparison of regression equations of the form ($\sigma_p = 10^{(a + b\,\theta m)}$) for preconsolidation pressure (σ_p) and soil water content (θ_m) for Capac loam, Kalamazoo loam, and Misteguay silty clay 50

CHAPTER 3

Table 1. Preconsolidation pressure (σ_p) obtained from current literature and using method 1 through 5 for saturated and unsaturated soil conditions 99

Table 2. Regression equations of preconsolidation pressure (σ_p) from current literature and as determined by methods 1 through 5 101

LIST OF FIGURES

CHAPTER 1

Figure 1. Soil water characteristic curves for the Capac loam, Kalamazoo loam, and Misteguay silty clay soils at 0-3 cm and 15-18 cm depth for the NTBT treatment 51

Figure 2. Soil compression curves for the Capac loam, and Misteguay silty clay soils and normalized compression curves for the Misteguay soils as affected by water content (θ_m). (Error bars represent the standard error of the mean; error bars for some points are masked by symbols due to very small std error values) 52

Figure 3. The relationship between the compression index (m) and soil water content (θ_m) for the Capac loam for the 0-3 cm and 15-18 cm depths . 53

Figure 4. The relationship between compression index (m) and soil water content (θ_m) for the Kalamazoo loam and Misteguay silty clay for 0-3 cm depth 54

Figure 5. Compression curves at -6 kPa and -100 kPa matric potential for Capac loam, Kalamazoo loam, and Misteguay silty clay soils under CTBT treatments at 0-3 cm depth. (Error bars represent the standard error of the mean; error bars for some points are masked by symbols due to small std error values) 55

Figure 6. Compression curves at -100 kPa matric potential (ψ_m) for Capac loam, Kalamazoo loam, and Misteguay silty clay soils under different tillage treatments at 0-3 cm depth. (Error bars represent the standard error of the mean; error bars for some points are masked by symbols due to small std error) 56

Figure 7. The relationship between the preconsolidation pressure (σ_p) and soil water content (θ_m) for the Capac loam, Kalamazoo loam , and Misteguay silty clay soils for the 0-3 cm depth for different tillage and traffic positions 57

Figure 8. Unconfined strength (US) as a function of soil water content (θ_m) for the Capac loam for the 0-3 cm depth for different tillage and traffic positions 58

CHAPTER 2

Figure 1. The secondary compression, rebound, and virgin compression components of a typical soil compression curve illustrating the position of the preconsolidation pressure (σ_p), the critical stress (σ_c), the compression index (m), and the shift down and to the left of the curve with increasing soil water content (θ_m). The dashed line represents a field compression curve constructed from the proposed model 74

Figure 2. The stress history model (a) expressing preconsolidation pressure (σ_p) as a function of soil water content (θ_m); and the virgin compression model (b) expressing bulk density (ρ_b) as a function of applied stress (σ) of the 0-3 cm depth for the Capac loam for four different θ_m 75

Figure 3. Soil compression curves expressing bulk density (ρ_b) as a function of applied stress (σ) for the 0-3 cm depth for the Capac loam at four different θ_m. The dashed line represents the line of the regression of preconsolidation pressure (σ_p) as a function of soil water content (θ_m) . 76

Figure 4. Preconsolidation pressure (σ_p) (from Kassa, 1992 and Reinert, 1990) and critical stress (σ_c) (from Kassa, 1992 and Larson and Gupta, 1980) as a function of soil water content (θ_m) compared with σ_p predicted from the stress history models obtained from the 0-3 cm depth of the Capac loam, Kalamazoo loam, and Misteguay silty clay for the conventionlly tilled treatment 77

Figure 5. Predicted and measured (Reinert, 1990) values of preconsolidation pressure (σ_p) using the stress history model for the 0-3 cm depth of Kalamazoo loam (5a) and the stress history model for the 0-3 cm depth of the Capac loam to compare with measurements of Kassa (1992) (5b). The stress history models used were for conventionlly tilled treatment 78

Figure 6. The relationship between critical stress (σ_c) and preconsolidation pressure (σ_p) from Kassa (1992) 79

Figure 7. The relationship between critical stress (σ_c) measured by Kassa (1992) and Larson and Gupta (1980) and preconsolidation pressure (σ_p) predicted using the stress history model derived from the 0-3 cm depth

of Capac loam when conventionlly tilled 80

Figure 8. Unconfined strength (US) or predicted preconsolidation pressure (σ_p) as related to soil water content (θ_m) in (a) and σ_p as predicted US from (b) using data from 0 - 3 cm depth of the Capac loam in no-till-track (NTT) and conventionally-tilled-between-track (CTBT) treatments . . . 81

Figure 9. The relationship between critical strength at which root elongation ceases, (as predicted from Gerard et al., 1982) and predicted preconsolidation pressure (σ_p) for θ_m = 0.10 kg kg^{-1} or ψ_m at -1.5 MPa matric potentials for the 0 - 3 cm depth of the Capac loam, Kalamazoo loam, and Misteguay silty clay soils for conventionally tilled between tracks 82

CHAPTER 3

Figure 1. Illustration of published methods for determination of the preconsolidation pressure (σ_p) for soil compression curves 102

Figure 2. Illustration of methods 1 through 4 for determination of the preconsolidation pressure (σ_p) for soil compression curves 103

Figure 3. The effect of water content on the soil compression curves for a Capac loam soil 104

Figure 4. Regression of preconsolidation pressure determined by the Casagrande (1936) procedure (σ_{pC}) on preconsolidation pressure estimated by methods 1 through 5 (σ_{pM}) for 288 compression curves from three soil series in Michigan 105

Figure 5. Regression of preconsolidation pressure determined by the Casagrande (1936) procedure (σ_{pC}) on preconsolidation pressure estimated by combinations of methods 1 and 5 with methods 2 and 3 (σ_{pM}) for 288 compression curves from three soil series in Michigan 106

Figure 6. Reproduction of the computer screen of the spreadsheet for determination of the preconsolidation pressure for soil compression curves 107

LIST OF SYMBOLS

a	.... Vertical intercept on q-axis
A, B, C, E	.... Soil parameters
A_H, B_H, C_H	.... Soil parameters determined from load compaction data during hydrostatic load, $\tau_{oct} = 0$
AWC	.... Available water capacity
b	.... Constant
c	.... Cohesion
[C]	.... Stress strain matrix
CI	.... Cone index
CI_o	.... Initial cone index
Cl	.... Clay content
C_p	.... Ratio between σ_3 and σ_1
D	.... Particle packing density
D_o	.... Maximum limiting packing density
D_{opt}	.... Optimal degree of compaction
e	.... Void ratio
E	.... Coefficient for the component of natural volummetric strain due to shearing stress

F	....	Stress of compactive force
Fe	....	Dithionite Fe
J	....	Parameters for adjusting the compression curve
H	....	Humus content
k	....	Measures of how rapidly the maximum packing density is attained with increasing pressure, σ
kf	....	Saturated hydraulic conductivity
L	....	Measures of how rapidly the maximum packing density is attained with increasing pressure, σ
Lk	....	Air capacity
LL	....	Liquid limit
n	....	Porosity
NAWC	....	Non-available water capacity
n_o	....	Initial porosity
m	....	Compression index
m_s	....	Slope of the secondary compression curve
p'	....	Effective vertical overburden pressure
OC	....	Organic C content
R	....	Ratio of maximum shear stress and mean normal stress
s	....	Sand content
S	....	Degree of saturation
Su	....	Undrained shear strength

RP	.... Resistance to penetration at field capacity
S_1	.... Desired degree of saturation
S_T	.... Slope of the bulk density vs degree of water saturation curve
S_k	.... Degree of saturation corresponding to ρ_k and σ_k
u_m	.... Minimum pore water pressure
u	.... Pore water pressure
U	.... Silt content
V	.... Volume
V_o	.... Initial volume
Y	.... Aggregate tensile strength
YF	.... Yield function for the plastic behavior
z	.... Depth of the specific layer
Δz	.... Change in the depth of specific layer
α	.... Slope of failure surface
$\delta_i = \rho_i/\rho_{iavg}$	.... Normalized initial bulk density
$\delta_c = (\delta_i - 1)\ \rho_i$	.... Adjusts the compressive curve for differences in the initial bulk density of each sample
ε_1	.... Major principal strain
ε_3	.... Minor principal strain
$\{\varepsilon\}$	.... Equal to $\{ \varepsilon_{xx}\ \varepsilon_{yy}\ \varepsilon_{xy}\ \varepsilon_{zz}\}^T$
$\hat{\varepsilon}_{oct}$	.... Natural octahedral normal strain

$\tilde{\epsilon}_{octH}$ .... Equal to $\tilde{\epsilon}_{oct}$, when the coefficients have been determined from triaxial test where $\sigma_1/\sigma_3 = 1$

$\tilde{\epsilon}_{octR}$ .... Equal to $\tilde{\epsilon}_{oct}$, when the coefficients have been determined from triaxial test where $\sigma_1/\sigma_3 > 1$

$\varepsilon_v = \Delta V/V_o$ .... Volumetric strain

$\tilde{\epsilon}_v = \ln (V/V_o)$ .... Natural volummetric strain

ε_{vT} .... Total volummetric strain

ε_z .... Volummetric strain in the vertical direction

ε_r .... Volummetric strain in the radial direction

ε_θ .... Volummetric strain in the tangential direction

ϕ .... Angle of internal friction

θ .... Volummetric soil water content

θ_m .... Water content by weight

θ_{mo} .... Initial water content by weight

θ_{mop} .... Optimum water content

ρ_b .... Bulk density

ρ_{bf} .... Final bulk density

ρ_{bi} .... Initial bulk density

ρ_{bk} .... Bulk density at a know stress σ_k

ρ_{boavg} .... Mean of initial bulk density

ρ_{bo}^* .... Bulk density resulting from previous vehicle loading

σ .... Applied stress

$\{\sigma\}$ .... Equal to $\{ \sigma_{xx}\ \sigma_{yy}\ \sigma_{xy}\ \sigma_{zz}\}^T$

σ_1 .... Major principal stress

σ_3 .... Minor principal stress

σ_c .... Critical stress

σ_f .... Final stress

σ_h .... Confining strain

σ_i .... Initial stress

σ_k .... Reference applied stress = 98 kPa

σ_m .... Mean normal stress

σ_n .... Normalized stress at $u_m = 1$

$\sigma_{oct} = (\sigma_x + \sigma_y + \sigma_z)/3$..... Mean normal stress or octahedral normal stress or spherical pressure

σ_p .... Preconsolidation pressure

σ_r .... Residual stress (soil without preconsolidation pressure σ_r=0)

σ_s .... Applied stress at u = 0

σ_x .... Stress at x axis

σ_z .... Stress at z axis

σ' .... Effective vertical overburden pressure

τ_{max} .... Maximum shearing stress

τ_{oct} .... Octahedral shearing stress

υ .... Specific volume = total volume / volume of solids

υ_r .... Specific volume at σ_r = 100 kPa and θ_{mr} = 0.20 kg kg^{-1}

ψ .... Angle of internal friction in degrees

ψ_m .... Matric potential

INTRODUCTION

Extremes in weather during critical periods, together with a move to conservation tillage systems, has renewed concerns over soil compaction during field operations in agricultural soils. Consequently, considerable research has been conducted (Barnes et al., 1971; Pidgeon and Soane, 1977; Bauder et al., 1981; Voorhees, 1983; Gupta et al., 1985; Voorhees et al., 1986; Håkansson et al., 1988; Larson et al., 1989; Hill and Meza-Montalvo, 1990; Bicki and Simens, 1991; Lebert and Horn, 1991) to obtain quantitative measurements of changes in soil physical properties caused by tillage operations and wheel traffic that would affect plant development and food production.

Field operations done when soil is too wet for tillage can lead to stress application that exceeds the soil strength, resulting in unrecoverable deformations. Farmers, however, have reported that soil managed under no-tillage are more easily trafficked under high moisture conditions than tilled soils. This could be an important advantage, particularly in the harvest of crops in wet seasons. However, the exact condition that defines when a soil is too wet to till or traffic still remains to be determined. Therefore, not only is the management system an important economical factor in industrialized agriculture (Bouma, 1984), but knowing when a soil is too wet for agricultural operations is critical. While moisture conditions and stress history primarily govern soil compressive behavior, there are no studies that had quantified the effects of drying on soil compressibility (McNabb and Boersma, 1993).

In this study, a stress history approach was developed in order to improve understand of the soil compaction process. The purpose of the first study was to examine how changes in soil properties induced by tillage and wheel traffic impacted the compressive behavior of different soils and the extent to which no-tillage and/or wheel traffic improves trafficability under high soil moisture conditions. The second study proposes a two component model of soil compressibility, consisting of a stress history submodel that describes the load carrying capacity of the soil in terms of the preconsolidation pressure and a classical virgin compression submodel that describes the plastic, non-recoverable deformation in terms of bulk density and applied stress, with both submodels as a function of the soil water content. Also, a field based soil compression curve was proposed based on field measurements of unconfined strength and water content, which were related to laboratory measurements of preconsolidation pressure, critical stress, and compression index. Finally, a spreadsheet procedure was developed to estimate the preconsolidation pressure from uniaxial compression test for unsaturated soil conditions which was used in the proposed model as a measure of the soil carrying capacity.

LIST OF REFERENCES

Barnes, K.K, W.M. Carleton, H.M. Taylor, R.I. Throckmorton, and G.E. Vanden Berg. 1971. Compaction of agricultural soils. ASAE. Monogr., St. Joseph, MI.

Bauder, J.W., G.W. Randall, and J.B. Swan. 1981. Effect of four continuous tillage systems on mechanical impedance of a clay loam soil. Soil Sci. Soc. Am. J. 45:802-806.

Bicki, T.J., and J.C. Siemens. 1991. Crop response to wheel traffic soil compaction. Trans. ASAE 34:909-913.

Bouma, J. 1984. Estimating moisture-related land qualities for land evaluation. p. 61-75. *In* Miller, F.P., E.L. Skidmore, D.T. Lewis, and D.M. Bandel (eds.) Land use planning techniques and policies. SSSA Spec. Publ. 12. ASA, CSSA, and SSSA, Madison, WI.

Gupta, S.C., A. Hadas, W.B. Voorhees, D. Wolf, W.E. Larson, and E.C. Schneider. 1985. Development of quids for estimating the ease of compaction of world soils. Research Report, Binational Agric. Res. Development, Bet Dagan, Israel, University of Minnesota, USA.

Håkansson, I., W.B. Voorhees, and H. Riley. 1988. Vehicle and wheel factors influencing soil compaction and crop response in different traffic regimes. Soil Tillage Res. 11:239-282.

Hill, R.L., and M. Meza-Montalvo. 1990. Long-term wheel traffic effects on soil physical properties under different tillage systems. Soil Sci. Soc. Am. J. 54:865-870.

Larson, W.E., G.R. Blake, R.R. Allmaras, W.B. Voorhees, and S.C. Gupta. 1989. Mechanics and related processes in structured agricultural soils. NATO Applied Science 172. Kluwer Academic Publishers, The Netherlands.

Lebert, M., and R. Horn. 1991. A method to predict the mechanical strength of agricultural soils. Soil Tillage Res. 19:275-286.

McNabb, D.H, and L. Boersma. 1993. Evaluation of the relationship between compressibility and shear strength of Andissols. Soil Sci. Soc. Am. J. 57:923-929.

Pidgeon, J.D., and B.D. Soane. 1977. Effects of tillage and direct drilling on soil properties during the growing season in a long-term barley monoculture system. J. Agric. Sci. 88:431-442.

Voorhees, W.B. 1983. Relative effectiveness of tillage and natural forces in alleviating wheel-induced soil compaction. Soil Sci. Soc. Am. J. 47:129-133.

Voorhees, W.B., W.W. Nelson, and G.W. Randall. 1986. Extend and persistence of subsoil compaction caused by heavy axle loads. Soil Sci. Soc. Am. J. 50:428-433.

LITERATURE REVIEW

SOIL COMPACTION PROCESS

Soil compaction refers to the compression of unsaturated soils during which there is an increase in soil density with a reduction in soil volume (Gupta and Allmaras, 1987; Gupta et al., 1989). Research has clearly shown the effect of soil compaction on soil physical properties (Barnes et al., 1971; Gupta et al., 1985; Larson et al., 1989; Binger and Wells, 1992). Soil compaction increases bulk density and soil strength (Trouse, 1971; Taylor, 1971; Hillel, 1982; Lebert et al., 1989; Wagger and Denton, 1989; Hill and Meza-Montalvo, 1990; Lebert and Horn, 1991), and decreases total porosity, size and continuity of the pores (Warkentin, 1971; Hillel, 1982; Smucker and Erickson, 1989). Significant reductions occur mainly in the volume of large pores, while small pores remain unaffected (Hillel, 1982). Soil compaction may have beneficial or adverse effects (Parish, 1971; Gupta and Allmaras, 1987; Smucker and Erickson, 1989; Raghavan et al., 1990). Beneficial effects have been attributed to improved seed soil contact (Smucker and Erickson, 1989) and increased available water in dry years (Raghavan and McKyes, 1983). However, excessive soil compaction can limit nutrient uptake, water infiltration and redistribution, gas exchange, and root development (Smucker and Erickson, 1989; Bicki and Siemens, 1991) resulting in decreased yields, increased erosion and increased power requirements for tillage (Soane, 1990).

Soil compaction, by definition, refers to a compression of unsaturated soil due to an applied external stress, that results in a decrease in soil volume. The ease with which unsaturated soil decreases in volume when subjected to a mechanical stress is called soil compressibility (Gupta and Allmaras, 1987). The compressibility behavior of a soil has been described as a function of the external and internal soil factors (Lebert and Horn, 1991). Soil external factors are characterized by the kind of load (Koolen and Kuispers, 1983; Horn, 1988; Raghavan et al., 1990), while soil internal factors are influenced by stress history (Harris, 1971; Horn, 1988; Gupta et al., 1989; Reinert, 1990), water content (Gupta et al., 1985; Bailey et al., 1986), soil texture (Gupta et al., 1985; Horn, 1988; McBride, 1989), soil structure (Dexter and Tanner, 1974; Horn, 1988), and initial bulk density (Gupta et al., 1985; Culley and Larson, 1987; Reinert, 1990).

Under dry conditions, soil strength may be great enough to support loads and soil compaction may be not significant (Trouse, 1971; Taylor, 1971; Larson and Allmaras, 1971). However, any compaction is detrimental to crop yield under wet conditions (Swan et al., 1987) and could cause yield reduction (Negi et al., 1980; Carter, 1985; Gameda et al., 1985; Negi et al., 1990; Bicki and Siemens, 1991). In areas with a short growing season, field operations are carried out as soon as the soils are considered trafficable, however, under such conditions the soils are probably still too wet to be trafficable (Håkansson et al., 1988) and traffic often leads to unrecoverable soil deformation. In contrast, farmers have indicated that soil managed under no-tillage are more easily trafficked under high moisture conditions than tilled soils. This could be an important advantage, particularly in the sowing and harvesting of crops in wet seasons. This may be explained by the fact that no-tilled soils and wheel-traffic increases bulk density and soil strength greater than 50% than conventionally tilled soils (Hill and Meza-Montalvo, 1990) at moisture conditions at saturation and slightly above and below field capacity. In addition, Soane et al., (1982) suggested that a no-tilled soil becomes precompacted and may have acquired sufficient soil strength to carry traffic without further compaction occurring. In spite of these observations, the necessity of quantification of the effect of drying on the compressibility of soils still remains to be determined (McNabb and Boersma, 1993). Therefore, while the stress history of a soil is greatly affected by the drying process, there are few studies that have quantified the effects of long-term no-tillage or drying on soil compressibility. Thus, there are little quantitative data to support the observation of increased trafficability of soil managed under no-till.

The persistence of soil compaction beyond the current crop caused by previous traffic have been reported by several researchers (Smith et al., 1969; Black et al., 1976; Voorhees, 1977; Voorhees et al., 1978; Pollard and Elliot, 1978; Logsdon et al., 1992). Some of these studies showed the effects of compaction are only temporarily harmful, however, in the majority of cases, little or no change in the persistence of soil compaction was observed. Therefore, restoration of soil compaction, if possible, is costly and time consuming.

MODELING SOIL COMPACTION

The critical concern with soil compaction is to determine when the soil is too wet to till or traffic and what level of damage will occur to the soil when applied stresses exceed its carrying capacity. Thus, a soil is too wet at any water content if plastic deformation occurs. While much is known about the compaction process (Barnes et al., 1971; Gupta and Allmaras, 1987; and Gupta et al., 1989), there are no studies that had quantified the effects of drying on soil compressibility (McNabb and Boerma, 1993), particularly under field conditions. The emphasis on modeling soil compaction has been focused on the virgin compression curve which, by definition, defines plastic, unrecoverable deformation, and is generally well described (Larson and Gupta, 1980; Gupta et al., 1985; Horn, 1989). However, it is the region of elastic, recoverable deformation (the secondary compression curve) that defines when a soil can be tilled or trafficked. It is this component of the soil compression curve that defines the stress history of soil and it not been modeled. Thus, a model that predicts the maximum stress that a soil can withstand over a range of water contents without causing soil compaction is needed. This would answer the question whether a soil can be tilled or trafficked without soil damage.

In order to assess the susceptibility of soils to compaction, the relationship between compaction and soil properties must be determined. A summary of the relationship between soil properties used to assess soil compaction is presented in Table 1. These relationships were obtained using disturbed soil samples (Bailey and VandenBerg, 1968; Larson et al., 1980; Larson and Gupta, 1980; Grisso et al., 1987;

Bailey and Johnson, 1989; O'Sullivan, 1992), and undisturbed soil samples (Smith, 1985; Reinert, 1990; Lebert and Horn, 1991; McNabb and Boersma, 1993). Also different types of tests, such as uniaxial compression test (Larson et al., 1980; Larson and Gupta, 1980; Reinert, 1990; O'Sullivan, 1992) and triaxial (Bailey and VandenBerg, 1968; Bailey et al., 1986; Bailey and Johnson; 1989, Grisso, 1987) were used with saturated soil samples (MacNabb and Boerma, 1993) and with different water contents (Bailey and VandenBerg, 1968; Dexter and Tanner, 1973; Larson and Gupta, 1980; Larson et al., 1980; Reinert, 1990; Lebert and Horn, 1991; O'Sullivan, 1992) to obtain those relationship. Thus, there is no agreement upon which soil properties should be used in order to predict soil compaction.

In general, five different approaches have been used as the basis for modeling the compression behavior of the soil: (1) the virgin compression curve (Soehne, 1958; Bailey and VandenBerg, 1968; Bowen, 1975; Larson et al.,1980; Lebert and Horn, 1991; Binger and Well, 1992), (2) critical stress (Larson and Gupta, 1980; Gupta and Larson, 1982; Gupta et al. 1985); (3) the relationship between strain and applied stress during triaxial tests (Bailey et al., 1984; Bailey et al., 1985; Bailey et al., 1986; Grisso et al.,1987; Bailey and Johnson, 1989); (4) finite element analysis (Perumpral et al, 1971; Colleman and Perumpral, 1974; Pollock, Jr. et al. 1986; Gassman et al., 1989; Raper and Erbach, 1990 a; Raper and Erbach, 1990 b); and (5) generalized curve fitting techniques (Blackwell and Soane, 1981; Howard et al; 1981; Leeson and Campbell, 1983; Angers et al, 1987, Lebert et al., 1989; Canarache, 1991; Lebert and Horn, 1991) (Table 1). However, none of these models account for the stress history of the soil, although Lebert et al. (1989), Reinert (1990) and Lebert and Horn (1991), predict the preconsolidation pressure (σ_p) from soil properties. The diminished importance of stress history in current models may be related to the fact that compression tests are usually performed on disturbed soil samples and at relatively high soil water contents, both of which would tend to mask the stress history of a soil.

The σ_p is an indication of the maximum previously applied stress sustained by a soil (Holtz and Kovacs, 1981) and defines the limit of elastic deformation in the soil compression curve. Thus, in agriculture application of stress greater than the highest previously applied stress should be avoided (Gupta et al, 1989; Lebert and Horn, 1991) in order to avoid unrecoverable soil deformations. Therefore, σ_p is more likely to be the maximum stress applied to a soil to prevent further soil compaction.

METHODS TO DETERMINE THE PRECONSOLIDATION PRESSURE

A change in the stress acting on a soil will result in some deformation until a new equilibrium is reached. These deformations are relatively small and recoverable during secondary compression and unrecoverable during primary compression of the soil (Stone and Larson, 1980; Gupta et al.,1989; Lebert and Horn, 1991). The preconsolidation pressure has been used to divide the compression curve into regions of small, elastic and recoverable deformations (secondary compression curve) and in regions of plastic and unrecoverable deformations (virgin compression curve) (Holtz and Kovacs, 1981; Jamiolkowski et al., 1985). Thus, additional soil compaction only occurs in the virgin compression curve (Gupta et al., 1989; Lebert and Horn, 1991). Hence, a consistent, fast, repeatable and reliable method for determination of the preconsolidation pressure is often of considerable importance from the point of view of avoiding and predicting soil compaction.

Several methods have been proposed for determining the preconsolidation pressure from laboratory tests. The Casagrande (1936) method involves selecting the point of minimum radius of curvature. This is accomplished by drawing horizontal and tangent lines at this point and bisecting the angle between them, then extending the straight line portion of the virgin compression curve until it intersects the bisector of the angle. The pressure corresponding to this point of intersection is the estimated preconsolidation pressure.

Burmister (1951) proposed a procedure in which the unloading-reloading stress cycle defines the slope of a typical unloading curve and the form and size of the characteristic triangle on a semi logarithmic plotting of the curve. By shifting the unloading curve upward parallel to itself to a point where a geometrically similar triangle of the same vertical intercept is found, the preconsolidation pressure can be determined. The preconsolidation pressure is equal to the position of the vertical leg.

Schmertmann (1955) suggested a procedure in which a horizontal line is drawn parallel to the log of applied stress from the initial void ratio to the existing vertical overburden pressure. A line parallel to the rebound-reload curve is drawn through the vertical overburden pressure, and the laboratory initial virgin compression curve is extended until it intersects either the initial void-ratio or the rebound line. The intersection point is defined as the preconsolidation pressure.

Sällfors (1975, as cited by Larson, 1986) suggested a method in which the two straight parts of the stress-strain curve are extended and intersected. An isosceles triangle is inscribed between the lines and the stress-strain curves. The intersection point between the base of the triangle and the upper line represents the preconsolidation pressure.

Anderson and Lukas (1981) predict the preconsolidation pressure (σ_p) from the undrained shear strength (Su) and the effective vertical overburden pressure (σ'):

$$\sigma_p = Su/(Su/\sigma')$$

Culley and Larson (1987) used a statistical procedure to estimate the preconsolidation pressure. First, a least square regression was determined considering that all points lay on the virgin compression curve. Next, the compression curve was divided into two regions assuming an initial estimate of preconsolidation pressure of 15 kPa. Regression equations for each region was them developed and a combined sums of square calculated. The estimate preconsolidation pressure was then incrementally increased by 5 kPa and the statistics recalculated until the lowest residual sums of squares was achieved.

Jose et al. (1989) used a log-log method in which the applied pressure and corresponding void ratio are plotted in logarithmic scale for each segment of the curve. The preconsolidation pressure is assumed to be equal to the applied stress at the intersection of these two distinct lines. The authors did not reveal their criteria for choosing which points were included in the calculation of the two lines.

Lebert and Horn (1991) estimated the preconsolidation pressure as the intersection of the regression lines fitted through the secondary compression curve and the virgin compression curve. The authors did not reveal their criteria for choosing which points were included in the calculation of the two lines.

Therefore, there are no agreed upon methods for determining the preconsolidation pressure. However, according to Leonards (1962) the earliest and most widely used procedure to determine the preconsolidation pressure is the Casagrande (1936) procedure.

LIST OF REFERENCES

Amir, I., G.S.V. Raghavan, E. McKyes, and R.S. Broughton. 1976. Soil compaction as a function of contact pressure and soil moisture content. Can. Agric. Eng. 18:54-57.

Anderson, T.C., and R.G. Lukas. 1981. Preconsolidation pressure predicted using Su/p' ratio. p. 502-515. *In* Yong, R.N. and F.C. Townsend (eds.) Laboratory shear strength of soil. Symposium ASTM. Special Technical Publication 740. Chicago, Ill, 25 June 1980. Philadelphia, Pa.

Angers, D.A., B.D. Kay, and P.H. Groenevelt. 1987. Compaction characteristics of a soil cropped to corn and bromegrass. Soil Sci. Soc. Am. J. 51:779-783.

Bailey, A.C., and C.E. Johnson. 1989. A soil compaction model for cylindrical stress state. Trans. ASAE 32:822-825.

Bailey, A.C., C.E. Johnson and R.L. Schafer. 1984. Hydrostatic compaction of agricultural soils. Trans. ASAE 27:952-995.

Bailey, A.C., C.E., Johnson, and R.L., Schafer, 1986. A model for agricultural soil compaction. J. Agric. Eng. Res. 33:257-262.

Bailey, A.C., C.E. Johnson, R.L. Schafer, T.A. Nichols, and R.D. Grisso. 1985. A compaction model for agricultural soil. p. 2:203-212. *In* Taction and transport as related to cropping systems. Proc. Int. Conf. Soil Dynamics. Auburn, AL. June 17-19, 1985. Natl. Tillage Mach. Lab. and Agric. Eng. Dept., Alabama Exper. Sta., Auburn, AL.

Bailey, A.C., and G.E. VandenBerg. 1968. Yielding by compaction and shear in unsaturated soils. Trans. ASAE 11:307-311,317.

Barnes, K.K., W.M. Carleton, H.M. Taylor, R.I. Throckmorton, and G.E. Vanden Berg. 1971. Compaction of agricultural soils. ASAE. Monogr., St. Joseph, MI.

Bicki, T.J., and J.C. Siemens. 1991. Crop response to wheel traffic soil compaction. Trans. ASAE 34:909-913.

Binger, R.L., and L.G. Wells. 1992. Compact - a reclamation soil compaction model part I. model development. Trans. ASAE 35:405-413.

Black, G.R., W.W. Nelson and R.R. Allmaras. 1976. Persistence of subsoil compaction in a mollisol. Soil Sci. Soc. Am.J. 40:943-948.

Blackwell, P.S., and B.D. Soane. 1981. A method of predicting bulk density changes in field soils resulting from compaction by agricultural traffic. J. Soil Sci. 32:51-65.

Bolling, I.H. 1985. How to predict the soil compaction of agricultural tires. p. 936-952. In Taction and transport as related to cropping systems. Int. Conf. on Soil Dynamics. Auburn, AL. June 17-19,1985. National Tillage Machinery Laboratory and Agricultural Engineering Dept., Alabama, Experimental Station, Auburn, AL.

Bowen, H.D. 1975. Simulation of soil compaction under tractor-implement traffic. ASAE paper No. 75-1569. Am. Soc. Agric. Eng. St. Joseph, MI.

Brandon, J.R., T. Kuppusamy, and J.V. Perumpral. 1987. A stress-strain model for agricultural soils. ASAE paper No. 87-1552. Am. Soc. Agric. Eng. St. Joseph, MI.

Burmister, D. 1951. The application of controlled test methods in consolidation testing. p. 83-98. *In* Fifty-Fourth Annual Meeting of the ASTM. Symposium on consolidation testing of soils. Special Technical Publication 126. Atlantic City, N.J. June 18, 1951. Philadelphia, Pa.

Canarache, A. 1991. Factors and indices regarding excessive compactness of agricultural soils. Soil Tillage Res. 19:145-164.

Carter, L.M. 1985. Wheel traffic is costly. Trans. ASAE 28:430-434

Casagrande, A. 1936. The determination of the pre-consolidation load and its practical significance. p. 60-64. *In* Int. Conf. on Soil Mech. and Found. Eng. Proc. of ICSMFE. Cambridge, Mass. June 22-26, 1936. vol. 3. Cambridge, Mass.

Colleman, G.E., and J.V. Perumpral. 1974. The finite element analysis of soil compaction. Trans ASAE 17:856-860.

Culley, J.L.B., and W.E. Larson. 1987. Susceptibility to compression of a clay loam Haplaquoll. Soil Sci. Soc. Am. J. 51:562-567.

Dexter, A.R., and D.W. Tanner. 1973. The response of unsaturated soils to isotropic stress. J. Soil Sci. 24:491-502.

Dexter, A.R., and D.W. Tanner. 1974. Time dependence of compressibility for remolded and undisturbed soils. J. Soil Sci. 25:153-164.

Gameda, S., G.S. V. Raghavan, R. Theriault, and McKyes. 1985. High axle load compaction and corn yield. Trans. ASAE 28:1759-1765.

Gassman, P.W., D.C. Erbach, and S.W. Melvin. 1989. Analysis of track and wheel soil compaction. Trans. ASAE 32:23-29.

Grisso, R.D., C.E. Johnson, and A.C. Bailey. 1987. Soil compaction by continuous deviatoric stress. Trans. ASAE 30:1293-1301.

Gupta, S.C., A. Hadas, and R.L. Schafer. 1989. Modeling soil mechanical behavior during compaction. p. 137-152. *In* Larson, W.E., G.R. Blake, R.R. Allmaras, W.B. Voohees, and S.C. Gupta (eds.). Mechanical and related process in structured agricultural soils. NATO applied sciences 172. Kluwer Academic Publishers, The Netherlands.

Gupta, S.C., A. Hadas, W.B. Voorhees, D. Wolf, W.E. Larson, and E.C. Schneider. 1985. Development of quids for estimating the ease of compaction of world soils. Research Report, Binational Agric. Res. Development, Bet Dagan, Israel. University of Minnesota, USA.

Gupta, S.C., and R.R. Allmaras. 1987. Models to access the susceptibility of soil to excessive compaction. Adv. Soil Sci. 6:65-100.

Gupta, S.C., and W.E. Larson. 1982. Modeling soil mechanical behavior during tillage. p. 151-178. *In* P.W. Unger, D.M. Van Doren, Jr., F.D. Whisler, and E.L. Skidmore (eds.). Predicting tillage effects on soil physical properties and process. Spec. Pub. 44. Am. Soc. Agron. Madison, WI.

Håkansson, I. 1988. A method for characterizing the state of compactness of an arable soil. Catena Suppl. 11:101-105.

Håkansson, I., W.B. Voorhees, and H. Riley. 1988. Vehicle and wheel factors influencing soil compaction and crop response in different traffic regimes. Soil Tillage Res. 11:239-282.

Harris, W.L. 1971. The soil compaction process. p. 9-44 *In* K.K. Barnes, W.M. Carleton, H.M. Taylor, R.L. Throckmorton, and G.E. Vanden Berger.(eds.). Compaction of Agricultural Soils. Am. Soc. Agric. Eng., St. Joseph, MI.

Hill, R.L., and M. Meza-Montalvo. 1990. Long- term wheel traffic effects on soil physical properties under different tillage systems. Soil Sci. Soc. Am. J. 54:865-870.

Hillel, D. 1982. Introduction to soil physics. Academic Press, Inc. San Diego, CA.

Holtz, R.D., and Kovacs, W.D. 1981. An introduction to geotechnical engineering. Prentice-Hall, Inc., Englewood Cliffs, NJ.

Horn, R. 1988. Compressibility of arable land. Catena Sup. 11:53-71.

Horn, R. 1989. Strength of structured soils to loading - a review of process on macro and microscale; European aspects. p. 9-22. *In* W.E. Larson, G. R. Blake, R. R. Allmaras, W. B. Voorhees, and S. C. Gupta (eds.) Mechanics and related processes in structured agricultural soils. NATO applied sciences, vol. 172. Kluwer Academic Publishers, The Netherlands.

Howard, R.F., M.J. Singer, and G.A. Frantz. 1981. Effects of soil properties, Water content, and compactive effort on the compaction of selected California forest and range soils. Soil Sci. Soc. Am. J. 45:231-236.

Jamiolkowski, M., C.C. Ladd, J.T. Germaine, and R. Lancellotta. 1985. New development in field and laboratory testing of soils. p. 57-153. *In* Publications Committee of XI ICSMFE (ed.). Proc. of the Eleventh Int. Conf. on Soil Mech. and Found. Eng. San Francisco, CA, 12-16 August 1985. Netherlands.

Johnson, C.E., A.C. Bailey, T.A. Nichols and R.D. Grisso. 1984. Soil behavior under repeated hydrostatic loading. ASAE paper No.84-1548. Am. Soc. Agric. Eng. St. Joseph, MI.

Jones, C.A. 1983. Effect of soil texture on critical bulk densities for root growth. Soil Sci. Am. J. 47:1208-1211.

Jose, B.T., A. Sridharan, and B.M. Abraham. 1989. Log-log method for determination of preconsolidation pressure. Geotechnical Testing Journal. 12:230-237.

Koolen, A.J., and Kuipers, H. 1983. Agricultural soil mechanics. Springer Verlag, Berlin.

Larson, R. 1986. Consolidation of soft soils. Swedish Geotechnical Institute. Report 29. Linköping, Swedish.

Larson, W.E., G.R. Blake, R.R. Allmaras, W.B. Voorhees, and S.C. Gupta. 1989. Mechanics and related processes in structured agricultural soils. NATO Applied Science 172. Kluwer Academic Publishers, The Netherlands.

Larson, W.E., and R.R. Allmaras. 1971. Management factors and natural forces as related to compaction. p. 367-427. *In* k.K Barnes, W.M. Carleton, H.M. Taylor, R.I. Throckmorton, and G.E. Vanden Berg. Compaction of agricultural soils. ASAE. Monogr., St. Joseph, MI.

Larson, W.E., and S.C. Gupta. 1980. Estimating critical stress in unsaturated soils from changes in pore water pressure during confined compression. Soil Sci. Soc. Am. J. 44:1127-1132.

Larson, W.E., S.C. Gupta, and R.A. Useche. 1980. Compression of agricultural soils from eight soil orders. Soil Sci. Soc. Am. J. 44:450-457.

Lebert, M., N. Burger, and R. Horn. 1989. Effects of dynamic and static loading on compaction of structured soils. p. 73-80. *In* W.E. Larson, G. R. Blake, R. R. Allmaras, W. B. Voorhees, and S. C. Gupta (eds.) Mechanics and related processes in structured agricultural soils. NATO applied sciences, vol. 172. Kluwer Academic Publishers, The Netherlands.

Lebert, M., and R. Horn. 1991. A method to predict the mechanical strength of agricultural soils. Soil Tillage Res. 19:275-286.

Leeson, J.J., and D.J. Campbell. 1983. The variation of soil critical state parameters with water content and its relevance to the compaction of two agricultural soils. J. Soil Sci. 34:33-44.

Leonards, G.A. 1962. Foundation Engineering. McGraw Hill Book Company, Inc., NY.

Logsdon, S.D., R.R. Allmaras, W.W. Nelson, and W.B. Voohees. 1992. Persistence of subsoil compaction from heavy axle loads. Soil Tillage Res. 23:95-110.

McBride, R.A. 1989. Estimation of density-moisture-stress function from uniaxial compression on unsaturated structured soils. Soil Tillage Res. 13:383-397.

McNabb, D.H., and L. Boersma. 1993. Evaluation of the relationship between compressibility and shear strength of Andisols. Soil Sci. Am. J. 57:923-929.

Negi, S.C., E. McKyes, F. Taylor, G.S.V. Raghavan. 1980. Crop performance as affected by traffic and tillage in a clay soil. ASAE 23:1364-1368.

Negi, S.C., G.S.V. Raghavan, E. McKyes, and F. Taylor. 1990. The effect of compaction and minimum tillage on corn yield sand soil properties. Trans. ASAE 33:744-748.

O'Sullivan, M.F. 1992. Uniaxial compaction effects on soil physical properties in relation to soil type and cultivation. Soil Tillage Res. 24:275-286.

Parish, D.H. 1971. Effects of compaction on nutrient supply to plants. p. 277-291. *In* k.K Barnes, W.M. Carleton, H.M. Taylor, R.I. Throckmorton, and G.E. Vanden Berg. Compaction of agricultural soils. ASAE. Monogr., St. Joseph, MI.

Pollard, F. and J.G. Elliott. 1978. The effect of soil compaction and method of fertilizer placement on the growth of barley using a concrete track technique. J. Agric. Eng. Res. 23:203-216.

Pollock, Jr. D., J.V. Perumpral, and T. Kuppusamy. 1986. Finite element analysis of multipass effects of vehicles on soil compaction. Trans. ASAE 29:45-50.

Prumpral, J.V., J.B. Lijedahl, and W.H. Perloff. 1971. The finite element method for predicting stress distribution and soil deformation under a tractive device. Trans. ASAE 14:1184-1188.

Raghavan, G.S.V., and E. McKyes. 1983. Physical and hydraulic Characteristics in compacted clay soils. J. Terramechanics. 19:235-242.

Raghavan, G.S.V., P. Alvo, and E. McKyes. 1990. Soil compaction in agriculture: A review toward managing the problem. Advances in Soil Sci. 11:1-36.

Raper, R.L., and D.C. Erbach. 1990 a. Prediction of soil stresses using the finite element method. Trans. ASAE 33:725-730.

Raper, R.L., and D,C. Erbach. 1990 b. Effect of variable linear elastic parameters on finite element prediction of compaction. Trans. ASAE 33:731-736.

Reinert, D.J. 1990. Soil structural form and stability induced by tillage in a Typic Hapludalf. Ph.D diss. Michigan State Univ. East Lansing.

Saini, G.R., and T.L. Chow. 1984. Compactibility indexes of some agricultural soils of New Brunswick, Canada. Soil Sci. 137:33-38.

Sällfors, G. 1975. Preconsolidation pressure of soft high plastic clays. Thesis. Department of Geotechinical Engineering. Gothenburg.

Schmertmann, J.H. 1955. The undisturbed consolidation behavior of clay. Trans. ASCE 120:1201-1233.

Smith, D.L.O. 1985. Compaction by Wheels: a numerical model for agricultural soils. J. Soil Sci. 36:621-632.

Smith, S.T., T.C. Stoneman, and C.V. Malcolm. 1969. Cultivation and traffic hardpans in Swan Valley Vineyards. West. Aust. Dept. Agric., Tech. Bull. 1.

Smucker, A.J.M., and A.E. Erickson. 1989. Tillage and compactive modifications of gaseous flow and soil aeration. p. 205-221. *In* W.E. Larson, G.R. Blake, R.R. Allmaras, W.B. Voorhees, and S.C. Gupta (eds.). Mechanics and related processes in structured agricultural soils. NATO applied sciences, vol. 172. Kluwer Academic Publishers, The Netherlands.

Soane, B.D. 1990. The role of organic matter in soil compactibility: a review of some practical aspects. Soil Tillage Res. 16:179-201.

Soane, B.D., J.W. DicKson, and D.J. Campbell. 1982. Compaction by agricultural vehicles: a review III. Incidence and control of compaction in crop production. Soil Tillage Res. 2:3-36.

Soehne, W.H. 1958. Fundamentals of pressure distribution and soil compaction under tractors tires. J. Agric. Eng. 276-291.

Stone, J.A., and W.E. Larson. 1980. Rebound of five one-dimensionally compressed unsaturated granular soils. Soil Sci. Soc. Am. J. 44:819-822.

Swan, J.B., J.F. Moncrief, and W.B. Voohees. 1987. Soil compaction-causes, effects, and control. University of Minnesota, Agric. Bull. 3115. St. Paul, Minnesota.

Taylor, H.M. 1971. Effects of soil strength on seedling emergence, root growth and crop yield. p. 292-305. *In* k.K Barnes, W.M. Carleton, H.M. Taylor, R.I. Throckmorton, and G.E. Vanden Berg. Compaction of agricultural soils. ASAE. Monogr., St. Joseph, MI.

Trouse, JR., A.C. 1971. Present knowledge and need for research. p. 225-240. *In* k.K Barnes, W.M. Carleton, H.M. Taylor, R.I. Throckmorton, and G.E. Vanden Berg. Compaction of agricultural soils. ASAE. Monogr., St. Joseph, MI.

Vanden Berg, G.E. 1966. Triaxial measurements of shear strain and compaction in unsaturated soil. Trans. ASAE 9:460-463,467.

Voorhees, W.B. 1977. Soil compaction: our newest natural resource. Crops Soils Mag. 29:13-15.

Voorhees, W.B., C.G. Senst, and W.W. Nelson. 1978. Compaction and soil structure modification by wheel traffic in the Northern Corn Belt. Soil Sci. Soc. Am. J. 42:344-349.

Wagger, M.G., and H.P. Denton. 1989. Influence of cover crop and wheel traffic on soil physics properties in continuous no-till corn. Soil Sci. Soc. Am. J. 53:1206-1210.

Warkentin, B.P. 1971. Effects of compaction on content and transmission of water in soils. p. 126-153. *In* k.K Barnes, W.M. Carleton, H.M. Taylor, R.I. Throckmorton, and G.E. Vanden Berg. Compaction of agricultural soils. ASAE. Monogr., St. Joseph, MI.

Wlodek, S. 1991. Depth indicators method for determination of bulk density dynamics. Soil Tillage Res. 19:197-201.

Table 1. Relationship between soil properties used to assess soil compaction.

Reference	Relationship
Soehne, 1958	$n = m \ln \sigma + n_o$
VandenBerg, 1966	$\rho = A + B \log [\sigma_{oct} (1 + \tau_{max})]$
Bailey & VandenBerg, 1968	$1/\rho_b = m \log \sigma + B$
	$1/\rho_b = A \log \zeta + B (\tau_{max} / \sigma_m) + C$
	$\zeta = (\sigma_m{}^2 + \tau_{max}{}^2)^{1/2}$
	$\sigma_m = (\sigma_1 + 2\sigma_3)/3$
	$\tau_{max} = (\sigma_1 - \sigma_3)/3$
Dexter & Tanner, 1973	$D = D_o + B \exp (-k\sigma) + C \exp (-L\sigma)$
	$D = (\rho / 2660) [(100\text{-}OC) / (100+\theta_m)]$
Colleman & Perumpral, 1974	$\varepsilon_{vT} = (-0.007 + 1.72 R - 15.854R^2 +$
	$96.107 R^3 - 237.304 R^4 + 213.301 R^5)* 10^{-3}$
Bowen, 1975	$n = - m \log \sigma + C$
	$\rho_b = 2.65 (1 - n / 100)$
Amir et al., 1976	$n = A - B \ln (\sigma_r + \sigma) - C \ln \theta$
	$\rho_b = A + B \ln (\sigma_r + \sigma) - C \ln \theta$
Larson et al., 1980	$\rho_b = \rho_{bk} + S_T (S_1 - S_k) + m \log (\sigma/\sigma_k)$
Larson & Gupta, 1980	$\log \sigma_c = \sigma_n \log \sigma_s$
Blackwell & Soane, 1981	m and $\rho_b = f (\theta_m)$
	$\rho_{bf} = 1.166 + 0.252 \ln \sigma_{octmax}$

Table 1 (cont'd).

Howard et al., 1981	$\rho_b = 1.19 - 0.596\ OC - 0.076\ LL + 0.0019\ s + 0.0058\ Fe$
	$\rho_b = 1.93 - 0.0628\ OC - 0.0063\ LL + 0.0012\ s$
	$\rho_b = 3.27 - 0.0231\ OC - 0.528 \ln \theta_{mop} - 0.0008\ s + 0.0039\ Fe$
Gupta & Larson, 1982	$n = f(\theta_m, \sigma)$
	criteria of : critical air-filled porosity, critical stress for shearing, aggregates and critical soil resistance for root growth was superimposed.
Jones, 1983	$\rho_b = 1.52 - 0.00646\ Cl$
Leeson & Campbell, 1983	for sandy loam soil
	$\upsilon = 2.25 - 0.008\ \theta_m$
	for loam soil
	$\upsilon = 2.28 - 0.011\ \theta_m$
Bailey et al., 1984	$\varepsilon_v = (A + B\sigma)(1 - e^{-C\sigma})$
	$\varepsilon_v = \Delta V/V_o \quad \Delta V = V_o - V$
	$1/\rho_b = 1/\rho_{bi} - 1/\rho_{bi}(A + B\sigma)(1 - e^{-C\sigma})$

Table 1 (cont'd).

Johnson et al., 1984	$\varepsilon_v = (A + B\sigma)(1 - \exp(-C\sigma))$
	$\ln \rho_b = \ln \rho_{bi} - (A + B\sigma)(1 - \exp(-C\sigma))$
Saini et al., 1984	$\rho_b = 1.2926 - 0.2504\,\theta_m + 0.8353\,\theta_m^2 + 0.9932\,\theta_m^3 + 0.1203\,F - 0.0330F^2 + 0.0026\,F^3 + 1.0635\,\theta_m F + 7.4289\,\theta_m^2 F + 12.96350\theta_m^3 F + 0.0984\,\theta_m F^2 - 0.3842\,\theta_m^2 F^2 - 0.1272\,\theta_m^2 F^3 + + 0.02880\theta_m F^3 - 0.2231\,\theta_m^2 F^3 + 0.45880\theta_m^3 F^3$
Gupta et al., 1985	$\rho_b = f(S, \sigma)$
Bailey et al., 1985	$\hat{\varepsilon}_v = (A + B\sigma_h)(1 - e^{-C\sigma_h})$
and	$\hat{\varepsilon}_v = \ln(V/V_0)$
Bailey et al., 1986	$\ln(\rho_b) = \ln(\rho_{bi}) - (A + B\sigma_h)(1 - e^{-C\sigma_h})$
Bolling, 1985	$n = n_o - (\theta_m/\theta_{mo})^3\,[CI/CI_o)]^{1/2}$
	$n = n_o - (n_o - 0.225)\,/\,(35C_p + 1)(\theta_m/12)^{3/2}\,\sigma_1$
Smith, 1985	$\Delta\sigma_1 = \sigma_i - (\rho_b - \rho_{bi})\,[(\sigma_i - \sigma_f)\,/\,(\rho_{bf} - \rho_{bi})]$
Pollock, Jr. et al., 1986	$\varepsilon_v = \varepsilon_z + \varepsilon_r + \varepsilon_\theta$
Angers et al., 1987	$Y = -112.2 + 88.9\,\rho_b$
Grisso et al., 1987	$\hat{\varepsilon}_{oct} = (\hat{\varepsilon}_{octR}\,/\,\hat{\varepsilon}_{octH})(A_H + B_H\sigma_{oct})(1 - e^{-C_H\sigma_{oct}})/3$
Brandon et al., 1987	$YF = a + \alpha[(\sigma_x + \sigma_y)/2] - \{[(\sigma_x - \sigma_y)/2]^2 + \sigma_{xy}^2\}^{1/2}$

Table 1 (cont'd).

Håkansson, 1988	for $0 < Cl < 60\%$; $1 < H < 11\%$
	$D_{opt} = 90.5 - 0.29\ Cl + 0.0059\ Cl^2 - 0.139\ H$
	for $0 < Cl < 60\%$
	$D_{opt} = 86.5 + 0.041\ Cl$
Bailey & Johnson, 1989	$\hat{\varepsilon}_v = (A + B\sigma_{oct})(1 - e^{-C\sigma_{oct}}) + E(\tau_{oct} / \sigma_{oct})$
	$\ln \rho_b = \ln \rho_{bi} - (A + B\sigma_{oct})(1 - e^{-C\sigma_{oct}}) +$
	$+E(\tau_{oct}/\sigma_{oct})$
Lebert et al., 1989	$\sigma_p = 2.1592\ \rho_b + 0.234\ LK + 0.0360\ AWC$
	$+ 0.0770\ NAWC - 3.426$
	$\sigma_p = (3.0975\ \rho_b - 0.0475\ Cl - 0.0280U -$
	$- 0.9659 \log s + 0.3369\ LK - 0.0268\ \psi$
	$+ 2.1330 \log c + 0.0839)^2$
Raper & Erbach, 1990 a	$\varepsilon_v = \exp[(A + B\sigma_b)(1 - e^{-C\sigma_b})]-1$
Raper & Erbach, 1990 b	$\{\sigma\} = [c]\{\varepsilon\}$
Reinert, 1990	$\sigma_p = - 263 - 2.66\ S + 322\ \rho_{bi}$
Canarache, 1991	$\log RP = - 4.14 + 0.0858\ \rho_b - 0.000347\rho_b^2$
Lebert & Horn, 1991	$e = B + m \log \sigma$
	$\sigma_p = f(\phi, c, \rho_b, LK, AWC, NAWC, Kf, OC)$
Wlodek, 1991	$\rho_b = \rho_{bi}[z / (z + \Delta z)]$
Binger & Wells, 1992	Secondary compression curve
	$\rho_b = \rho_{bi}^* + m_s \log(\sigma / \sigma_k)$

Table 1 (cont'd).

	Virgin compression curve
	$\rho_b = \rho_{bk} + S_T (S_1 - S_k) + m \log (\sigma / \sigma_k)$
O'Sullivan, 1992	$\upsilon = \upsilon_r - m \ln (\sigma / \sigma_r) - b(\theta_m - \theta_{mr})$
McNabb & Boersma, 1993	$\ln \rho_b = \ln (\rho_{bi} \cdot \delta_i) - (A + B\sigma + J\delta_c) (1 - e^{-C\sigma})$
	$\delta_i = \rho_{bi} / \rho_{biavg}$
	$\delta_c = (\delta_i - 1) \rho_{bi}$

CHAPTER 1

SOIL COMPRESSIBILITY OF THREE GLACIAL SOILS IN RESPONSE TO TILLAGE AND WHEEL TRAFFIC

ABSTRACT

Field observations indicate soils managed under no-tillage are more easily trafficked than tilled soils. This study examined how changes in soil properties induced by tillage and wheel traffic impacted the compressive behavior of three Michigan soils. Intact soil cores, from track and between track positions in conventional moldboard or chisel plow (CT) and no-tillage (NT) treatments from the Kalamazoo loam (Fine loamy, mixed, mesic, Typic Hapludalfs), the Capac loam (Fine loamy, mixed, mesic, Aeric Ochraqualfs), and the Misteguay silty clay (Fine, mixed (calcareous), mesic, Aeric Haplaquepts) were equilibrated at four soil water contents and subjected to uniaxial confined compression tests over the range 25-1600 kPa of applied stresses. In general, NT shifted the compression curves down due to higher bulk densities, increased the preconsolidation pressure (σ_p) in the Capac loam and Kalamazoo loam soils but not in the Misteguay, and had little effect on the compression index (m) in any of the soils. Unconfined strength (US) of the Capac loam soil confirmed laboratory measurements of σ_p, with NT and wheel tracked soil

having higher US than CT. Wheel traffic also shifted the position of the compression curves, increased σ_p, and decreased m. NT treatment had a small effect but wheel traffic did more to decrease susceptibility of these soils to further compaction by decreasing m and increasing σ_p. Perceptions of increased trafficability of soils in NT relates not so much to tillage induced differences in soil physical properties but is due, primarily, to wheel traffic.

INTRODUCTION

In recent years, extremes in weather during critical periods, together with a move to conservation tillage systems, has renewed concern over soil compaction during field operations in agricultural soils. Also, farmers have reported that soils managed under no-tillage (NT) are more easily trafficked under high soil water content than tilled soils. Therefore, increasing soil strength could be an important advantage of NT treated soils for trafficability under high soil water content, for example, at harvest. In general, NT increases bulk density (ρ_b) and soil strength when compared with conventional tillage (Soane et al., 1982; Hill and Meza-Montalvo, 1990). However, there are few studies that have quantified the effects of long-term NT on soil compressibility.

Soil management under NT and conventional tillage (CT) has produced differences in soil physical properties (Pidgeon and Soane, 1977; Bauder et al., 1981) and quantitative measurements of those changes have been reported for a number of soils (Voorhees et al., 1978; Gupta et al, 1985; Culley and Larson, 1987; Horn, 1988; Johnson et al., 1989; Hill and Meza-Montalvo, 1990; Muller et al., 1990; Meek et al., 1992; Pierce et al., 1992; Pierce et al., 1994). However, few studies have considered changes in soil compressibility with changes in soil water content (Culley and Larson, 1987; Reinert, 1990; Kassa, 1992). Therefore, quantification of the effect of drying on soil compressibility remains to be determined (McNabb and Boersma, 1993).

The stress history of a soil greatly affects its compressive behavior (Culley and

Larson, 1987; Harris, 1971; Soane et al., 1982). However, soil compressibility is strongly regulated by soil water content and the concern over soil damage has focused mainly on soil behavior at high soil water content. Additionally, most soil compression measurements have been made on disturbed soil samples and at high soil water content (Bailey and VandenBerg, 1968; Larson and Gupta, 1980; Larson et al., 1980; Gupta et al., 1985; Grisso et al., 1987; Bailey and Johnson, 1989; O'Sullivan, 1992). Thus, some if not all may have had the stress history altered by the sieving process or by the high soil water content at which compression tests were conducted.

The purpose of this study was to examine how changes in soil properties induced by tillage and wheel traffic impacted the compressive behavior of different soils and the extent to which no-tillage and/or wheel traffic improves trafficability under high soil water conditions.

MATERIAL AND METHODS

Soils

Soil from experiments managed under long term NT and CT were sampled to characterize compressive behavior of three glacial soils in Michigan. Soils used in this study were: Kalamazoo loam (Fine loamy, mixed, mesic, Typic Hapludalfs) located at the Kellogg Biological Station (KBS), Hickory Corners, MI; Capac loam (Fine loamy, mixed, mesic, Aeric Ochraqualfs) located on the Michigan State University Agronomy Farm, East Lansing, MI; and Misteguay silty clay (fine, mixed (calcareous), mesic, Aeric Haplaquepts) located near Saginaw, MI. Prior to sampling, the experiments have been managed under NT for 13, 14, and 9 yr, respectively (Bronson, 1989; Pierce et al., 1994; Martinson, 1993; Xu, 1994). Conventional tillage consisted of fall moldboard plowing for the Capac loam and Misteguay silty clay soils and spring chisel plowing for the Kalamazoo loam soil, with secondary tillage in the spring consisting of one pass of a tandem disk and one pass of a harrow prior to planting for all three soils.

Soil sampling

For each soil, the NT and CT treatments were sampled in three transects perpendicular to crop rows, both in track (T) and between track (BT) positions, and at two depths, 0-3 cm and 15-18 cm. The soils were sampled on the following dates: the Capac loam on 25 August, 1992, the Kalamazoo loam on 18 August, 1992 and again on 7 May, 1993, and the Misteguay silty clay on 5 April, 1993, with all spring sampling occurring prior to any field operations. Four soil cores were taken at each position to allow for compression measurements at four gravimetric soil water contents (θ_m). Intact soil cores (6.35 cm diameter and 2.54 cm length) were sampled using a metal soil sampler containing rings of polyvinyl chloride (PVC) pipe placed within a cutting metal device with a bevelled cutting edge. The sampling device was pushed carefully into the soil using a falling weight. The ring filled with soil was removed from the metal device and the ends were trimmed to the dimension of the PVC ring. Soil cores were stored in plastic at 4 °C until compressibility tests were performed.

Disturbed soil samples were obtained near the intact soil cores, air dried and subjected to standardized test for plastic and liquid limits (Sowers, 1986), particle size analysis by the pipette method, and sand fractionation by sieving (Day, 1986). Bulk density was determined as dry soil weight per unit volume of the intact soil cores (Blake and Hartge, 1986). Total organic C and N were determined by dry combustion of 5 replicate samples of 50 mg on a Carlo Erba CHN analyzer Model 1104 (Carlo Erba Instruments, Milano, Italy).

Laboratory Compression Measurements

To achieve a range of θ_m, soil cores were saturated and equilibrated to a matric potential (ψ_m) equal to -6 kPa and -100 kPa on a ceramic plate inside a pressure chamber (Klute, 1986). For lower θ_m, soil cores were first equilibrated at a matric potential of -100 kPa and then air dried at room temperature until within the desired θ_m (0.07 to 0.10 and 0.03 to 0.07 kg kg^{-1} for Kalamazoo loam, 0.08 to 0.14 and 0.03 to 0.06 kg kg^{-1} for Capac loam, and 0.16 to 0.23 and 0.09 to 0.14 kg kg^{-1} for Misteguay silty clay).

Uniaxial compression tests were conducted according to Bowles (1986), using a pneumatic Brainard-Kilman consolidometer (2175 West Park Ct. Stone Mountain, GA). The strain measuring device uses a dial gage reading with 2.54 μm/division. The loads were applied until 90% of maximum deformation was reached. The 90% of maximum deformation was determined by drawing a straight line through the data points in the initial part of the curve obtained when dial readings were plotted versus

$\sqrt{}$time, until this line intercepts the y axis (dial readings). A second straight line was drawn from this intersection with all abscissas 1.15 times as large as corresponding values on the first line. The intersection of this second line and the laboratory curve is the point corresponding to 90% consolidation (Taylor, 1948 as cited by Holtz and Kovacs, 1981). After this condition was reached, a new successive stress was applied. Increasing stresses were applied in succession using an applied stress (σ) sequence of 25, 50, 100, 200, 400, 800, and 1600 kPa. The compression index (m) was computed as the slope of the virgin compression line plotted as ρ_b versus log σ (Bradford and Gupta, 1986). The preconsolidation pressure (σ_p) was estimated by the Casagrande (1936) procedure.

Field Unconfined Strength Measurements

Three replications of penetrometer measurements were made in the field weekly in 1993 over a 9-wk period (May, June, and July) for Capac loam soil, with measurements in track and between track positions of both tillage treatments. A pocket penetrometer (Soiltest model CL-700, 2205 Lee Street, Evaston, Illinois) was pushed into the soil until a reference mark was reached and the reading was recorded. θ_m were determined for each penetrometer reading by drying soil at 105°C for 24 hours.

Statistics

Regression equations were performed using the computer program Sigma Plot 1.02 (Jandel Scientific, P.O. Box 7005, San Rafael, CA) for ρ_b prior to compression tests, σ_p, m and θ_m. Intercepts and slopes of the regression equations of ρ_b prior to the compression test and preconsolidation pressure were compared using procedures of Snedecor and Cochran (1967).

RESULTS AND DISCUSSION

The compressibility of soil is a function of several soil factors, primarily soil water content, texture, structure, stress history, and initial ρ_b (Culley and Larson, 1987; Gupta and Allmaras, 1987; Gupta et al., 1987; Gupta et al., 1989; Horn, 1988; Larson et al., 1980). Therefore, soil physical properties of the three soils and the effects of tillage and traffic on the initial conditions prior to compression tests will be discussed first.

Initial Soil Properties

The Kalamazoo loam and Capac loam had similar particle size distribution, with clay contents between 90 to 110 g kg^{-1}, but the sand size distribution was coarser in the Kalamazoo loam than the Capac loam with geometric mean diameters 0.076 mm and 0.031 mm, respectively (Table 1). The Capac loam had higher OC and N, slightly higher consistency limits (Table 1), higher water holding capacity (Figure 1), and lower ρ_b at both depths (Table 2). ρ_b was similar between tillage systems but was higher in the wheel-track than between tracks (Table 2). Differences in soil physical properties between these two soils were related to differences in OC and associated differences in soil structure (Reinert, 1990; Pierce et al., 1994). Additionally, the surface 3 cm of all three soils had higher water holding capacities than the 15-18 cm depth, indicative of lower bulk density (Table 2) and higher OC.

The Misteguay silty clay had clay contents of 480 to 490 g kg^{-1}, with very little sand (50 g kg^{-1} Table 1), and had a high water holding capacity (Figure 1). The consistency limits of the Misteguay silty clay were more than double the other soils and the plastic index more than tripled (Table 1).

The initial ρ_b of the Misteguay silty clay, prior to the compression tests, decreased linearly as θ_m increased, although the strength of the regression varied with tillage and traffic condition (Table 3). This is in contrast with the Capac loam and Kalamazoo loam soils, for which ρ_b was invariant to θ_m. Tillage and wheel traffic shifted the regression curve either in the slope, in the intercept, or both, in the Misteguay silty clay soil. Statistical tests comparing the regression lines for different treatments and depths showed that the regression lines were parallel (equal slopes) with the exception that CTT had a higher slope than CTBT at 0-3 cm depth (Table 3). Therefore, shrinkage upon drying in the conventionally tilled Misteguay silty clay soil was greater in the wheel track. Differences in the intercept of the regression lines are indicative of soil compaction. In the 0-3 cm depth, the tracked soil (both NTT and CTT) had a higher ρ_b than between tracked (NTBT and CTBT) and the NTBT was more compact than CTBT. In the 15-18 cm depth, only the NTT was initially more compact than the untracked soil (both NTBT and CTBT). Therefore, not only did θ_m effect ρ_b in the Misteguay soil, stress history was also very important in determining this relationship.

Soil compression curves

Soil compression curves were obtained by plotting ρ_b versus applied stress (σ). The compression curve is comprised of two regions: a region of plastic and unrecoverable deformation called the virgin compression curve, and a region of small, elastic and recoverable deformation called the secondary compression curve. The slope of the virgin compression curve is called the compression index (m). The point that divides these two regions in a compression curve is the preconsolidation pressure (σ_p). These parameters define the soil compression curve and may change with soil type, initial θ_m, and management history (Culley and Larson, 1987; Larson et al., 1988).

Soil water content was the major factor regulating the compressive behavior of these soils (Figure 2). Larson et al. (1980) reported that as initial θ_m increases, soil compression curves are generally displaced down and to the left in a parallel manner, indicating an increase in susceptibility of soil to compaction with increasing θ_m. This shift in the compression curves with increasing θ_m was true for both the Capac loam (Figure 2) and Kalamazoo loam (data not shown). The shift in the compression curves for the Misteguay silty clay was reversed (Figure 2). This appeared to be related to moisture effects on initial ρ_b as the Misteguay silty clay soil shrinks upon drying (Table 3). This apparent paradox was resolved when the curves were normalized (ρ_b at each stress was divided by initial ρ_b prior to compression test). When normalized, compression curves for the Misteguay silty clay soil conformed to the same pattern of shifting down and to left as θ_m increased.

The virgin compression curves for these soils were not parallel, as reported by Larson et al. (1980). The non-parallel nature of the virgin compression curves were apparently here due to the broad range of θ_m measured compared to the moisture range measured by Larson et al. (1980). This is consistent with Schmertmann (1955), who reported that compression curves intersect within a narrow range of void ratio, with an average estimate of 0.42 of the initial void ratio reasonable for most clays. For these soils, m was a function of θ_m, but the form of the relationship varied with soil type. For the Capac loam and Misteguay silty clay soils, the general relationship between m and θ_m followed

$$m = a + b\,\theta_m + c\,\theta_m^2 \qquad [1]$$

with R^2 ranging from 0.26 to 0.61, with higher R^2 for the 0-15 cm depth (Figure 3 and 4 and Table 4). The m was lower for tracked than between tracked soil in the 0-3 cm depth but not in the 15-18 cm depth and m_{max} occurred at θ_m near the plastic limit. For the Kalamazoo loam, m decreased linearly with increasing θ_m for the 0-3 cm depth regardless of wheel traffic (R^2 =0.37), but showed little change with θ_m at the 15-18 cm depth (Figure 4). While the relationships between m and θ_m are weak, and we do not understand why the behavior is different for the Kalamazoo loam, the change in m with θ_m has important implications in predicting the amount of deformation per applied stress that will occur in the virgin compression curve.

These soils, however, exhibited a strong dependence of stress history on θ_m. At -6 kPa ψ_m, the compression curves showed little stress history (slight curvature at low applied stress as indicated by a significant fit of the second order polynomial) (Figure 5a). This relates to the fact that θ_m was near the liquid limit for Capac loam, Kalamazoo loam, and Misteguay silty clay (0.25, 0.22, and 0.53 kg kg^{-1}, respectively), where the stress bearing capacity is limited. Note that the curves for the three soils are nearly parallel, indicating a similar deformation for a given applied stress. At -100 kPa ψ_m, θ_m was near the plastic limit for Capac loam, Kalamazoo loam, and Misteguay silty clay (0.17, 0.15, and 0.26 kg kg^{-1}, respectively). The compression curves clearly show the presence of a stress history (curvature at low applied stress), although this was less so for the Misteguay silty clay than the other soils (Figure 5b). Therefore, less deformation is expected at -100 kPa ψ_m at low applied stress due to the presence of stress history, but higher deformation at higher applied stresses due to higher m. In the Capac loam and Misteguay silty clay soils, CTBT and NTBT treatments exhibited a similar compression behavior at -100 kPa ψ_m i.e., the two curves were similar for the Capac loam and parallel for the Misteguay silty clay (Figure 6). In the Kalamazoo loam, the NTBT had a higher initial ρ_b than the CTBT but lower deformation (curves cross). The effects of tillage were similar at other θ_m. Thus, although NTBT had the same load carrying capacity (similar σ_p) as CTBT in the Kalamazoo loam, the NTBT had lower deformation than CTBT at applied stress > σ_p. θ_m, therefore, affects both σ_p and m, and thus regulates the shape of the compression curve.

Overall, as illustrated in Figure 7, σ_p decreases as a function of increasing θ_m, following the relationship

$$\sigma_p = 10^{(a + b\theta m)} \qquad [2]$$

The coefficients varied with soil, tillage, and wheel traffic, with R^2 ranging from 0.83 to 0.98 (Table 5). Tillage and wheel traffic influenced the relationships between σ_p and θ_m (Table 5). For example, NTT was often different from CTBT but not different from either CTT or NTBT (Figure 7). In the Capac loam and Kalamazoo loam, the NTT could sustain a higher stress than the other treatments while in the Misteguay at high θ_m, this was true for CTT, although NTT was greater than NTBT. A clear difference did not exist between wheel track and no wheel track for Misteguay silty clay soil.

Based on the relationships in Equations [1] and [2], at high soil moisture, σ_p is unimportant when the soil is near the liquid limit and m is moderate, therefore, deformation is not at a maximum. As the soil drains, σ_p increases only slightly, but since the soil must increasingly support more of the applied stress, m increases and deformation increases. As further drying takes place, σ_p increases exponentially and the soil can support considerable loads without further deformation.

Field measurements

Field penetrometer measurements for the Capac loam showed that unconfined strength (US) increased exponentially with decreasing θ_m (Figure 8). The form of this relationship is consistent with that between σ_p and θ_m measured in the laboratory (Figure 7). As was the case with σ_p, NTT had the highest US and CTBT the lowest. The NTBT was intermediate but approximately parallel to CTBT and CTT is the same as NTBT, which upon careful inspection of Figure 7 and Table 5, is also consistent with the laboratory measurements. At the plastic limit, the NTT soil strength values were five times greater than for CTBT. Therefore, field data support conclusions from laboratory measurements.

SUMMARY

Changes in soil properties induced by tillage and wheel traffic affected the compressive behavior of these three soils. θ_m regulated the shape of the curve while initial bulk density ρ_b regulated its position. The initial ρ_b of the Misteguay silty clay, and subsequently the compressive behavior, was greatly affected by θ_m, and required a normalization of the compression curves to fit the generalized relationship of shifts in soil compression curves with changes in θ_m. In general, no-tillage shifted the compression curves, increased σ_p in the Capac loam and Kalamazoo loam soils but not in the Misteguay, and had little effect on m in any of the soils. No-tillage also had higher field measured unconfined strength than CT in the Capac loam soil. Wheel traffic shifted the position of the compression curves, due to their influence on initial conditions, increased σ_p, and decreased m. These shifts would support the notion of improved trafficability on no-tilled and trafficked soils. No-tillage had some effect but wheel traffic did more to decrease susceptibility of these soils to further compaction by decreasing m and increasing σ_p. Specifically, wheel traffic in no-tillage (NTT) had a higher σ_p in the Capac loam and Kalamazoo loam soil, although CTT was higher in the Misteguay silty clay soil. The perception of increased trafficability of soils in no-tillage, as reported by farmers, relates not so much to tillage induced differences in soil physical properties but is primarily due to wheel traffic effects and the fact that controlled traffic is likely in long-term NT. Additionally, soils that dry faster would support higher loads earlier. Therefore, farmers must not only consider the adoption of controlled traffic patterns to reduce overall soil compaction but should focus mainly on the enhanced resistance due to soil drying.

LIST OF REFERENCES

Bailey, A.C. and C.E. Johnson. 1989. A soil compaction model for cylindrical stress state. Trans. ASAE. 32:822-825.

Bailey, A.C., and G.E. VandenBerg. 1968. Yielding by compaction and shear in unsaturated soils. Trans. ASAE. 11:307-311,317.

Bauder, J.W., G.W. Randall, and J.B. Swan. 1981. Effect of four continuous tillage systems on mechanical impedance of a clay loam soil. Soil Sci. Soc. Am. J. 45:802-806.

Blake, G.R. and K.H. Hartge. 1986. Bulk density. p. 363-375. *In* A. Klute (ed.) Methods of soil analysis. Part 1. 2nd ed. Agron. Monogr. 9. ASA, Madison, WI.

Blackwell, P.S., and B.D. Soane. 1981. A method of predicting bulk density changes in field soils resulting from compaction by agricultural traffic. J. Soil Sci. 32:51-65.

Bradford, J.M and S.C. Gupta. 1986. Compressibility. p. 479-492. *In* A. Klute (ed.) Methods of soil analysis. Part 1. 2nd ed. Agron. Monogr. 9. ASA, Madison, WI.

Bowles, J.A. 1986. Engineering properties of soils and their measurements. Third edition. McGraw-Hill Book Company, Inc., NY.

Bronson, J.A. 1989. The effect of tillage system on corn production and soil properties on a Kalamazoo loam. MS Thesis. Michigan State University. East Lansing.

Casagrande, A. 1936. The determination of the pre-consolidation load and its practical significance. 3:60-64. *In* Int. Conf. on Soil Mech. and Foundation Eng. Proc. of the First ICSMFE. Cambridge, Mass. June 22-26,1936. Cambridge, Mass.

Culley, J.L.B., and W.E. Larson. 1987. Susceptibility to compression of a clay loam Haplaquoll. Soil Sci. Soc. Am. J. 51:562-567.

Day, P.R. 1986. Particle fractionation and particle size analysis. p. 545-567. *In* A. Klute (ed.) Methods of soil analysis. Part 1. 2nd ed. Agron. Monogr. 9. ASA, Madison, WI.

Grisso, R.D., C.E. Johnson, and A.C. Bailey, 1987. Soil compaction by continuous deviatoric stress. Trans. ASAE. 30:1293-1301.

Gupta, S.C., and R.R. Allmaras. 1987. Models to access the susceptibility of soil to excessive compaction. Adv. Soil Sci. 6:65-100.

Gupta, S.C., A. Hadas, and R.L. Schafer. 1989. Modeling soil mechanical behavior during compaction. p. 137-152. *In* W.E. Larson, G.R. Blake, R.R. Allmaras, W.B. Voorhees and S.C. Gupta (eds.). Mechanics and related process in structured agricultural soils. Kluwer Academic Publishers, The Netherlands.

Gupta, S.C., A. Hadas, W.B. Voorhees, D. Wolf, W.E. Larson, and E.C. Schneider. 1985. Development of quids for estimating the ease of compaction of world soils. Research Report, Binational Agric. Res. Development, Bet Dagan, Israel. University of Minnesota. USA.

Gupta, S.C., E.C. Schneider, W.E. Larson, and A. Hadas. 1987. Influence of corn residue on compression and compaction behavior of soils. Soil Sci. Soc. Am. J. 51:207-212.

Harris, W.L. 1971. The soil compaction process. p. 9-44 *In* K.K. Barnes, W.M. Carleton, H.M. Taylor, R.L. Throckmorton, and G.E. Vanden Berger.(eds.). Compaction of Agricultural Soils. Am. Soc. Agric. Eng., St. Joseph, MI.

Hill, R.L., and M. Meza-Montalvo. 1990. Long- term wheel traffic effects on soil physical properties under different tillage systems. Soil Sci. Soc. Am. J. 54:865-870.

Holtz, R.D., and W.D. Kovacs. 1981. An introduction to geotechnical engineering. Prentice-Hall, Inc., Englewood Cliffs, NJ.

Horn, R. 1988. Compressibility of arable land. Catena Sup. 11:53-71.

Johnson, B.S., A.E. Erickson, and W.B. Voorhees. 1989. Physical conditions of lake plain soil as affected by tillage and wheel traffic. Soil Sci. Soc. Am. J. 53:1545-1551.

Kassa, Z. 1992. Pore water pressure and some associated mechanical responses to uniaxial stress in structured agricultural soil. MS thesis. University of Minnesota.

Klute, A. 1986. Water retention: laboratory methods. p. 635-662. *In* A. Klute (ed.) Methods of soil analysis. Part 1. 2 nd ed. Agron. Monog. 9. ASA, Madison, WI.

Larson, W.E., and S.C. Gupta. 1980. Estimating critical stress in unsaturated soils from changes in pore water pressure during confined compression. Soil Sci. Soc. Am. J. 44:1127-1132.

Larson, W.E., S.C. Gupta, and J.L.B. Culley. 1988. Changes in bulk density and pore water pressure during soil compaction. Catena Sup. 11:123-128.

Larson, W.E., S.C. Gupta, and R.A. Useche. 1980. Compression of agricultural soils from eight soil orders. Soil Sci. Am. J. 44:450-457.

Martinson, O. K. 1993. N dynamics in and under a fixing dry bean using ^{15}N as tracer. MS. Thesis, Michigan State University.

McNabb, D.H., and L. Boersma. 1993. Evaluation of the relationship between compressibility and shear strength of Andisols. Soil Sci. Am. J. 57:923-929.

Meek, B.D., E.R. Rechel, L.M. Carter, and W.R. DeTar. 1992. Bulk density of a sandy loam: traffic, tillage, and irrigation-methods effects. Soil Sci. Soc. Am. J. 56:562-565.

Muller, L., P. Tille, and H. Krestschmer. 1990. Trafficability and workability of alluvial clay soils in response to drainage. Soil Tillage Res. 16:273-287.

O'Sullivan, M.F. 1992. Uniaxial compaction effects on soil physical properties in relation to soil type and cultivation. Soil Tillage Res. 24:275-286.

Pidgeon, J.D. and B.D. Soane. 1977. Effect of tillage and direct drilling on soil properties during the growing season in a long-term barley monoculture system. J. Agric. Sci. 88:431-442.

Pierce, F.J., M.C. Fortin, and M.J. Staton. 1992. Immediate and residual effects of zone-tillage in rotation with no-tillage on soil physical properties and corn performance. Soil Tillage Res. 24:149-165.

Reinert, D.J. 1990. Soil structural form and stability induced by tillage in a Typic Hapludalf. Ph.D diss. Michigan State Univ. East Lansing.

Snedecor, G.W. and Cochran. 1967. Statistical methods. Sixth edition. The Iowa State University Press, Ames, Iowa.

Soane, B.D., J.W. DicKson, and D.J. Campbell. 1982. Compaction by agricultural vehicles: a review III. Incidence and control of compaction in crop production. Soil Tillage Res. 2:3-36.

Sowers, G.F. 1986. Consistency. p. 391-399. *In* A. Klute (ed.) Methods of soil analysis. Part 1. 2nd ed. Agron. Monogr. 9. ASA, Madison, WI.

Voorhees, W.B., C.G. Senst, and W.W. Nelson. 1978. Compaction and soil structure modification by wheel traffic in the Northern Corn Belt. Soil Sci. Soc. Am. J. 42:344-349.

Xu, Chuanguo. 1994. Conservation tillage, chemical input, and manure history in regulating corn (*Zea mays* L.) and soybean (*Glycine max* (L). Merr.) production and fate of nitrogen in soil. Ph. D. diss., Michigan State University.

Table 1. Soil properties of the Capac loam, Kalamazoo loam and Misteguay silty clay soils averaged across treatments.

Soil	LL†	PL	PI	OC	N	Clay	Silt	Sand	GMD
	(kg kg^{-1})			(g kg^{-1})					(mm)
				0-3cm					
Capac	0.25	0.17	0.08	17	1.6	110	340	550	0.076
Kalamazoo	0.22	0.15	0.07	11	1.1	90	350	560	0.032
Misteguay	0.53	0.26	0.27	31	2.1	480	470	50	-----
n‡	4	12	4	20	20	12	12	12	3
				15-18cm					
Capac	0.25	0.17	0.08	17	1.5	100	350	550	0.076
Kalamazoo	0.21	0.13	0.08	7	0.8	100	350	550	0.031
Misteguay	0.53	0.26	0.27	30	1.9	490	460	50	-----
n	4	12	4	19	19	12	12	12	3

†LL = Liquid limit, PL = Plastic limit, PI = Plasticity index, OC = Organic carbon, N = Nitrogen, GMD = geometric mean diameter of sand particles.
‡n for LL and PI consisted of 1 measure for each treatment while 3 replications were measured for each treatment for the other parameters.

Table 2. Bulk density prior to compression test for the Capac loam, and Kalamazoo loam soils.

Soil	Bulk Density (Mg m^{-3})			
	NTT†	CTT	NTBT	CTBT
		0 - 3 cm		
Capac	1.47±0.02‡	1.57±0.02	1.38±0.01	1.37±0.02
Kalamazoo	1.55±0.03	1.50±0.03	1.49±0.02	1.47±0.03
		15 - 18 cm		
Capac	1.53±0.01	1.57±0.02	1.50±0.02	1.48±0.01
Kalamazoo	1.64±0.03	1.64±0.01	1.63±0.02	1.66±0.02

† NTT = No tillage in the track, CTT = Conventional tillage in the track, NTBT = No tillage between tracks, CTBT = Conventional tillage between tracks.
‡ mean ± standard error of the mean. Each value represents an average of 12 measurements.

Table 3. Coefficients of the regression of bulk density (ρ_b) on soil water content (θ_m) prior to compression test for the Misteguay silty clay using the regression model ($\rho_b = a + b\ \theta_m$).

Tillage/traffic	Intercept (a)	slope (b)	R^2
		0 - 3 cm	
NTT†	1.77 a	- 1.29 ab	0.60
CTT	1.90 a	- 1.68 a	0.84
NTBT	1.69 b	- 1.35 ab	0.66
CTBT	1.47 c	- 0.85 b	0.66
		15 - 18 cm	
NT	2.10 a‡	- 2.09 a	0.96
CTT	1.96 ab	- 1.64 a	0.82
NTBT	2.01 b	- 1.94 a	0.97
CTBT	1.98 b	- 1.78 a	0.94

Coefficients followed by the same letter are not significantly different at $p = 0.05$.
† NTT = No tillage in the track, CTT = Conventional tillage in the track, NTBT = No tillage between tracks, CTBT = Conventional tillage between tracks.
‡ The NTT was not significantly different from CTT due to higher variation at CTT ($R^2 = 0.82$).
n = 16 for each regression.

Table 4. Comparison of regression equations of the form ($m = a + b\theta_m + c\theta_m^2$) for compression index (m) and soil water content (θ_m) for Capac loam, and Misteguay silty clay.

Depth (cm)	Tillage/Traffic	a	b	c	R^2	θ_{mmax} ($kgkg^{-1}$)	m_{max} (Mgm^{-3})	n
				Capac loam				
0-3	T†	0.08	2.63	- 7.78	0.49	0.17	0.30	24
	BT	0.26	1.75	- 7.03	0.32	0.13	0.37	24
15-18	All	0.08	3.61	-12.59	0.45	0.14	0.34	48
				Misteguay silty clay				
0-3	T	-0.16	3.53	- 7.46	0.28	0.24	0.26	24
	BT	0.14	1.98	- 4.17	0.26	0.24	0.38	24
15-18	All	0.02	1.04	- 1.26	0.61	0.41	0.23	48

† T = Track, BT = Between tracks, All = Track and between tracks combined together.

Table 5. Comparison of regression equations of the form ($\sigma_p = 10^{(a + b\,\theta_m)}$) for preconsolidation pressure (σ_p) and soil water content (θ_m) for Capac loam, Kalamazoo loam, and Misteguay silty clay.

Tillage/Traffic	Intercept (a)	Slope (b)	R^2	Intercept (a)	Slope (b)	R^2
			Capac loam			
	0 - 3 cm			15 - 18 cm		
NTT†	2.90 d	- 3.23 c	0.92	2.97 e	- 3.30 c	0.95
CTT	2.92 c	- 4.11 d	0.98	3.01 d	- 4.13 d	0.98
NTBT	2.87 c	- 3.96 cd	0.94	3.07 cd	- 4.86 de	0.95
CTBT	2.80 e	- 4.30 d	0.94	3.17 c	- 6.08 e	0.95
			Kalamazoo loam			
NTT	2.94 d	- 4.96 c	0.93	3.07 d	- 5.59 c	0.95
CTT	2.96 c	- 7.36 d	0.89	3.12 c	- 7.04 cd	0.88
NTBT	2.76 c	- 5.06 c	0.89	3.05 c	- 6.29 c	0.97
CTBT	2.90 c e	- 6.94 d	0.93	3.15 c	- 7.86 d	0.95
			Misteguay silty clay			
NTT	3.15 d	- 3.56 d	0.91	2.97 d	- 1.82 c	0.88
CTT	2.95 d	- 1.86 c	0.90	2.90 c	- 1.77 c	0.96
NTBT	3.32 c	- 4.86 e	0.93	3.11 c e	- 2.84 de	0.83
CTBT	3.04 d	- 2.97 d	0.91	2.91 e	- 2.08 c e	0.98

Coefficients followed by the same letter are not significantly different at $p = 0.05$.
† NTT = No tillage in the track, CTT = Conventional tillage in the track, NTBT = No tillage between tracks, CTBT = Conventional tillage between tracks.
n = 16 for each regression.

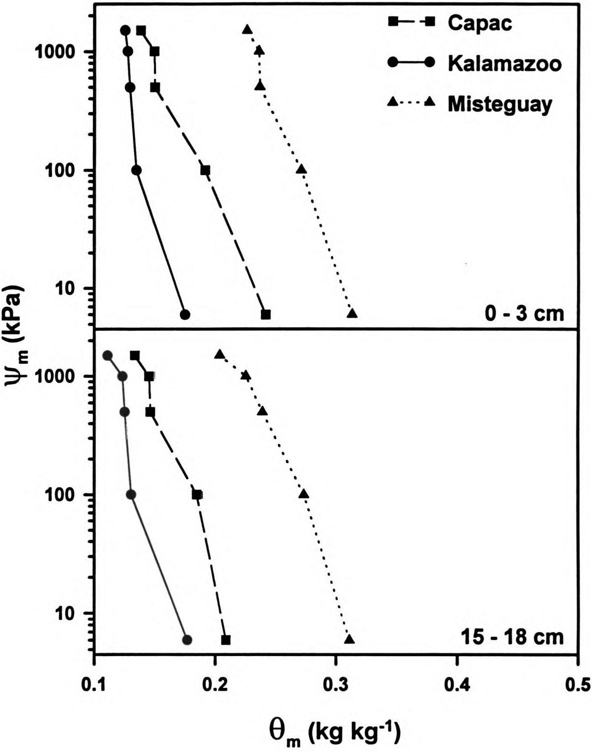

Figure 1. Soil water characteristic curves for the Capac loam, Kalamazoo loam, and Misteguay silty clay soils at 0-3 cm and 15-18 cm depths for the NTBT treatment.

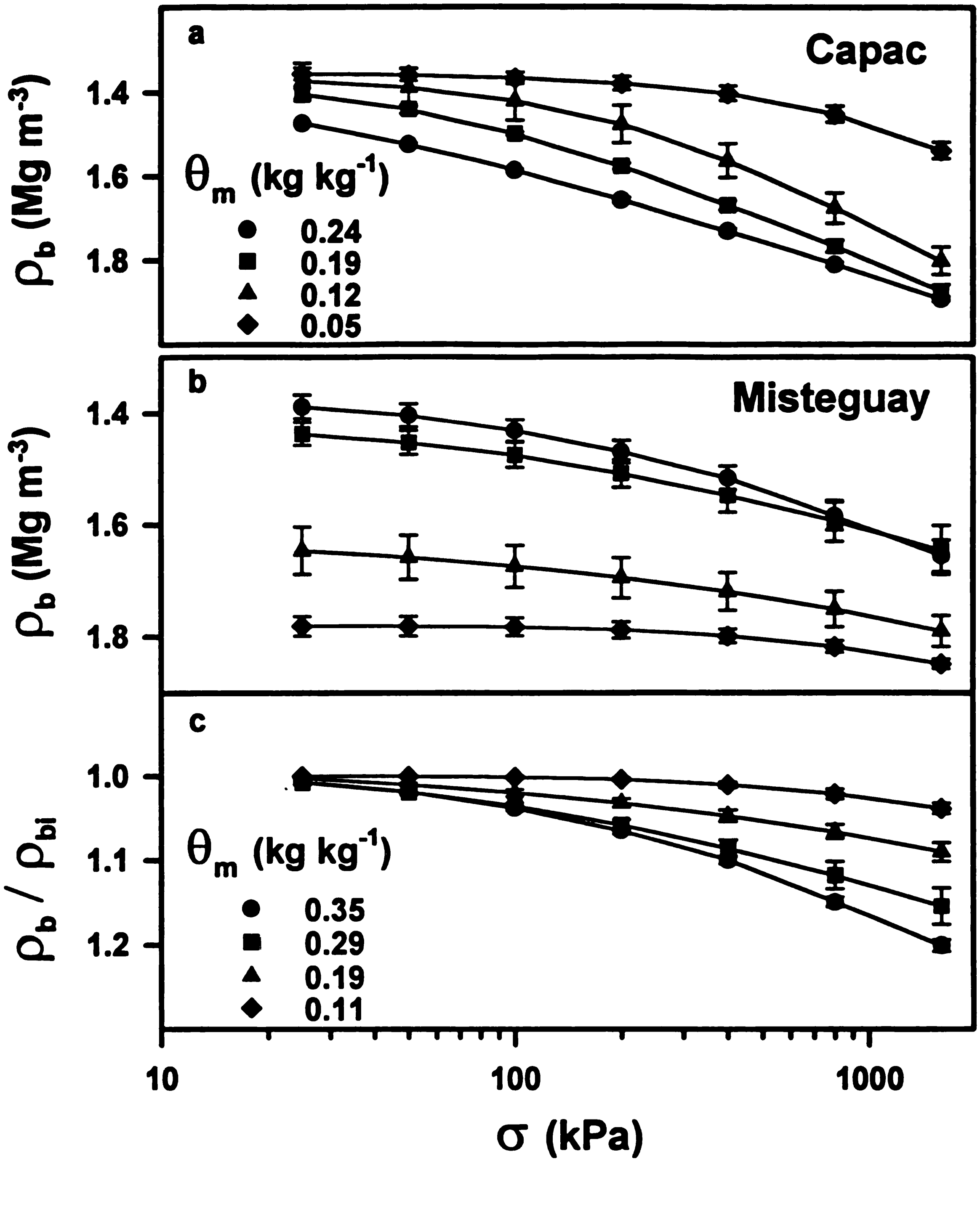

Figure 2. Soil compression curves for the Capac loam, and Misteguay silty clay soils and normalized compression curves for the Misteguay soils as affected by water content (θ_m). (Error bars represent the standard error of the mean; error bars for some points are masked by symbols due to very small std error values).

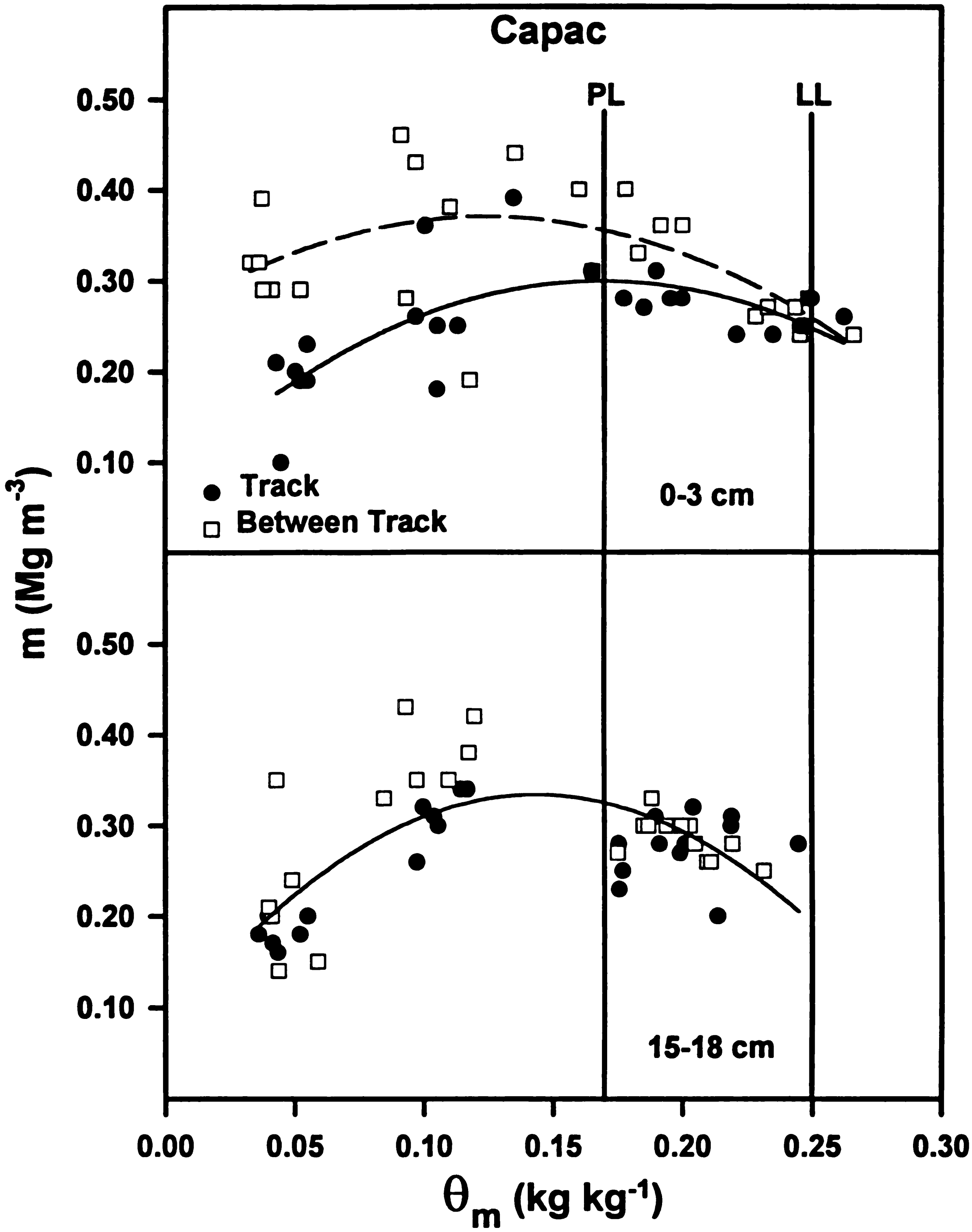

Figure 3. The relationship between the compression index (m) and soil water content (θ_m) for Capac loam for the 0-3 cm and 15-18 cm depths.

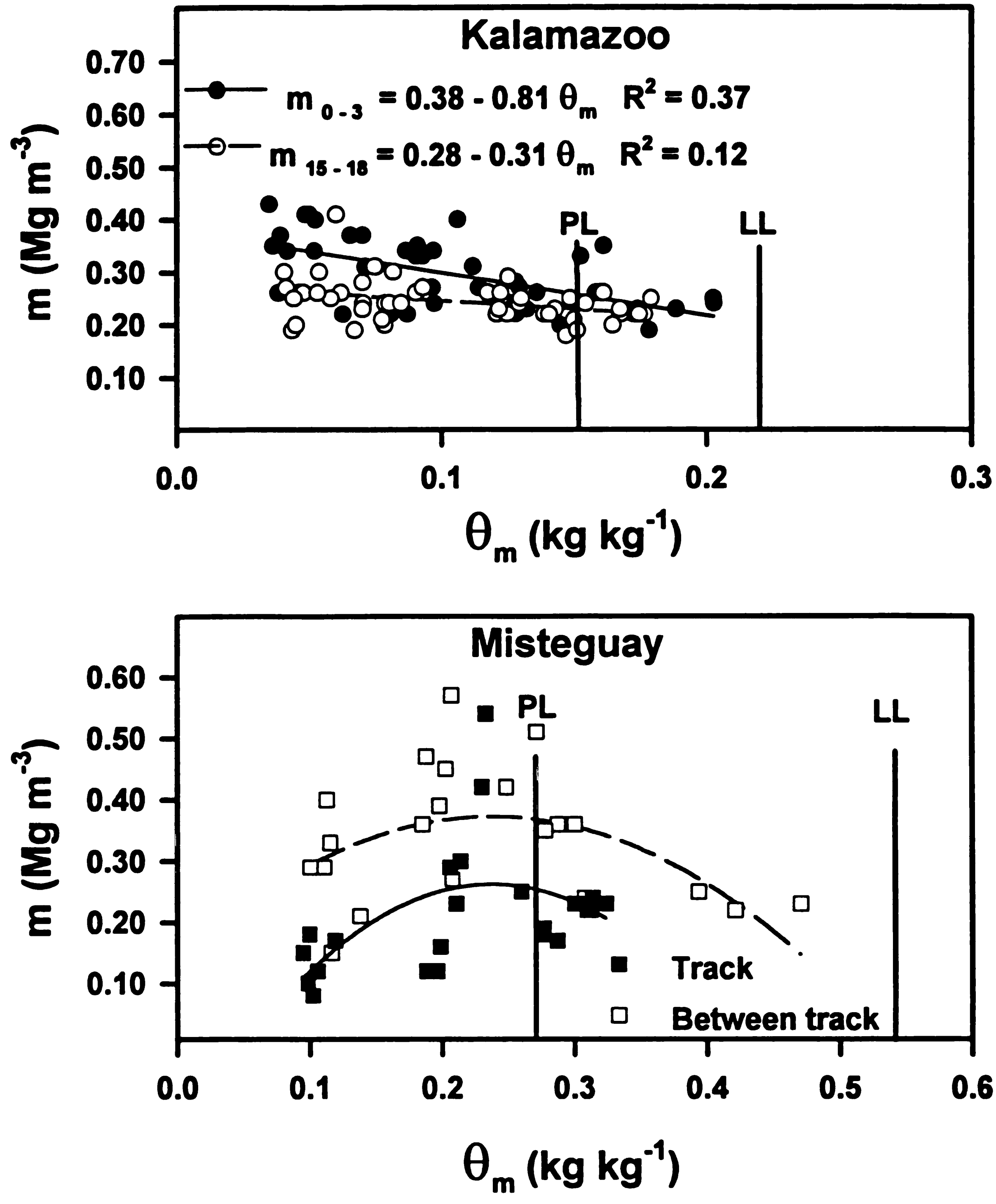

Figure 4. The relationship between the compression index (m) and soil water content (θ_m) for the Kalamazoo loam and Misteguay silty clay for the 0-3 cm depth.

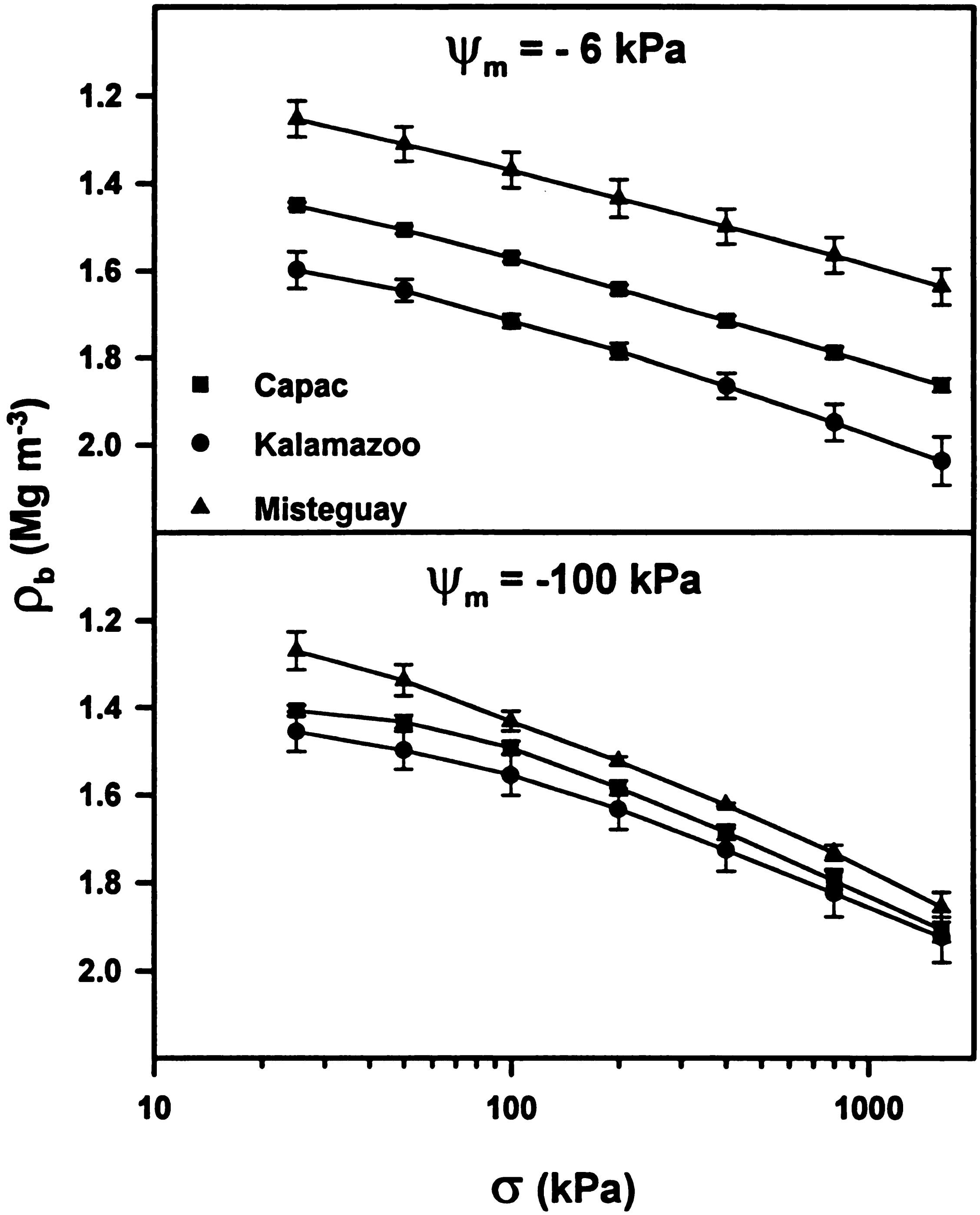

Figure 5. Compression curves at - 6 kPa and - 100 kPa matric potential (ψ_m) for Capac loam, Kalamazoo loam, and Misteguay silty clay soils under CTBT treatments at 0-3 cm depth. (Error bars represent the standard error of the mean; error bars for some points are masked by symbols due to small std error).

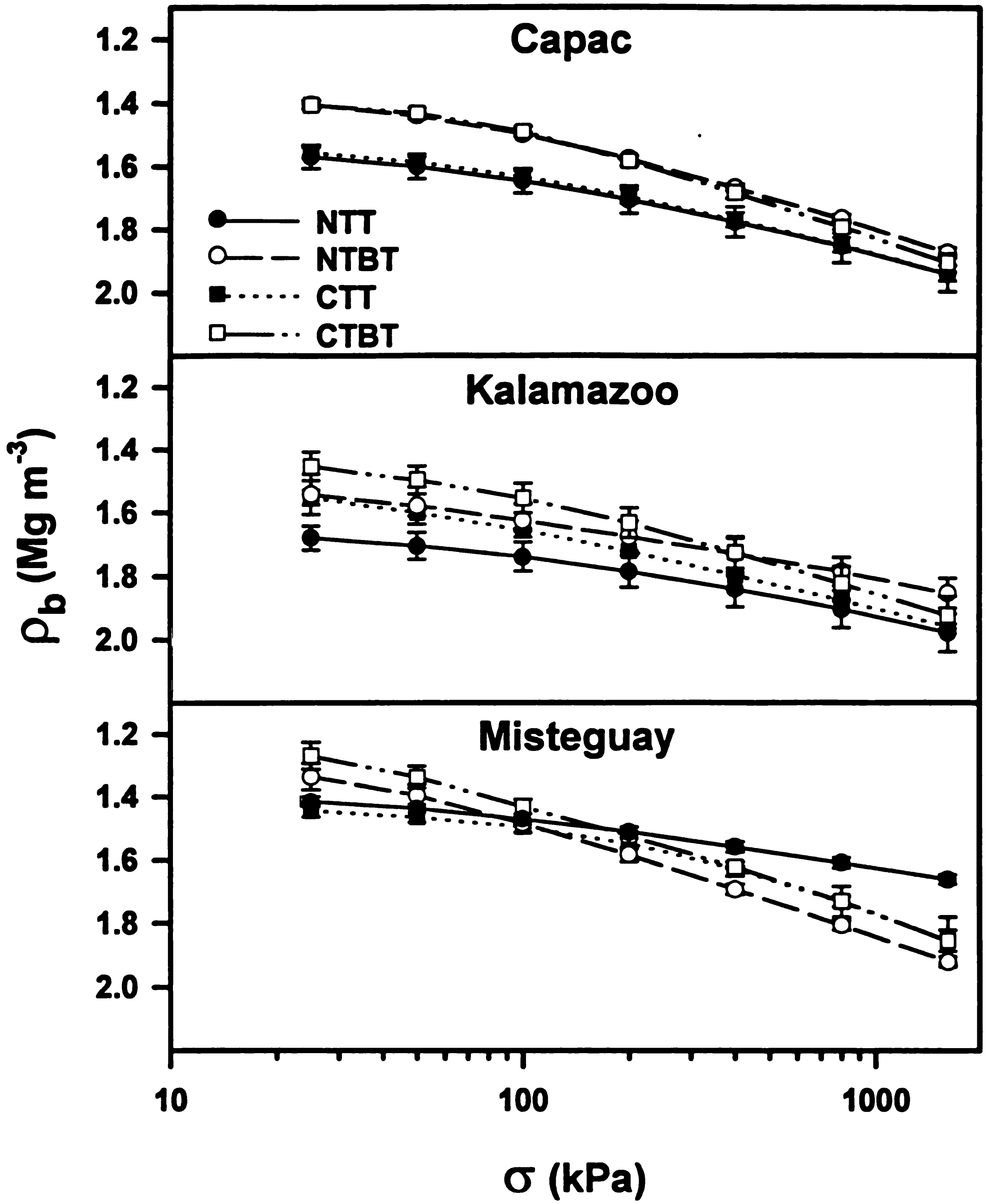

Figure 6. Compression curves at - 100 kPa matric potential (ψ_m) for Capac loam, Kalamazoo loam, and Misteguay silty clay soils under different tillage treatments at 0-3 cm depth. (Error bars represent the standard error of the mean; error bars for some points are masked by symbols due to small std error)

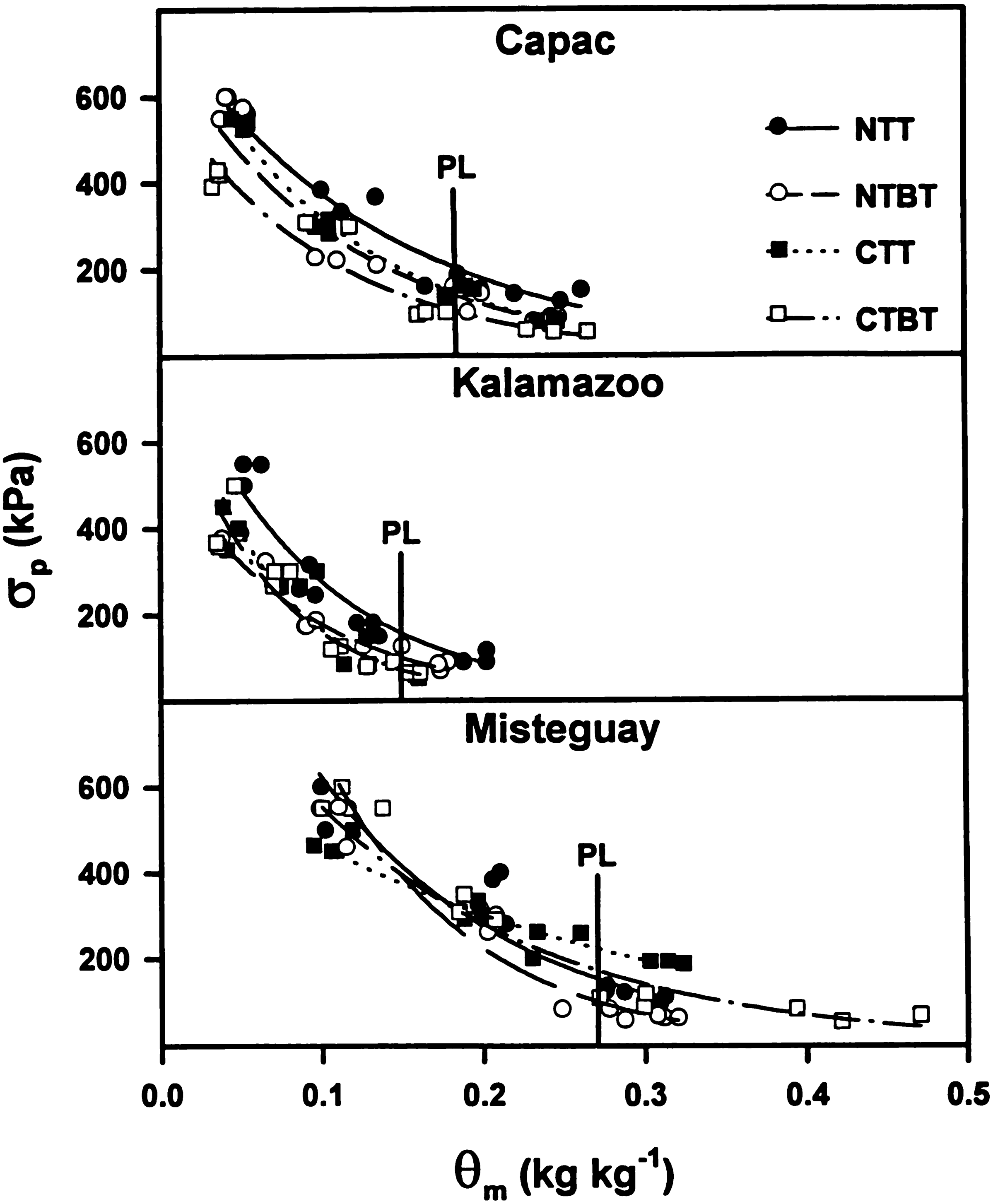

Figure 7. The relationship between the preconsolidation pressure (σ_p) and soil water content (θ_m) for the Capac loam, Kalamazoo loam, and Misteguay silty clay soils for the 0-3 cm depth for different tillage and traffic positions.

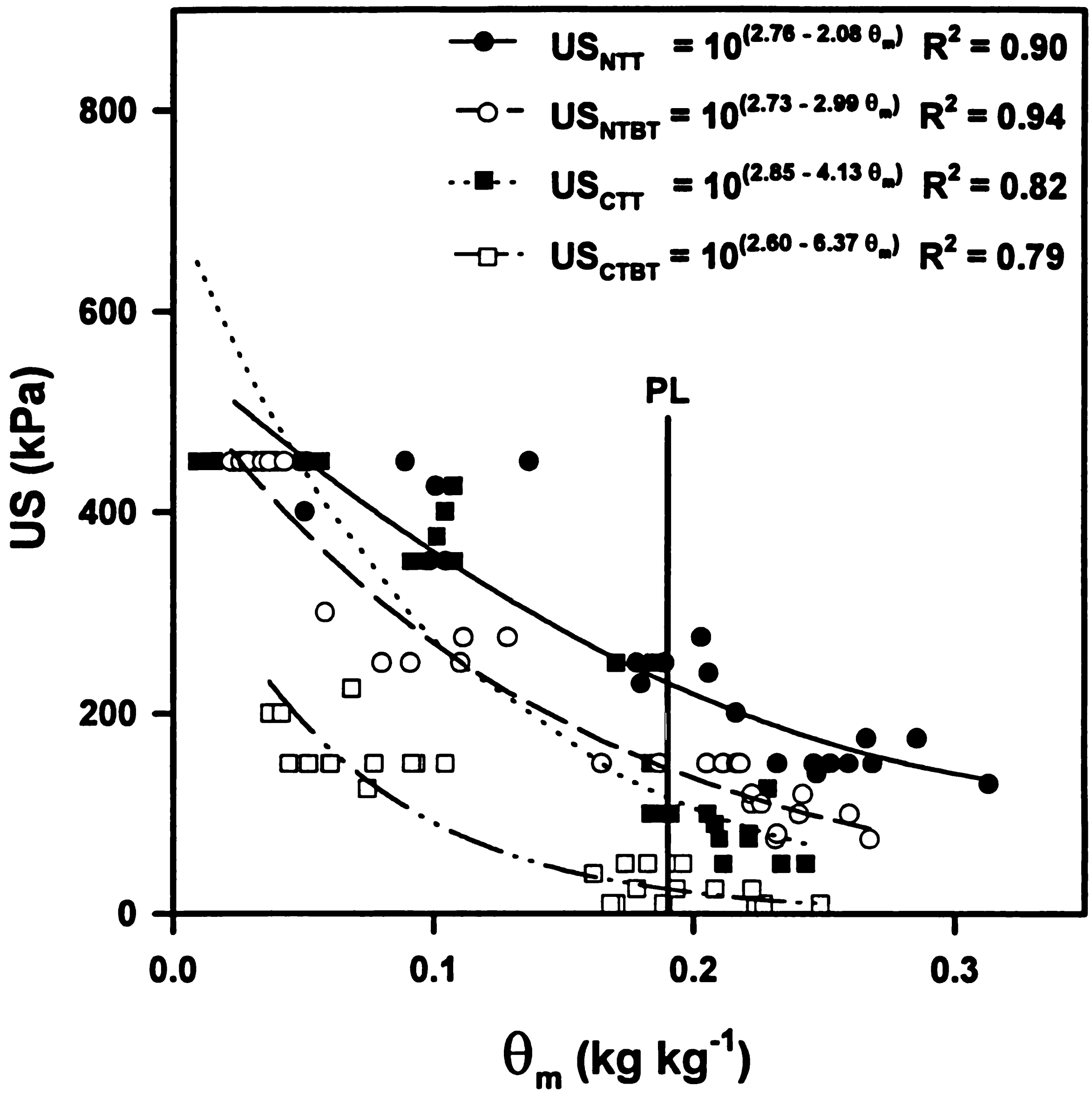

Figure 8. Unconfined strength (US) as a function of soil water content (θ_m) for the Capac loam for the 0-3 cm depth for different tillage and traffic positions.

CHAPTER 2

ACCOUNTING FOR STRESS HISTORY IN MODELING SOIL COMPACTION

ABSTRACT

While much is known about the soil compaction process, current models do not predict soil compressibility since they do not account for stress history and are not linked to the field measurements. This study proposes a model of soil compressibility, consisting of a stress history submodel that describes elastic, recoverable deformation combined with a classical virgin compression submodel that describes the plastic, unrecoverable deformation. The stress history model relates preconsolidation pressure (σ_p) as a function of soil water content (θ_m) as $\sigma_p = 10^{(a + b\theta m)}$. The virgin compression model takes the form $\rho_{bfinal} = \rho_b + m \log (\sigma_{final}/\sigma)$, where ρ_b is bulk density and σ is applied stress, and m is the compression index modeled as a function of θ_m as $m = c + d\theta_m + e\theta_m^2$. The stress history model predicted both σ_p and $\log_{10} \sigma_c$ reasonably well ($R^2 = 0.84$ and 0.86) and ($R^2 = 0.78$ and 0.89), respectively, for the data reported in the literature, where σ_c is the critical stress. Field unconfined stress (US) measurements followed the stress history model and were linearly related to σ_p ($R^2 > 0.98$). A procedure was proposed to construct field soil compression curves using field measurements of US,

ρ, and θ_m in conjunction σ_p, m, and σ_c determined from laboratory measured soil compression curves. It was also shown that σ_p is a good predictor of reported critical strengths at which root elongation ceases. This study quantifies the importance of stress history in modeling soil compaction and has immediate application in estimating soil workability or trafficability.

INTRODUCTION

A critical concern with soil compaction is the determination of when the soil is too wet to till or traffic and what damage will occur to soil when applied stresses exceed the carrying capacity of the soil. The soil compression curve is the basis for such an understanding. While much is known about the compaction process (Barnes et al., 1971; Gupta and Allmaras, 1987; Gupta et al., 1989), there are no studies that have quantified the effect of drying on soil compressibility (McNabb and Boersma, 1993), particularly under field conditions. A soil based emphasis on modeling soil compaction is the virgin compression curve which, by definition, defines plastic, unrecoverable deformation, and is generally well described (Larson and Gupta, 1980; Gupta et al., 1985; Horn, 1989). However, a soil is too wet and /or the stress excessive if plastic deformation occurs. It is the region of elastic, recoverable deformation (the secondary compression curve) within which a soil can be tilled or trafficked without serious damage. It is this component of the soil compression curve that reflects the stress history of soil and it is neglected in agriculture. By 'stress history' we mean that a soil has preserved, within its structure, remnants of previous stresses and other changes it has experienced in the past that give it the ability to sustain some level of stress without structural breakdown. Thus, a model that predicts the maximum stress that a soil can withstand over a range of water contents without causing soil compaction is very useful. Such a model will provide information to whether a soil can be tilled or trafficked without soil damage.

In general, five different approaches have been used as the basis for modeling the compression behavior of a soil: (1) the virgin compression curve (Soehne, 1958; Bailey and VandenBerg, 1968; Bowen, 1975; Larson et al.,1980; Lebert and Horn, 1991; Bingner and Well, 1992), (2) the critical stress (Larson and Gupta, 1980; Gupta and Larson, 1982; Gupta et al. 1985); (3) the relationship between strain and applied stress during triaxial tests (Bailey et al., 1984; Bailey et al., 1985; Bailey et al., 1986; Grisso et al.,1987; Bailey and Johnson, 1989); (4) a finite element analysis (Perumpral et al, 1971; Coleman and Perumpral, 1974; Pollock, Jr. et al. 1986; Gassman et al., 1989; Raper and Erbach, 1990 a; Raper and Erbach, 1990 b); and (5) generalized curve fitting techniques (Blackwell and Soane, 1981; Howard et al; 1981; Leeson and Campbell, 1983; Angers et al, 1987, Lebert et al., 1989; Canarache, 1991; Lebert and Horn, 1991). None of these models account for the stress history of the soil, although Lebert et al. (1989) and Lebert and Horn (1991) predict the preconsolidation pressure (σ_p) from soil properties. The neglect of stress history in current models may be related to the fact that compression tests are usually performed on disturbed soil samples and at relatively high soil water contents, both of which tend to mask the stress history of a soil.

The σ_p is an indication of the maximum previously applied stress sustained by a soil (Holtz and Kovacs, 1981) and defines the limit of elastic deformation in the soil compression curve. Thus, in agriculture, application of stress greater than the highest previously applied stress should be avoided (Gupta et al., 1989; Lebert and Horn, 1991) in order to avoid unrecoverable soil deformations. Since σ_p should be the maximum stress applied to a soil to prevent further soil compaction, a model of σ_p

can form the basis of a stress history model.

This study proposes a two component model of soil compressibility, consisting of a stress history submodel that describes elastic, recoverable deformation in terms of σ_p, and a virgin compression submodel, a submodel which describes the plastic, non-recoverable deformation in terms of bulk density (ρ_b) and applied stress (σ); both submodels are a function of soil water content (θ_m). Field unconfined stress (US) measurements are related to σ_p and used in conjunction with the compression index (m) and published values of critical stress (σ_c) to develop field based soil compression curves.

MATERIAL AND METHODS

Model Development

A common basis for compaction models is the soil compression curve, frequently expressed in terms of ρ_b as a function of log σ (Figure 1). The general position of this curve varies with soil type and θ_m (Larson and Gupta, 1980; Larson et al., 1980; Gupta et al., 1985; Gupta et al., 1987; Gupta and Allmaras, 1987; Lebert and Horn, 1991). For agricultural soils that have experienced previous stress, the compression curve consists of two distinct regions: the secondary compression curve, a region of small, elastic and recoverable deformation that defines the stress history of a soil; and the virgin compression curve, a region of plastic and unrecoverable deformations (Gupta et al, 1989; Lebert and Horn, 1991). The σ_p divides the compression curve into these two regions (Lebert and Horn, 1991) and the slope of the virgin compression curve is called the compression index (m) (Bradford and Gupta, 1986).

The soil compaction model proposed herein estimates a soil compression curve in terms of a stress history model and a virgin compression model (Figure 2). The stress history model takes the general form of the relationship between σ_p and θ_m (Figure 2a) expressed as

$$\sigma_p = 10^{(a + b\theta m)} \qquad [1]$$

where a and b are fitted parameters. The regressions of $\log_{10} \sigma_p$ on θ_m (Equation [1]) varied by tillage and traffic treatment as reported in chapter 1. The coefficient of determination (R^2) of the regressions ranged from 0.83 to 0.98, the intercepts ranged from 2.76 to 3.32, and the slopes ranged from -1.77 to -7.86. The virgin compression model takes the general form

$$\rho_{bfinal} = \rho_b + m \log (\sigma_{final}/\sigma) \qquad [2]$$

where σ is the applied stress (kPa) and m is the compression index (Figure 2b). Although the virgin compression curves for a given soil have been reported to be parallel, at least at high θ_m (Larson and Gupta, 1980; Larson et al., 1980; Saini et al., 1984; Håkansson et al., 1988; O'Sullivan, 1992), we found the virgin compression curves were not always parallel (Figure 3). This agrees with Schmertmann (1955) who reported that the curves for saturated soils intersect within a narrow range of void ratio. For a given soil type, m is described as a function of θ_m expressed as

$$m = c + d\,\theta_m + e\,\theta_m^2 \qquad [3]$$

The m_{max} was found to occur near the plastic limit. Although this relationship was weak and not consistent for all soils, it recognizes the variability of m, a portion of which is explained by θ_m. The variability in m needs further quantification.

The compaction model then describes the compressive behavior of soil as a function of ρ_b, σ, σ_p, θ_m, and soil management practices providing parameters for using Equations [1], [2], and [3]. The model works in the following manner. For applied stress less than the σ_p, deformation is elastic so that wheel traffic will cause no additional compaction. For applied stress greater than the σ_p, deformation is plastic, compaction increases in proportion to the applied stress, and the rate of deformation m is a maximum near the plastic limit. Thus, the degree to which an applied stress causes elastic or plastic deformation is largely a function of stress history, θ_m, and soil management for a given soil type.

Model validation

The stress history component of the proposed compaction model was evaluated relative to data reported by Larson and Gupta (1980), Reinert (1990), and Kassa (1992). Data on θ_m, σ_p,and σ_c were obtained from those studies. These data were then fit to the stress history portion of the proposed compaction model. Field validation of the stress history model was accomplished by evaluating field measured penetrometer measurements reported in chapter 1 for the Capac loam (Fine loamy, mixed, mesic Aeric Ochraqualfs) against σ_p predicted from Equation [1]. Appropriate regressions were performed in Sigma Plot 1.02 (Jandel Scientific, P.O. Box 7005, San Rafael, CA).

RESULTS AND DISCUSSION

Model Validation

The stress history model (Equation [1]) expressed in Figure 4 was obtained from the conventional tillage treatment at the 0-3 cm depth in the Capac loam (110 g kg^{-1} clay), the Kalamazoo loam (Fine loamy, mixed, mesic Typic Hapludalfs) (90 g kg^{-1} clay), and the Misteguay silty clay (Fine, mixed (calcareous), mesic Aeric Haplaquepts) (480 g kg^{-1} clay). The information was obtained between tracks in the field. Also shown in Figure 4 are data reported by others. The stress history model for the Kalamazoo loam predicted σ_p reasonably well ($R^2 = 0.84$) for data reported by Reinert (1990) for the same soil (Figure 5a). The stress history model for the Capac loam predicted σ_p of the Ves clay loam (300 g kg^{-1} clay) and the Webster clay loam (330 g kg^{-1} clay) reported by Kassa (1992) well, with an R^2 of 0.86 and a close fit to the 1:1 line, even though the range of soil water used for the compression tests was at the high end only (Figure 5b). Thus, the stress history model predicts the elastic deformation of a soil reasonably well.

Larson and Gupta (1980) proposed the use of critical stress (σ_c) to define the maximum stress a soil can withstand without damaging aggregates. The σ_c corresponds to the minimum pore water pressure at which soil aggregate ruptures and occurs at $\sigma_c > \sigma_p$. σ_c was not measured for the Michigan soils. However, we analyzed data from Kassa (1992) and found a strong linear relationship between $\log_{10}$

σ_c and σ_p, with R^2 ranging from 0.86 to 1.00 (Figure 6) given as

$$\sigma_c = 10^{(f + g\theta_m)} \qquad [4]$$

where f and g are fitted parameters. The stress history model for the Capac predicted the $\log_{10} \sigma_c$ well for data from Larson and Gupta (1980) and Kassa (1992), with R^2 of 0.78 and 0.89, respectively, even though these soils had higher clay contents than the Capac (Figure 7). Thus, σ_p and σ_c are closely related, both increasing with decreasing θ_m. Additionally, we found that the relationship between unconfined strength (US), as measured in the field with a pocket penetrometer (chapter 1), and θ_m follows the stress history model (Figure 8a) as

$$US = 10^{(h + i\theta_m)} \qquad [5]$$

where h and i are fitted parameters. Thus, field measures of US and θ_m can be used to estimate σ_{pfield} (Figure 8b) from

$$\sigma_{pfield} = j + k(US) \qquad [6]$$

where j and k are fitted parameters.

The importance of these findings are that estimates of field soil compression curves can be constructed from easily measured soil properties: US, θ_m, and ρ_{bi} in Equations [1-6]. This is possible because, by definition, σ_p divides the compression curve into two regions, the virgin compression curve is log-linear, and $\sigma_p < \sigma_c$. Therefore, the secondary compression curve can be constructed from a linear line segment between ρ_{bi} and σ_p, and the virgin compression curve can be constructed using σ_p and both m and σ_c (Figure 1).

We have shown the importance of σ_p and its relationship to σ_c and field measured US, but have not explored the relationship between σ_p and root penetration. Gerard et al. (1982) reported that soil strength was a function of soil water content, voids, and clay content and that the critical strength (MPa) at which root elongation ceased was solely a function of clay content (%) expressed as

$$\text{critical strength} = 18.57\ \text{clay}^{-0.49} \qquad [7]$$

We calculated the critical strength predicted by Equation [7] for the Capac loam, Kalamazoo loam, and Misteguay silty clay (clay contents 110, 90, and 480 g kg^{-1}, respectively) and regressed the predicted critical strength on σ_p predicted from Equation [1] for dry soil at a constant θ_m of 0.10 kg kg^{-1} and at θ_m corresponding to a matric potential of -1.5 MPa as reported in chapter 1 (Figure 9). The regression was linear and the relationship was strong (R^2 = 0.99 and 0.83 respectively). Therefore, σ_p is also a good predictor of the critical strength at which root elongation ceases and implies that soils with a considerable stress history are more likely to inhibit root growth.

CONCLUSIONS

The proposed soil compaction model accounts for stress history in terms of σ_p as a function of θ_m. The stress history model was a good predictor of σ_p and σ_c from the literature and is a good predictor of critical strength for root elongation. Because σ_p was closely related to field measured US, it was possible to construct soil compression curves from field measurements of US, ρ_b, and θ_m with knowledge of laboratory measured soil compression curves from which values of σ_p, m, and possibly σ_c can be obtained. The importance of stress history in modeling soil compaction is clear. Stress history models have immediate application in estimating soil workability or trafficability for a range of soils and soil management conditions.

LIST OF REFERENCES

Angers, D.A., B.D. Kay, and P.H. Groenevelt. 1987. Compaction characteristics of a soil cropped to corn and bromegrass. Soil Sci. Soc. Am. J. 51:779-783.

Bailey, A.C., and C.E. Johnson. 1989. A soil compaction model for cylindrical stress state. Trans. ASAE 32:822-825.

Bailey, A.C., C.E. Johnson and R.L. Schafer. 1984. Hydrostatic compaction of agricultural soils. Trans. ASAE 27:952-995.

Bailey, A.C., C.E., Johnson, and R.L., Schafer, 1986. A model for agricultural soil compaction. J. Agric. Eng. Res. 33:257-262.

Bailey, A.C., C.E. Johnson, R.L. Schafer, T.A. Nichols, and R.D. Grisso. 1985. A compaction model for agricultural soil. p. 2:203-212. *In* Taction and transport as related to cropping systems. Proc. Int. Conf. Soil Dynamics. Auburn, AL. June 17-19, 1985. Natl. Tillage Mach. Lab. and Agric. Eng. Dept., Alabama Exper. Sta., Auburn, AL.

Bailey, A.C., and G.E. VandenBerg. 1968. Yielding by compaction and shear in unsaturated soils. Trans. ASAE 11:307-311,317.

Barnes, K.K, W.M. Carleton, H.M. Taylor, R.I. Throckmorton, and G.E. Vanden Berg. 1971. Compaction of agricultural soils. ASAE. Monogr., St. Joseph, MI.

Binger, R.L., and L.G. Wells. 1992. Compact - a reclamation soil compaction model part I. model development. Trans. ASAE 35:405-413.

Blackwell, P.S., and B.O. Soane. 1981. A method of predicting bulk density changes in fields soils resulting from compaction by agricultural traffic. J. Soil Sci. 32:51-65.

Bowen, H.D. 1975. Simulation of soil compaction under tractor-implement traffic. ASAE paper No. 75-1569. Am. Soc. Agric. Eng. St. Joseph, MI.

Bradford, J.M. and S.C. Gupta. 1986. Compressibility. p. 479-492. In A. Klute (ed.) Methods of soil analysis. Part 1. 2nd ed. Agron. Monog. 9. ASA, Madison, WI.

Canarache, A. 1991. Factors and indices regarding excessive compactness of agricultural soils. Soil Tillage Res. 19:145-164.

Coleman, G.E., and J.V. Perumpral. 1974. The finite element analysis of soil compaction. Trans. ASAE 17:856-860.

Gassman, P.W., D.C. Erbach, and S.W. Melvin. 1989. Analysis of track and wheel soil compaction. Trans. ASAE 32:23-29.

Gerard, C. J., P. Sexton, and G. Shaw. 1982. Physical factors influencing soil strength and root growth. Agron. J. 74:875-879.

Grisso, R.D., C.E. Johnson, and A.C. Bailey. 1987. Soil compaction by continuous deviatoric stress. Trans. ASAE 30:1293-1301.

Gupta, S.C., and R.R. Allmaras. 1987. Models to access the susceptibility of soil to excessive compaction. Adv. Soil Sci. 6:65-100.

Gupta, S.C., A. Hadas, and R.L. Schafer. 1989. Modeling soil mechanical behavior during compaction. p. 137-152. *In* W.E. Larson, G.R. Blake, R.R. Allmaras, W. B. Voorhees and S.C. Gupta (eds.). Mechanics and related process in structured agricultural soils. Kluwer Academic Publishers, The Netherlands.

Gupta, S.C., A. Hadas, W.B. Voorhees, D. Wolf, W.E. Larson, and E.C. Schneider. 1985. Development of quids for estimating the ease of compaction of world soils. Research Report, Binational Agric. Res. Development, Bet Dagan, Israel. University of Minessota, USA.

Gupta, S.C., E.C. Schneider, W.E. Larson, and A. Hadas. 1987. Influence of corn residue on compression and compaction behavior of soils. Soil Sci. Soc. Am. J. 51:207-212.

Gupta, S.C., and W.E. Larson. 1982. Modeling soil mechanical behavior during tillage. p. 151-178. *In* P.W. Unger, D.M. Van Doren,Jr., F.D. Whisler, and E.L. Skidmore (eds.). Predicting tillage effects on soil physical properties and process. Spec. Pub. 44. Am. Soc. Agron. Madison, WI.

Håkansson, I., W.B. Voorhees, and H. Riley. 1988. Vehicle and wheel factors influencing soil compaction and crop response in different traffic regimes. Soil Tillage Res. 11:239-282.

Holtz, R.D., and W.D. Kovacs. 1981. An introduction to geotechnical engineering. Prentice-Hall, Inc., Englewood Cliffs, NJ.

Horn, R. 1989. Strength of structured soils to loading - a review of process on macro and microscale; European aspects. p. 9-22. *In* W.E. Larson, G.R. Blake, R.R. Allmaras, W. B. Voorhees and S.C. Gupta (eds.). Mechanics and related process in structured agricultural soils. Kluwer Academic Publishers, The Netherlands.

Howard, R.F., M.J. Singer, and G.A. Frantz. 1981. Effects of soil properties, water content, and compactive effort on the compaction of selected California forest and range soils. Soil Sci. Soc. Am. J. 45:231-236.

Kassa, Z. 1992. Pore water pressure and some associated mechanical responses to uniaxial stress in structured agricultural soil. M.S. Thesis. University of Minnesota.

Larson, W.E., and S.C. Gupta. 1980. Estimating critical stress in unsaturated soils from changes in pore water pressure during confined compression. Soil Sci. Soc. Am. J. 44:1127-1132.

Larson, W.E., S.C. Gupta, and R.A. Useche. 1980. Compression of agricultural soils from eight soil orders. Soil Sci. Soc. Am. J. 44:450-457.

Lebert, M., N. Burger, and Horn, R. 1989. Effects of dynamic and static loading on compaction of structured soils. p. 73-80. In W.E. Larson, G.R. Blake, R.R. Allmaras, W. B. Voorhees, and S.C. Gupta (eds.). Mechanics related process in structured agricultural soils. NATO applied sciences, vol. 172. Kluwer Academic Publishers, The Netherlands.

Lebert, M., and Horn, R. 1991. A method to predict the mechanical strength of agricultural soils. Soil Tillage Res. 19:275-286.

Leeson, J.J., and D.J. Campbell. 1983. The variation of soil critical state parameters with water content and its relevance to the compaction of two agricultural soils. J. Soil Sci. 34:33-44.

McNabb, D.H., and L. Boersma. 1993. Evaluation of the relationship between compressibility and shear strength of Andisols. Soil Sci. Soc. Am. J. 57:923-929.

O'Sullivan, M.F. 1992. Uniaxial compaction effects on soil physical properties in relation to soil type and cultivation. Soil Tillage Res. 24:275-286.

Perumpral, J.V., J.B. Lijedahl, and W.H. Perloff. 1971. The finite element method for predicting stress distribution and soil deformation under a tractive device. Trans. ASAE 14:1184-1188.

Pollock, Jr. D., J.V. Perumpral, and T. Kuppusamy. 1986. Finite element analysis of multipass effects of vehicles on soil compaction. Trans. ASAE 29:45-50.

Raper, R.L., and D.C. Erbach. 1990 a. Prediction of soil stresses using the finite element method. Trans. of ASAE 33:725-730.

Raper, R.L., and D.C. Erbach. 1990 b. Effect of variable linear elastic parameters on finite element prediction of soil compaction. Trans. ASAE 33:731-736.

Reinert, D.J. 1990. Soil structural form and stability induced by tillage in a Typic Hapludalf. Ph.D diss. Michigan State Univ., East Lansing.

Saini, G.R., and T.L. Chow. 1984. Compactibility indexes of some agricultural soils of New Brunswick, Canada. Soil Sci. 137:33-38.

Schmertmann, J.H. 1955. The undisturbed consolidation behavior of clay. Trans. ASCE 120:1201-1233.

Soehne, W.H. 1958. Fundamentals of pressure distribution and soil compaction under tractors tires. J. Agric. Eng. 276-291.

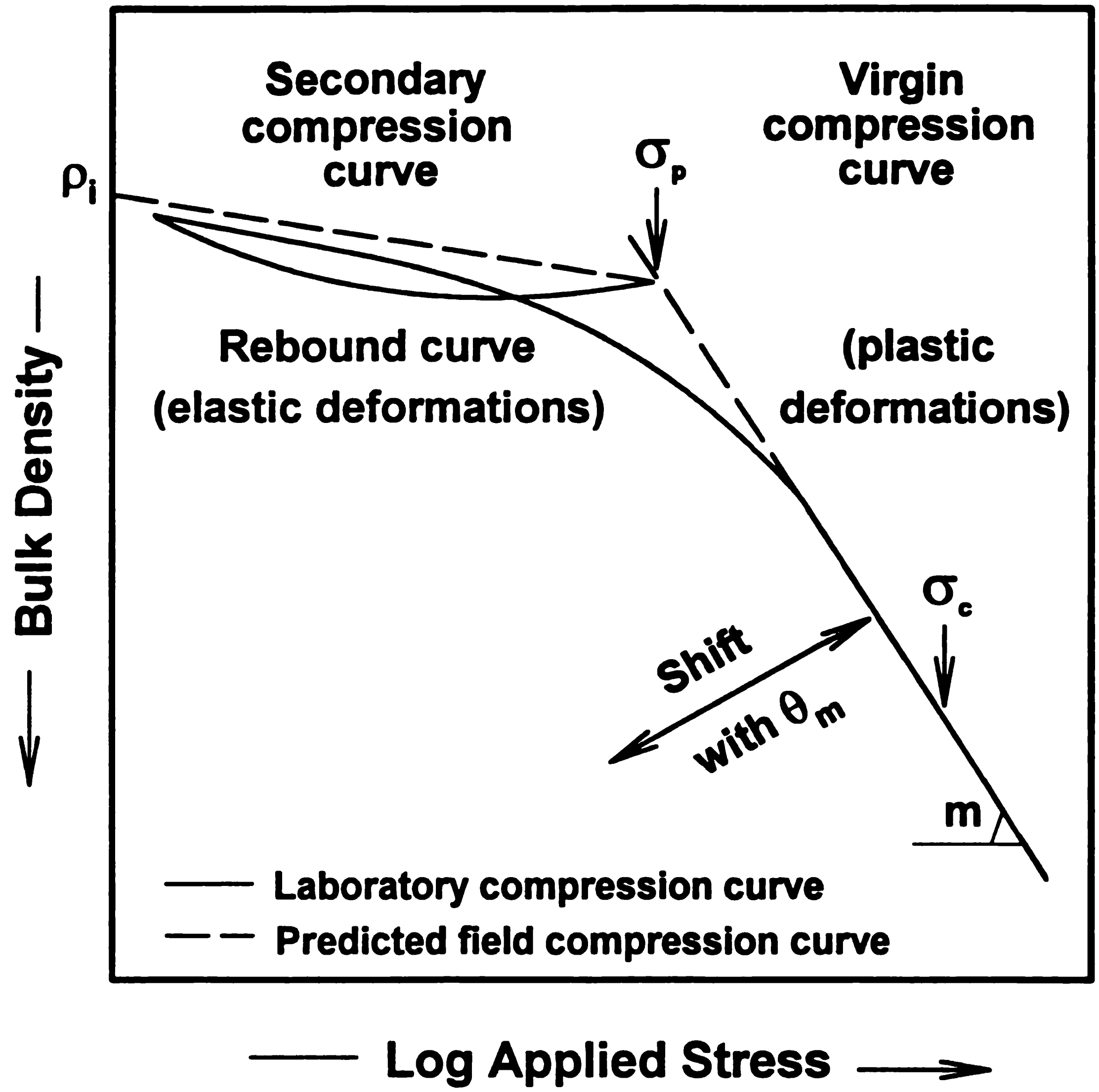

Figure 1. The secondary compression, rebound, and virgin compression components of a typical soil compression curve illustrating the position of the preconsolidation pressure (σ_p), the critical stress (σ_c), the compression index (m), and the shift down and to the left of the curve with increasing soil water content (θ_m). The dashed line represents a field compression curve constructed from the proposed model.

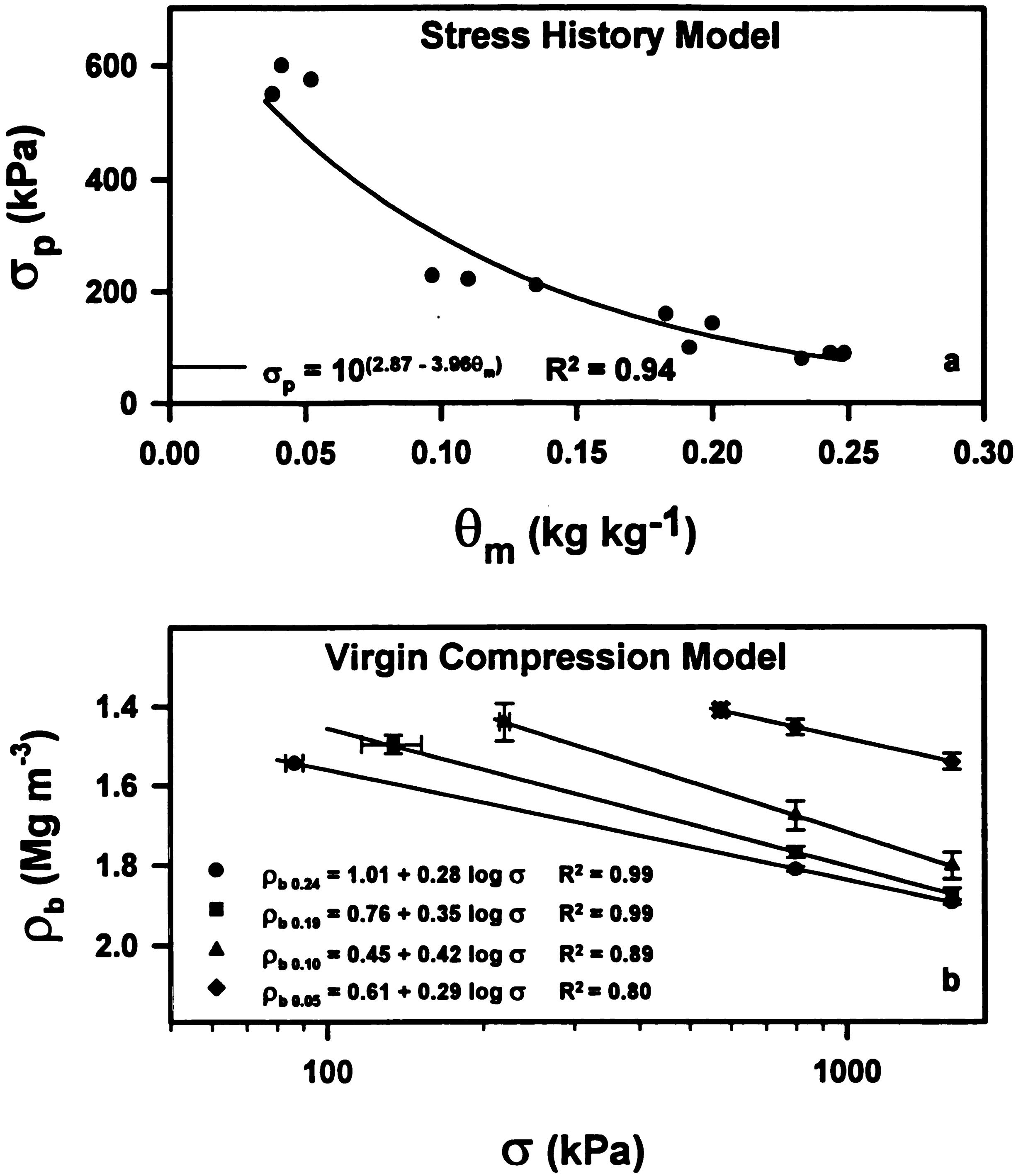

Figure 2. The stress history model (a) expressing preconsolidation pressure (σ_p) as a function of soil water content (θ_m); and the virgin compression model (b) expressing bulk density (ρ_b) as a function of applied stress (σ) of the 0-3 cm depth for the Capac loam at four different θ_m.

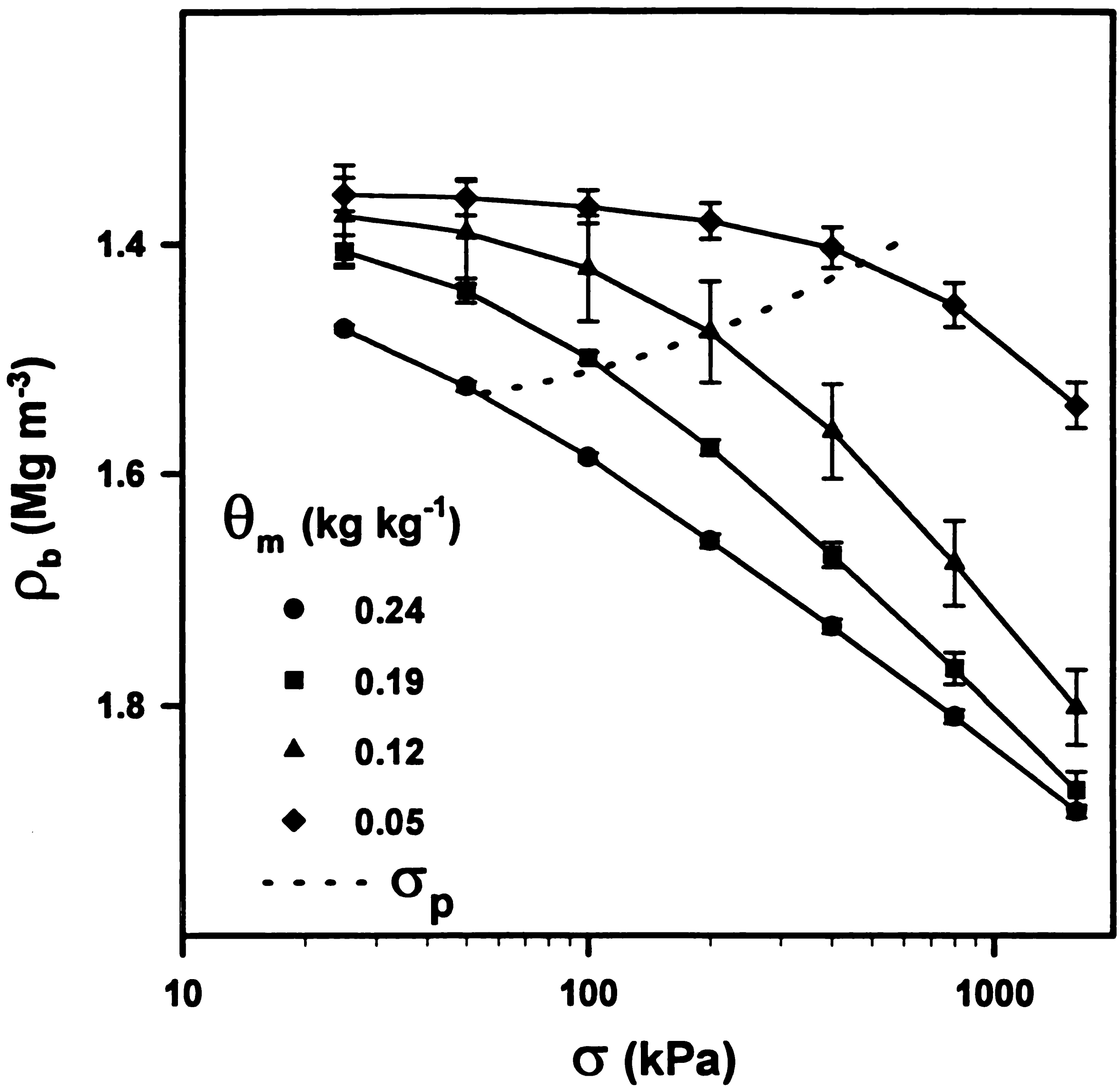

Figure 3. Soil compression curves expressing bulk density (ρ_b) as a function of applied stress (σ) for the 0-3 cm depth for the Capac loam at four different θ_m. The dashed line represents the line of the regression of preconsolidation pressure (σ_p) as a function of soil water content (θ_m).

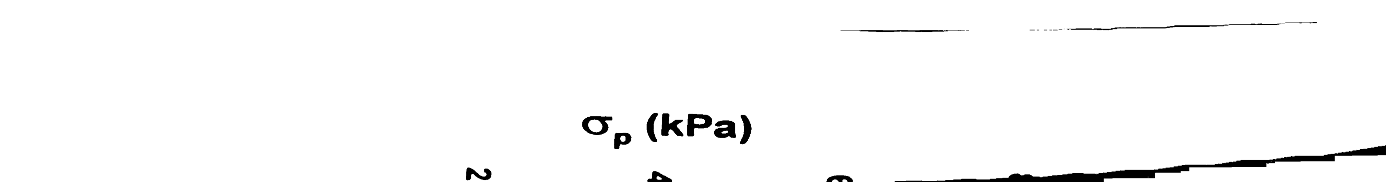

Figure 4

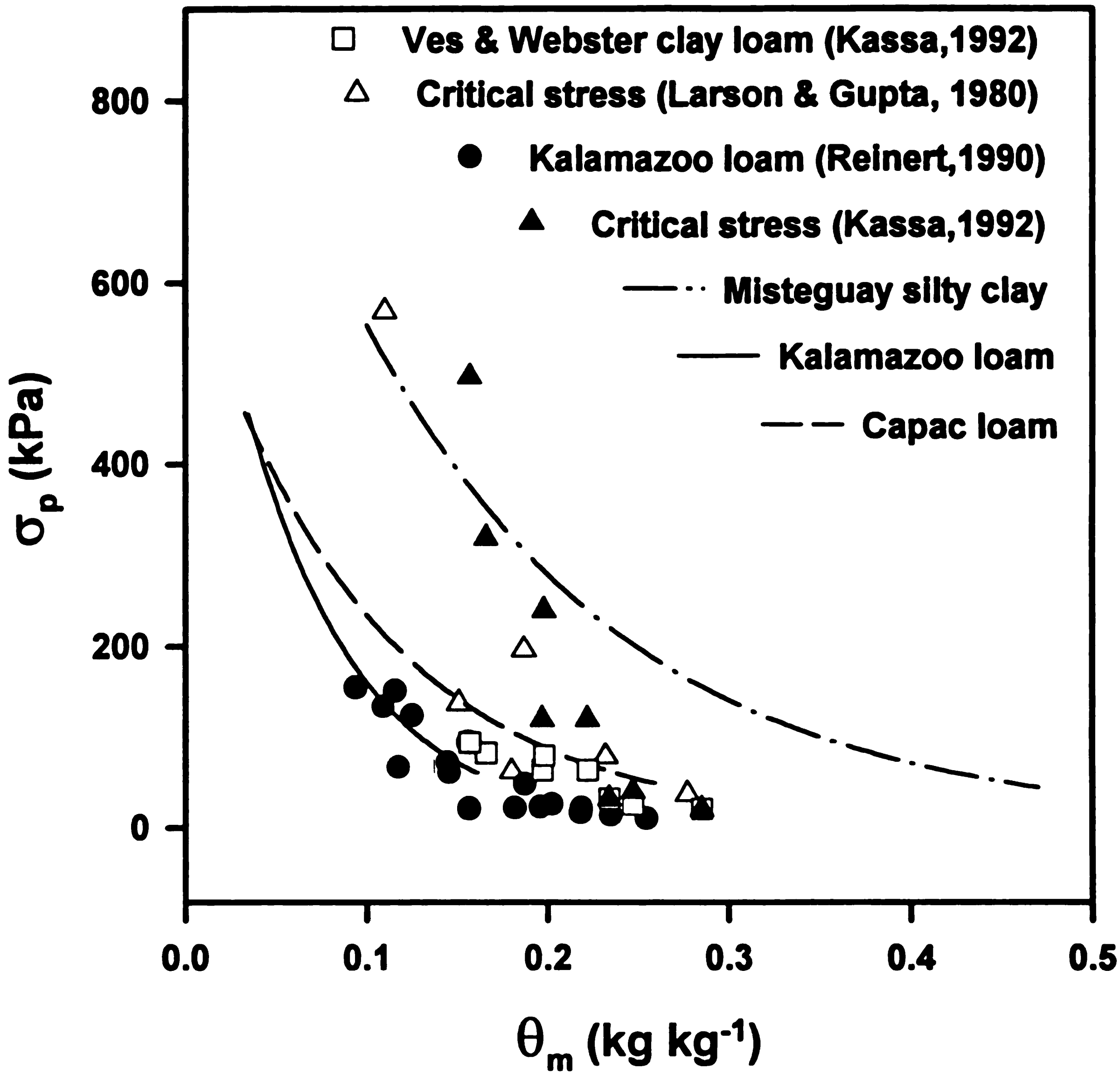

Figure 4. Preconsolidation pressure (σ_p) (from Kassa, 1992 and Reinert, 1990) and critical stress (σ_c) (from Kassa, 1992 and Larson and Gupta, 1980) each as a function of soil water content (θ_m) compared with σ_p predicted from the stress history models obtained from the 0-3 cm depth of the Capac loam, Kalamazoo loam, and Misteguay silty clay for the conventionally tilled treatment.

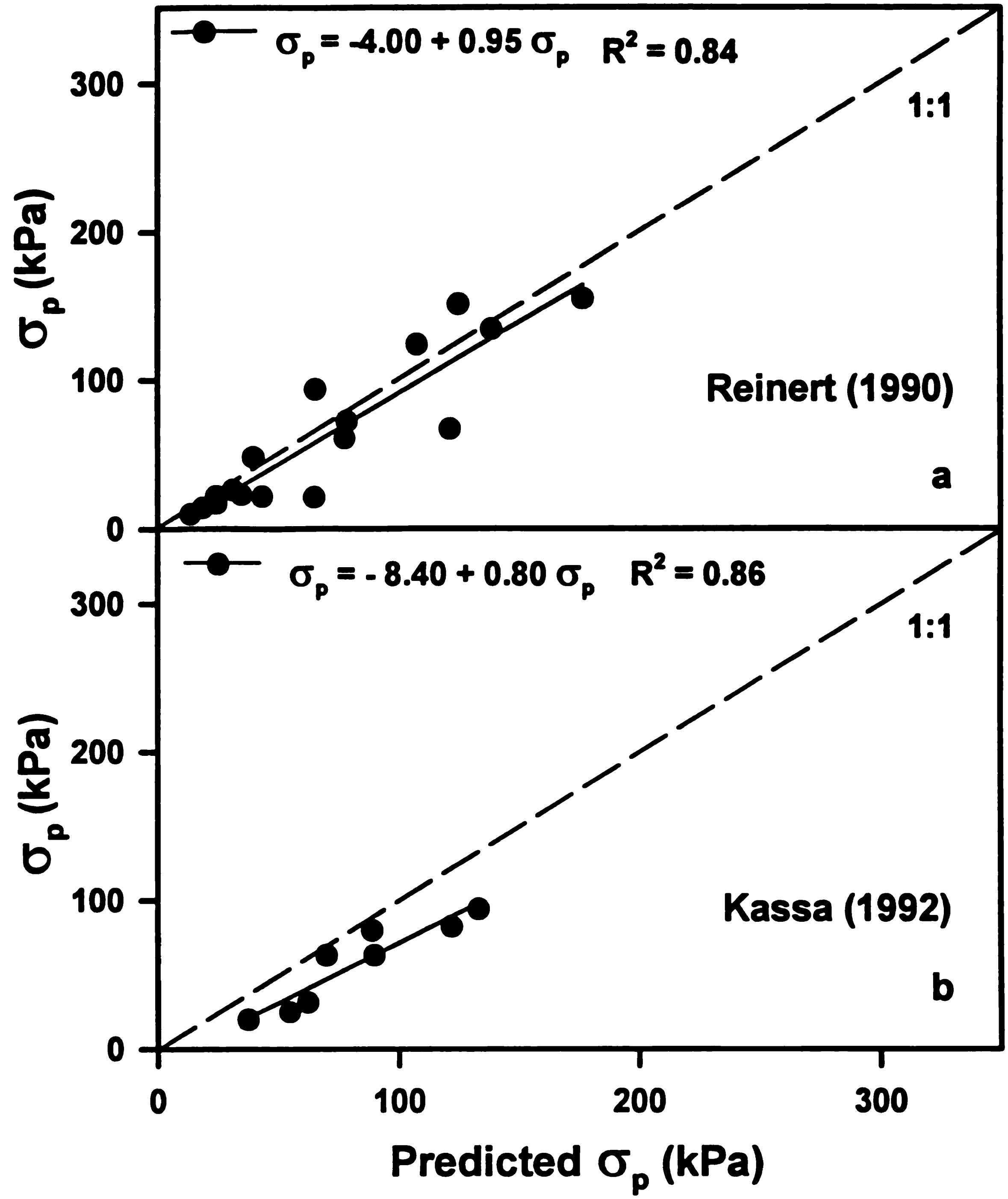

Figure 5. Predicted and measured (Reinert, 1990) values of preconsolidation pressure (σ_p) using the stress history model for the 0-3 cm depth of Kalamazoo loam (5a) and the stress history model for the 0-3 cm depth of the Capac loam to compare with measurements of Kassa (1992) (5b). The stress history models used were from the conventionally tilled treatment.

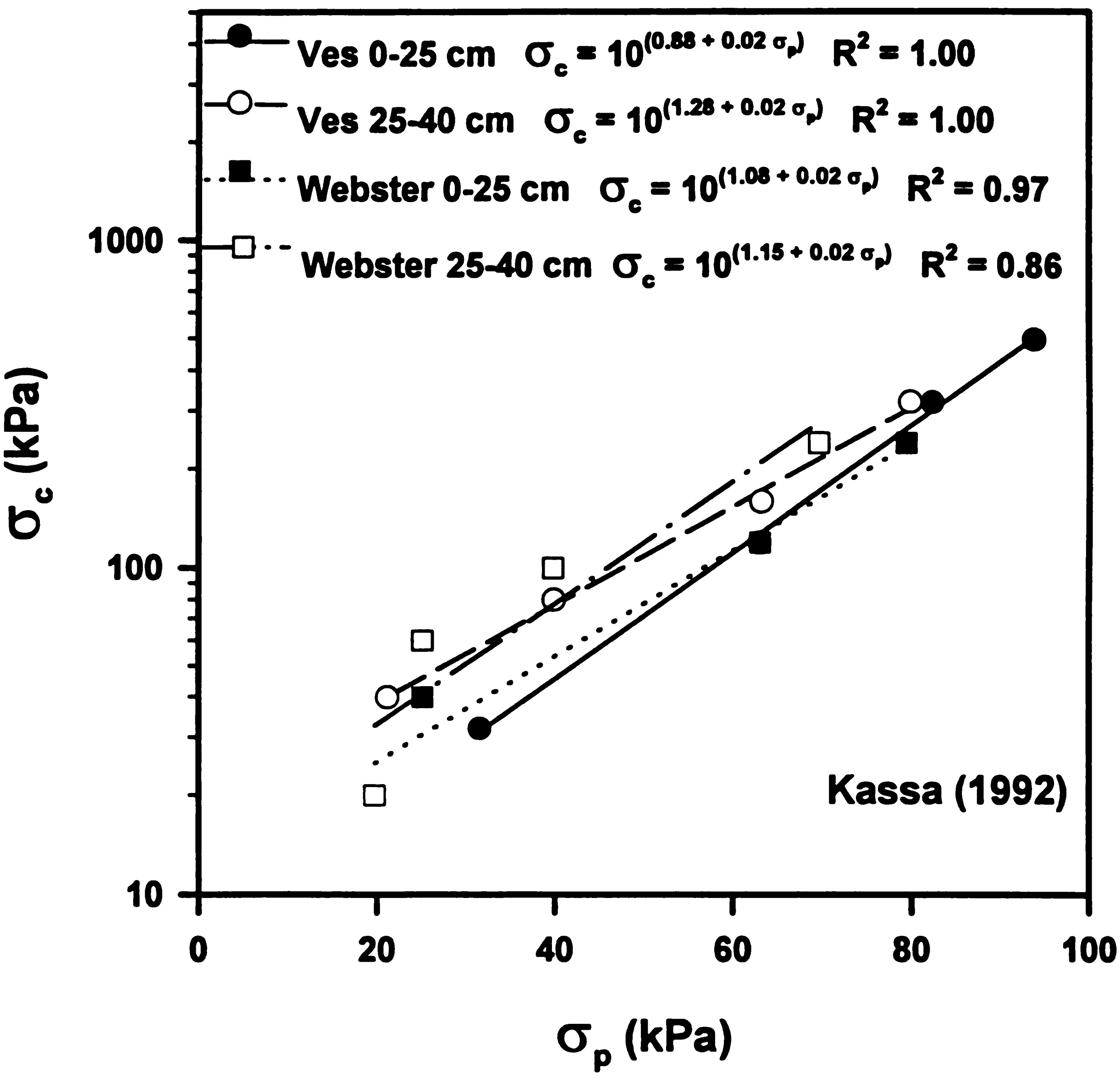

Figure 6. The relationship between critical stress (σ_c) and preconsolidation pressure (σ_p) from Kassa (1992).

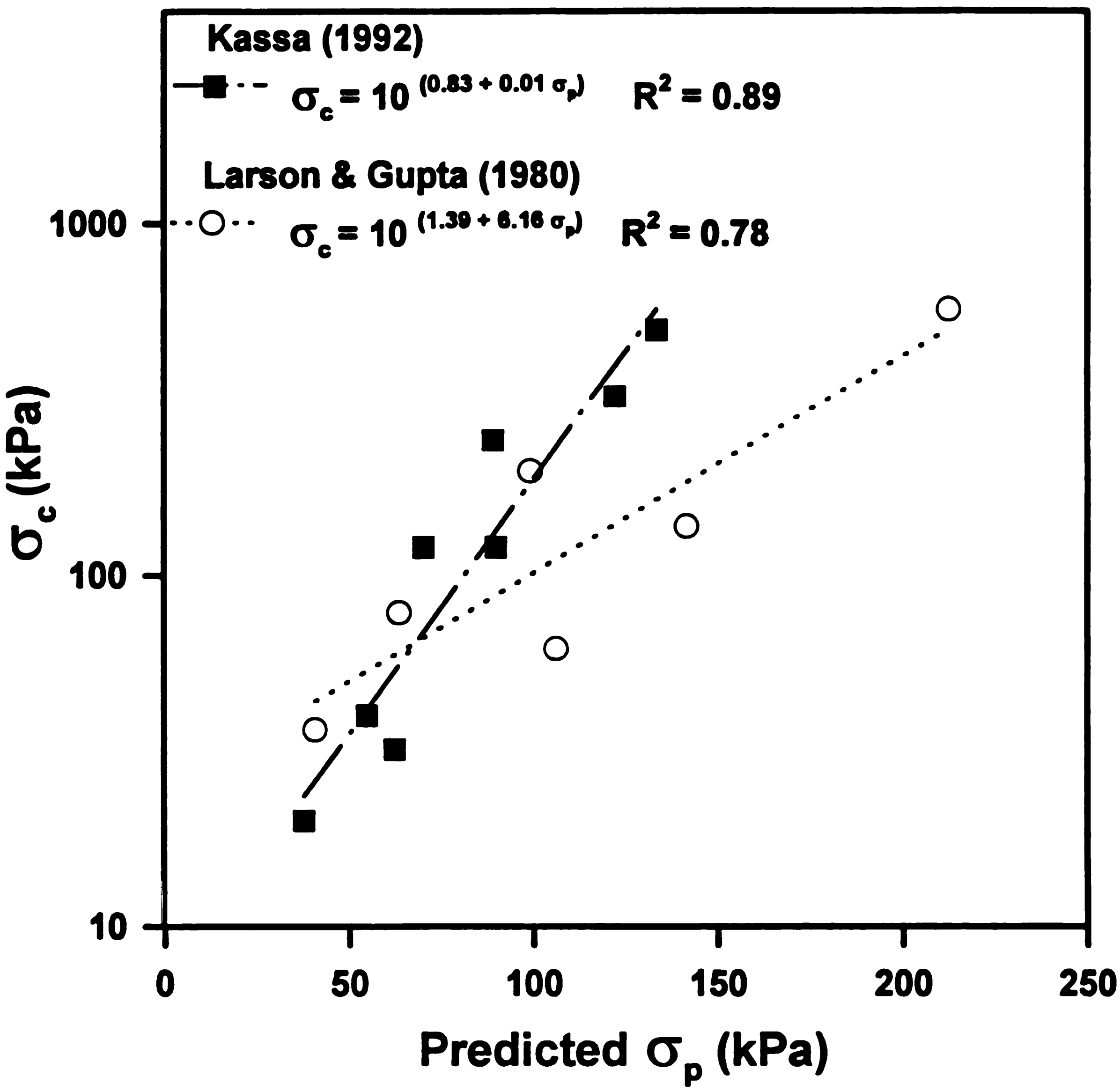

Figure 7. The relationship between critical stress (σ_c) measured by Kassa (1992) and Larson and Gupta (1980) and preconsolidation pressure (σ_p) predicted using the stress history model derived from the 0-3 cm depth of Capac loam when conventionally tilled.

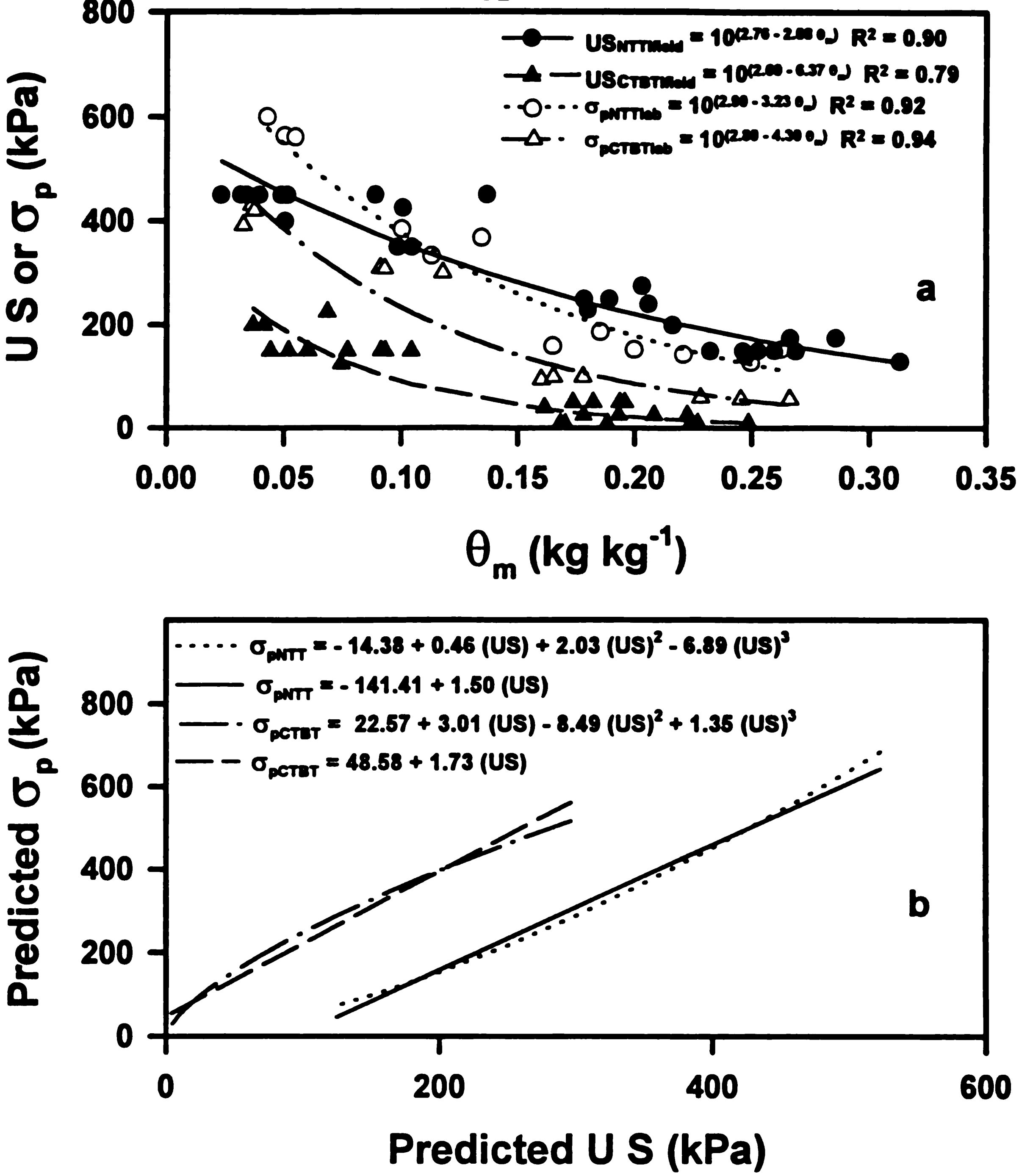

Figure 8. Unconfined strength (US) or predicted preconsolidation pressure (σ_p) as related to soil water content (θ_m) in (a) and σ_p as predicted US from (b) using data from the 0 - 3 cm depth of the Capac loam in the no-till-track (NTT) and conventionally-tilled-between-track (CTBT) treatments.

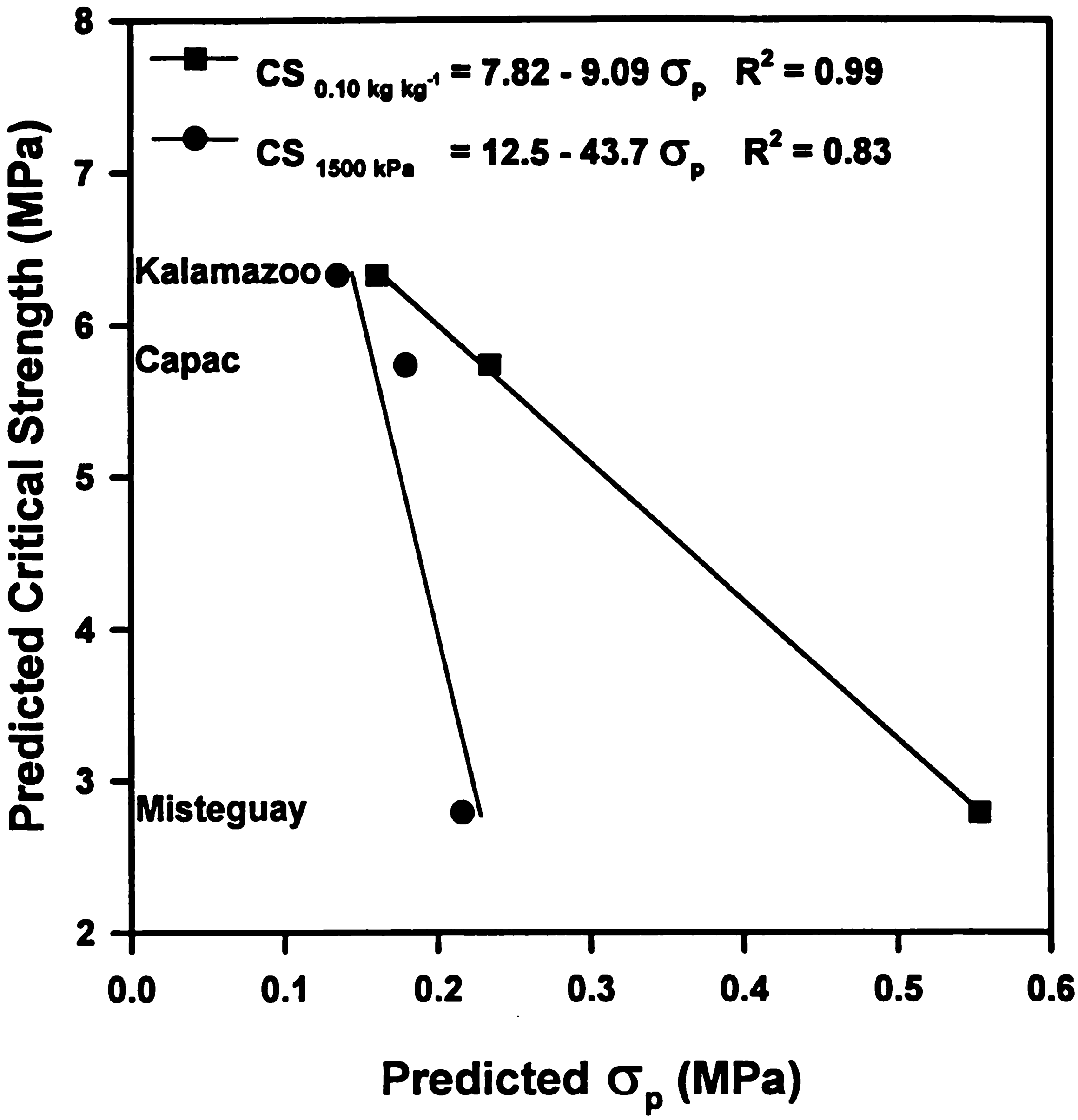

Figure 9. The relationship between critical strength at which root elongation ceases, (as predicted from Gerard et al., 1982) and predicted preconsolidation pressure (σ_p) for θ_m = 0.10 kg kg^{-1} or ψ_m at -1.5 MPa matric potential for the 0 - 3 cm depth of the Capac loam, Kalamazoo loam, and Misteguay silty clay soils for conventionally tilled between tracks.

CHAPTER 3

A SPREADSHEET PROCEDURE FOR ESTIMATING PRECONSOLIDATION PRESSURE FROM SOIL COMPRESSION CURVES

ABSTRACT

Classical graphics and regression procedures have been used to estimate preconsolidation pressure σ_p from soil compression curves, but none are easy to use and they often involve subjective judgement. This paper briefly reviews 9 methods used to estimate σ_p, describes a spreadsheet procedure for its estimation from soil compression curves, and evaluates the spreadsheet procedure with classical methods and published data. A spreadsheet was developed in Quattro Pro, Version 4.0, to calculate σ_p from soil compression curves. Five different estimation methods were programmed into the spreadsheet, for an applied stress sequence of 25, 50, 100, 200, 400, 800, and 1600 kPa. The σ_p was determined above for each method and compared to the σ_p estimated using the graphical procedure of Casagrande (1936) for 288 soil compression curves from three soils in Michigan and from values reported in the literature. Some methods fit the data best at low σ_p (high soil water content) while others fit the data better at high σ_p (low soil water content). Therefore, a combination of methods was found to fit the experimental data best. Methods 1 and 3

determine σ_p as the intersection of the line that passes through the first two points, or the regression line fitted to four points, respectively, in the secondary compression portion of the compression curve and the extension of the virgin compression line determined from the points associated with applied stress of 800 and 1600 kPa. The final spreadsheet procedure provides a fast and reliable estimation of σ_p and eliminates subjective judgment associated with classical graphical procedures.

INTRODUCTION

The compressive behavior of soil is expressed graphically in the relationship between the logarithm of applied stress and some parameter related to the packing state of soil, most often void ratio or bulk density (Casagrande, 1936; Leonards, 1962; Holtz and Kovacs, 1981). When no previous stress has been applied, this relationship is theoretically linear and the applied stress results in an unrecoverable deformation (Larson and Gupta, 1980; Larson et al., 1980; Culley and Larson, 1987; Gupta and Allmaras, 1987; Lebert and Horn, 1991). However, when a soil has experienced a previous stress, a change in the stress acting on a soil will result in some deformation, which can either be relatively small and recoverable or unrecoverable (Stone and Larson, 1980; Gupta et al.,1989; Lebert and Horn, 1991). As a result, the packing parameter versus log applied stress curve is still log-linear, but much flatter. The term preconsolidation pressure has been used to denote the "break" in the consolidation curve (Holtz and Kovacs, 1981; Jamiolkowski et al., 1985) between these two cases. Thus, the preconsolidation pressure divides the soil compression curve into a region of small, elastic and recoverable deformation (secondary compression curve) and a region of plastic and unrecoverable deformation (virgin compression curve).

In saturated soils, the preconsolidation pressure is used in settlement theory to estimate the load support capacity of soil (Leonards, 1962; Holtz and Kovacs, 1981). In agricultural soils, loads are applied to unsaturated soils. In theory, stress history is important to the compressive behavior of unsaturated soils since additional soil compaction occurs only when the load exceeds the preconsolidation pressure (Gupta et al., 1989; Lebert and Horn, 1991). Although the emphasis in soil compaction studies has been on the non-recoverable deformation that occurs with applied stresses within the range of the virgin compression curve (Larson et al., 1980; Gupta et al., 1989; Lebert and Horn, 1991; Binger and Wells, 1992), the importance of stress history is recognized, particularly as it relates to conservation tillage systems (Culley and Larson, 1987; Larson et al., 1988). However, its importance in predicting soil compaction and trafficability is poorly understood (Horn, 1989; Lebert and Horn, 1991; Binger and Well, 1992; McNabb and Boersma, 1993).

Preconsolidation pressure has been measured as part of recent soil compaction studies (Culley and Larson, 1987; Lebert et al., 1989; Lebert and Horn, 1991). However, its determination is somewhat imprecise. The most common methods in classical soil mechanics, such as Casagrande (1936) and Schmertmann (1955), are graphical and developed for saturated soils. These methods have been applied to unsaturated soils and the Casagrande method remains a standard for comparison to other methods (Jose et al., 1989). Additional methods have been used to estimate preconsolidation pressure in unsaturated soils, primarily involving regression (Lebert et al., 1989; Reinert, 1990; Lebert and Horn, 1991), but none are considered standard techniques. In all cases, none of the methods currently available are easy to use and often involve subjective judgement.

This paper briefly reviews methods used to estimate preconsolidation pressure, describes a spreadsheet procedure for estimating preconsolidation pressure from uniaxial compression tests for unsaturated soil conditions, and evaluates the spreadsheet procedure with classical methods and published results.

Review of Current Methods

The break in slope of a consolidation curve is not always sharp, and some methodology must be chosen to assign a best estimate of the presumed break (preconsolidation pressure). Thus, there is no agreed upon method of determining the preconsolidation pressure. However, according to Leonards (1962), the earliest and most widely used procedure to determine preconsolidation pressure is the Casagrande (1936) procedure. The following discussion briefly describes nine procedures for determining the preconsolidation pressure. The graphical methods are illustrated in Figure 1.

The Casagrande (1936) method involves selecting the point of minimum radius of curvature. This is accomplished by drawing horizontal and tangent lines at this point and bisecting the angle between them, then extending the straight line portion of the virgin compression curve until it intersects the bisector of the angle (Figure 1). The pressure corresponding to this point of intersection is the estimate of the preconsolidation pressure.

Burmister (1951) proposed a procedure in which the unloading-reloading stress cycle defines the slope of a typical unloading curve and the form and size of the characteristic triangle on a semi-logarithmic plotting of the curve (Figure 1). By shifting the unloading curve upward and parallel to itself to a point where a geometrically similar triangle of the same vertical intercept is found, the preconsolidation pressure can be determined. The preconsolidation pressure is equal to the position of the vertical leg.

Schmertmann (1955) suggested a procedure in which a horizontal line is drawn parallel to the log of applied stress from the initial void ratio to the existing vertical overburden pressure (Figure 1). A line parallel to the rebound-reload curve is drawn through the vertical overburden pressure, and the laboratory initial virgin compression curve is extended until it intersects either the initial void-ratio or the rebound line. The intersection point is defined as the preconsolidation pressure.

Sällfors (1975, as cited by Larson, 1986) used a method in which the two straight parts of the stress-strain curve are extended and intersected (Figure 1). An isosceles triangle is inscribed between the lines and the stress-strain curves. The intersection point between the base of the triangle and the upper line represents the preconsolidation pressure.

Anderson and Lukas (1981) predict the preconsolidation pressure (σ_p) from the undrained shear strength (Su) and the effective vertical overburden pressure (p'):

$$\sigma_p = Su/(Su/p') \qquad [1]$$

Culley and Larson (1987) used a statistical procedure to estimate the preconsolidation pressure. First, a least square regression was determined considering that all points lay on the virgin compression curve. Next, the compression curve was divided in two regions assuming an initial estimate of preconsolidation pressure of 15 kPa. Regression equations for each region were then developed and a combined sums of square calculated. The estimated preconsolidation pressure was then incrementally increased by 5 kPa and the statistics recalculated. The procedure was repeated until the lowest residual sums of squares was achieved.

Jose et al. (1989) used a log-log method in which the applied pressure and corresponding void ratio are plotted in logarithmic scale for each segment of the curve (Figure 1). The preconsolidation pressure is assumed to be equal to the applied pressure at the intersection of these two distinct lines. The authors did not reveal their criteria for choosing which points were included in the calculation of the two lines.

Lebert and Horn (1991) estimated the preconsolidation pressure as the intersection of the regression lines fitted through the secondary compression curve and the virgin compression curve (Figure 1). The authors did not reveal their criteria for choosing which points were included in the calculation of the two lines.

MATERIAL AND METHODS

Spreadsheet Procedure

A spreadsheet was developed in Quattro Pro (Version 4.0, Borland International, Inc., Scotts Valley, CA, USA) to calculate the preconsolidation pressure from soil compression curves. Equivalent procedures could be programmed in other modern spreadsheets. Five different estimation methods were programmed into the spreadsheet, for an applied stress sequence of 25, 50, 100, 200, 400, 800, and 1600 kPa. The first four methods estimated the preconsolidation pressure as the intersection of two lines: (a) one that passes through the first two points, or the regression line fitted to three, four, or five points, respectively, in the secondary compression portion of the compression curve and (b) the extension of the virgin compression line determined from the points associated with applied stress of 800 and 1600 kPa (Figure 2). Method 5 consisted of the Schmertmann (1955) method (Figure 1). The user simply enters the values of bulk density for the corresponding applied stress and the regressions are performed by entering the advanced math/regression menu under the tool subheading in Quattro Pro and executing the regression function.

The preconsolidation pressure was determined above for each method and compared to the preconsolidation pressure estimated using the graphical procedure of Casagrande (1936) for our data or from the preconsolidation pressure reported in the literature for selected studies. Our data included 288 compression curves determined as part of a study to evaluate the effects of tillage and wheel traffic on the compressive behavior of three soils in Michigan. The soil samples used are from experimental research plots managed under long term no-tillage and plowed plots including the Kalamazoo loam (Fine loamy, mixed, mesic, Typic Hapludalfs) located at Kalamazoo, MI, the Capac loam (Fine loamy, mixed, mesic, Aeric Ochraqualfs) located at East Lansing, MI, and the Misteguay silty clay (Fine, mixed (calcareous), mesic, Aeric Haplaquepts) located at Saginaw, MI. These soils had been cropped in no-tillage management for the last 13, 14, and 9 years, respectively. Measurements from the literature were taken from studies by Burmister (1951), Crawford (1964), Jose et al. (1989), Reinert (1990), and Kassa (1992). The relationships between applied stress and deformation were obtained by carefully extracting data from the graphics in those references. The methods were evaluated based on regression of σ_p, determined with the Casagrande method, on σ_p, determined by a given method, and nearness of the regression line to the 1:1 line. Based on these regressions, a single spreadsheet procedure was developed for unsaturated soil conditions.

RESULTS AND DISCUSSION

The graphical construction suggested by Casagrande (1936) is based in the choice of the point in the consolidation curve with minimum radius of curvature. Research has shown that as soil sample disturbance increases, the selection of this point is increasingly more difficult and the preconsolidation pressure will be lower than those obtained for undisturbed soil samples (Schmertmann, 1955; Brumund et al., 1976; Holtz and Kovacs, 1981). However, using undisturbed soil samples, the selection of the point of minimum radius can also be difficult to determine at high water content because the compression curve is almost linear (Figure 3). This could result in an overestimation of the preconsolidation pressure when compared with the values of minimum preconsolidation pressure determined according to Schmertmann (1955 - method 5).

As water content changes, the shape of the compression curve changes so that the number of points in the secondary or virgin compression portion of the curve changes (Figure 3). Therefore, a spreadsheet procedure to estimate the preconsolidation pressure should consider the possibility of changing the number of points that belong to the secondary compression curve in the fitting of the regression line. In addition, as the soil dries, the virgin compression curve is shifted up and to the right in a such away that for the lower water contents, only two points remain in the virgin compression curve for applied stress of 800 and 1600 kPa. Thus, if the procedures used by Culley and Larson (1987), Jose et al. (1989) and Lebert and Horn (1991) are used to estimate the preconsolidation pressure for a range of water contents, the preconsolidation pressure will be underestimated.

The regressions of predicted versus Casagrande method determined preconsolidation pressures for the 288 soil samples from the Michigan tillage studies are given in Figure 4. We evaluated overall performance of each method by examining the coefficient of determination (R^2) of the regression and the nearness of the regression line to the 1:1 line. Method 1 had the highest R^2 of 0.87 but tended to underpredict relative to the 1:1 line at preconsolidation pressures above 200 kPa (soil matric potentials < -100 kPa). Method 5 (Schmertmann, 1955) had a similar R^2 to method 1 and appeared to predict well at low preconsolidation pressures. However, all points were above the 1:1 line. Methods 2, 3, and 4 tended to over predict at low preconsolidation pressures (high water content) but did a better job at predicting at higher preconsolidation pressures (lower water contents). Since the performance of the methods varied depending on the range of preconsolidation pressures (and, therefore, water contents), the methods 1 and 5 were combined with methods 2 and 3 and the regression analyses calculated. Methods 1 and 5 were used to calculate preconsolidation pressures for matric potentials > -100 kPa and methods 2 and 3 were used for matric potentials < -100 kPa. This matric potential was chosen because it corresponded to one of the four potentials used in our compression measurements and preconsolidation pressures in the > -100 kPa matric potentials were generally below 200 kPa pressure. By inspection of Figure 4, methods 1 and 5 predicted well below 200 kPa and methods 2 and 3 predicted best above 200 kPa. All combinations improved R^2 to 0.90 to 0.92 (Figure 5). However, the combination of methods 1 and 3 showed the best correspondence to the 1:1 line. Therefore, the combination of method 1 and 3 was chosen as the best method for estimation of the preconsolidation pressure for unsaturated soil conditions for use in the final spreadsheet (Figure 6).

Table 1 shows the preconsolidation pressure obtained from the current literature and those estimated using methods 1 through 5. The regressions were performed for both saturated and unsaturated soil conditions, and for saturated and unsaturated combined (Table 2). For saturated, unsaturated, and combined regressions, all methods predicted the preconsolidation pressure well, but methods 1, 2, and 3 showed close correspondence to the 1:1 line, with slopes near 1 and intercepts near 0. The small difference between preconsolidation pressure obtained by methods 1, 2 and 3 and those from the literature was probably due to the well defined break point in the reported consolidation or compression curves. Also, the soil water contents evaluated in these studies were high and the range was narrow compared to the water content range evaluated in our soils. Therefore, the best overall method observed was the combination of method 1 and 3.

Spreadsheet Procedure Overview

The spreadsheet procedure is given in Appendix I. The spreadsheet screen is reproduced in Figure 6 and the regression plot is illustrated in Figure 2. The first step is to load the spreadsheet cell commands into the spreadsheet program in the order presented in Appendix I. For example, cell A1 is the heading for column A. Cell G2 is the equation to calculate the slope of the secondary compression curve. Once loaded, the spreadsheet will calculate all the necessary parameters for the preconsolidation pressure. First, type the bulk density corresponding to the applied pressures in the spreadsheet. The user enters "Tools" and then "Advanced Math" than "Regression" and enter "Go". This updates the spreadsheet for the regression output, the preconsolidation pressure, and the corresponding bulk density. At the same time, a graphic plot similar to the form in Figure 2 is redrawn and can be viewed by the user in the Graphics subdirectory ("View"). The user can alter the spreadsheet to different applied loads once the proposed spreadsheet has been entered.

CONCLUSIONS

For unsaturated soil conditions, the preconsolidation pressure can be estimated by using a spreadsheet procedure which uses a combination of method 1 for moisture conditions at matric potential higher than or equal to - 100 kPa, and method 3 for moisture conditions at matric potential lower than - 100 kPa. Preconsolidation pressures estimated with this procedure corresponded to standard graphical methods and literature values. This spreadsheet procedure, provides a fast and reliable estimation of the preconsolidation pressure. In addition, when used in the analysis of data for a research project involving σ_p, the use of a consistent, repeatable procedure rather than a graphical procedure will eliminate one source of variability, such as subjective judgment associated with classical graphical procedures.

LIST OF REFERENCES

Anderson, T.C., and R.G. Lukas. 1981. Preconsolidation pressure predicted using Su/p' ratio. p. 502-515. *In* Yong, R.N. and F.C. Townsend (eds.) Laboratory shear strength of soil. Symposium ASTM. Special Technical Publication 740. Chicago, Ill, 25 June 1980. Philadelphia, Pa.

Binger, R.L., and L.G. Wells. 1992. Compact - a reclamation soil compaction model part I. model development. Trans. ASAE 35:405-413.

Borland International, Inc. Scotts Valley, CA, USA.

Brumund, W.F., E. Jonas, and C.C. Ladd. 1976. Estimating in situ maximum past (preconsolidation) pressure of saturated clays from results of laboratory consolidometer test. p. 4-12. *In* Transportation Research Board, National Research Council. Estimation of consolidation settlement. Special Report 163. National Academy of Sciences. Washington, D.C.

Burmister, D. 1951. The application of controlled test methods in consolidation testing. p. 83-98. *In* Fifty-Fourth Annual Meeting of the ASTM. Symposium on consolidation testing of soils. Special Technical Publication 126. Atlantic City, N.J. June 18, 1951. Philadelphia, Pa.

Casagrande, A. 1936. The determination of the pre-consolidation load and its practical significance. p. 60-64. *In* Int. Conf. on Soil Mech. and Found. Eng. Proc. of ICSMFE. Cambridge, Mass. June 22-26, 1936. vol. 3. Cambridge, Mass.

Crawford, C.B. 1964. Interpretation of the consolidation test. p. 93-108. *In* ASCE, Soil Mechanics and Foundation Division. Design of foundations for control of settlement. Proc. of the ASCE, Evanston, ILL. June 16-19, 1964. Evanston, ILL.

Culley, J.L.B., and W.E. Larson. 1987. Susceptibility to compression of a clay loam Haplaquoll. Soil Sci. Soc. Am. J. 51:562-567.

Gupta, S.C., and R.R. Allmaras. 1987. Models to access the susceptibility of soil to excessive compaction. Adv. Soil Sci. 6:65-100.

Gupta, S.C., A. Hadas, and R.L. Schafer. 1989. Modeling soil mechanical behavior during compaction. p. 137-152. *In* Larson, W.E., G.R. Blake, R.R. Allmaras, W.B. Voohees, and S.C. Gupta (eds.). Mechanical and related process in structured agricultural soils. NATO applied sciences 172. Kluwer Academic Publishers, The Netherlands.

Holtz, R.D., and W.D. Kovacs. 1981. An introduction to geotechnical engineering. Prentice-Hall, Inc., Englewood Cliffs. NJ.

Horn, R., 1989. Strength of structured soils due to loading - A review of process on macro and microscale; European aspects. p. 9-22. *In* W.E. Larson, G.R. Blake, R.R. Allmaras, W.B. Voohees and S.C. Gupta (eds.), Mechanical and related process in structured agricultural soils. NATO applied sciences 172. Kluwer Academic Publishers, The Netherlands.

Jamiolkowski, M., C.C. Ladd, J.T. Germaine, and R. Lancellotta. 1985. New development in field and laboratory testing of soils. p. 57-153. *In* Publications Committee of XI ICSMFE (ed.). Proc. of the Eleventh Int. Conf. on Soil Mech. and Found. Eng. San Francisco, CA, 12-16 August 1985. Netherlands.

Jose, B.T., A. Sridharan, and B.M. Abraham. 1989. Log-log method for determination of preconsolidation pressure. Geotechnical Testing Journal. 12:230-237.

Kassa, Z. 1992. Pore water pressure and some associated mechanical responses to uniaxial stress in structured agricultural soils. M.S. thesis. University of Minnesota.

Larson, R. 1986. Consolidation of soft soils. Swedish Geotechnical Institute. Report 29. Linköping, Swedish.

Larson, W.E., and S.C. Gupta. 1980. Estimating critical stress in unsaturated soils from changes in pore water pressure during confined compression. Soil Sci. Soc. Am. J. 44:1127-1132.

Larson, W.E., S.C. Gupta, and J.L.B. Culley. 1988. Changes in bulk density and pore water pressure during soil compaction. Catena Sup. 11:123-128.

Larson, W.E., S.C. Gupta, and R.A. Useche. 1980. Compression of agricultural soils from eight soil orders. Soil Sci. Soc. Am.J. 44:450-457.

Lebert, M., N. Burger, and R. Horn. 1989. Effects of dynamic and static loading on compaction of structured soils. p. 73-80. *In* W.E. Larson, G.R. Blake, R.R. Allmaras, W.B. Voohees and S.C. Gupta (eds.), Mechanical and related process in structured agricultural soils. NATO applied sciences 172. Kluwer Academic Publishers, The Netherlands.

Lebert, M., and R. Horn. 1991. A method to predict the mechanical strength of agricultural soils. Soil Tillage Res. 19:275-286.

Leonards, G.A. 1962. Foundation Engineering. McGraw Hill Book Company, Inc., NY.

McNabb, D.H., and L. Boersma. 1993. Evaluation of the relationship between compressibility and shear strength of Andisols. Soil Sci. Soc. Am. J. 57:923-929.

Reinert, D.J. 1990. Soil structural form and stability induced by tillage in a Typic Hapludalf. Ph.D. diss. Michigan State Univ., East Lansing.

Sällfors, G., 1975. Preconsolidation pressure of soft high plastic clays. Thesis. Department of Geotechnical Engineering. Gothenburg.

Schmertmann, J.H. 1955. The undisturbed consolidation behavior of clay. Trans. ASCE 120:1201-1233.

Stone, J.A., and W.E. Larson. 1980. Rebound of five one-dimensionally compressed unsaturated granular soils. Soil Sci. Soc. Am. J. 44:819-822.

Table 1. Preconsolidation pressure (σ_p) obtained from current literature and using method 1 through 5 for saturated and unsaturated soil conditions.

Reference	Literature	Preconsolidation Pressure (kPa)				
		1	2	3	4	5
	Saturated					
Burmister, 1951	Burmister 75	81	89	109	155	71
	Burmister 350	372	351	360	441	270
Crawford, 1964	Casagrande 300	278	291	311	358	271
	Casagrande 262	238	256	289	343	224
Jose et al., 1989	Log - log 105	95	95	102	111	90
	Log - log 114	103	99	99	105	92
	Log - log 120	126	126	126	128	120
	Log - log 102	98	101	111	120	92
	Unsaturated					
Reinert, 1990	Casagrande 174	172	168	163	183	100
	Casagrande 134	139	117	138	178	89
	Casagrande 61	68	59	81	116	37
	Casagrande 17	14	13	11	7	11
Kassa, 1992	Statistical 94	95	94	104	138	29
	Statistical 82	73	92	126	156	18
	Statistical 63	60	63	69	79	31
	Statistical 32	29	31	34	35	9

Table 1 (cont'd)

	Statistical	70	63	67	79	118	44
	Statistical	40	37	45	51	71	34
	Statistical	25	23	25	29	43	16
	Statistical	20	18	21	26	38	10

Table 2. Regression equations of preconsolidation pressure (σ_p) from current literature and as determined by methods 1 through 5.

Method	Regression equations	R^2
	Saturated	
1	σ_p(Literature) = 7.92 + 0.98 σ_p(method 1)	0.98
2	σ_p(Literature) = 0.66 + 1.01 σ_p(method 2)	0.99
3	σ_p(Literature) = -1.99 + 0.96 σ_p(method 3)	0.98
4	σ_p(Literature) = 10.01 + 0.77 σ_p(method 4)	0.95
5	σ_p(Literature) = -11.13 + 1.23 σ_p(method 5)	0.98
	Unsaturated	
1	σ_p(Literature) = 3.50 + 0.97 σ_p(method 1)	0.99
2	σ_p(Literature) = -1.81 + 1.05 σ_p(method 2)	0.98
3	σ_p(Literature) = -4.16 + 0.95 σ_p(method 3)	0.92
4	σ_p(Literature) = -4.00 + 0.74 σ_p(method 4)	0.85
5	σ_p(Literature) = 15.66 + 1.46 σ_p(method 5)	0.82
	Saturated & Unsaturated	
1	σ_p(Literature) = 3.41 + 1.00 σ_p(method 1)	0.99
2	σ_p(Literature) = 0.12 + 1.02 σ_p(method 2)	0.99
3	σ_p(Literature) = -4.78 + 0.97 σ_p(method 3)	0.98
4	σ_p(Literature) = -5.13 + 0.80 σ_p(method 4)	0.95
5	σ_p(LIterature) = 21.05 + 1.10 σ_p(method 5)	0.94

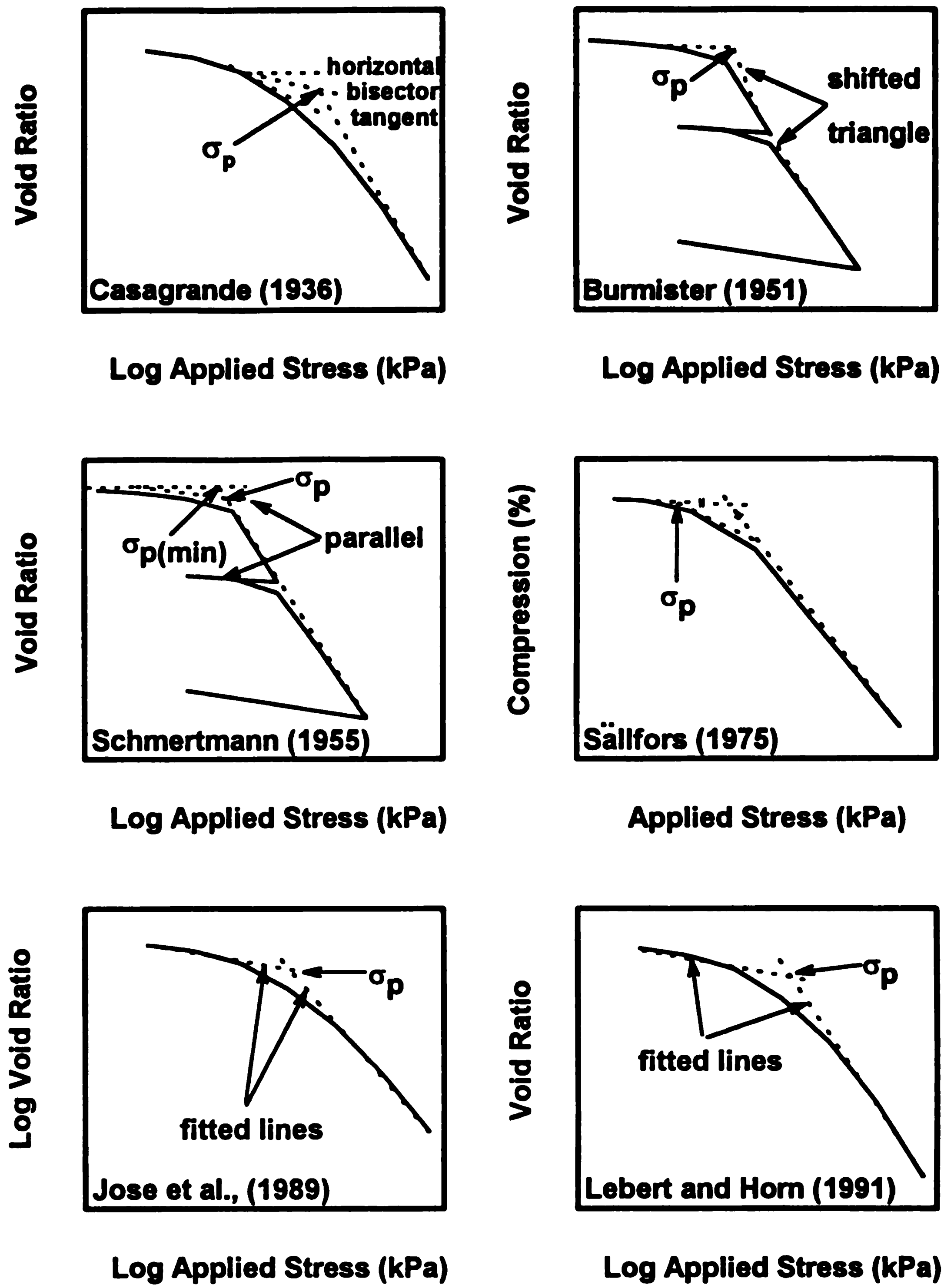

Figure 1. Illustration of published methods for determination of the preconsolidation pressure (σ_p) for soil compression curves.

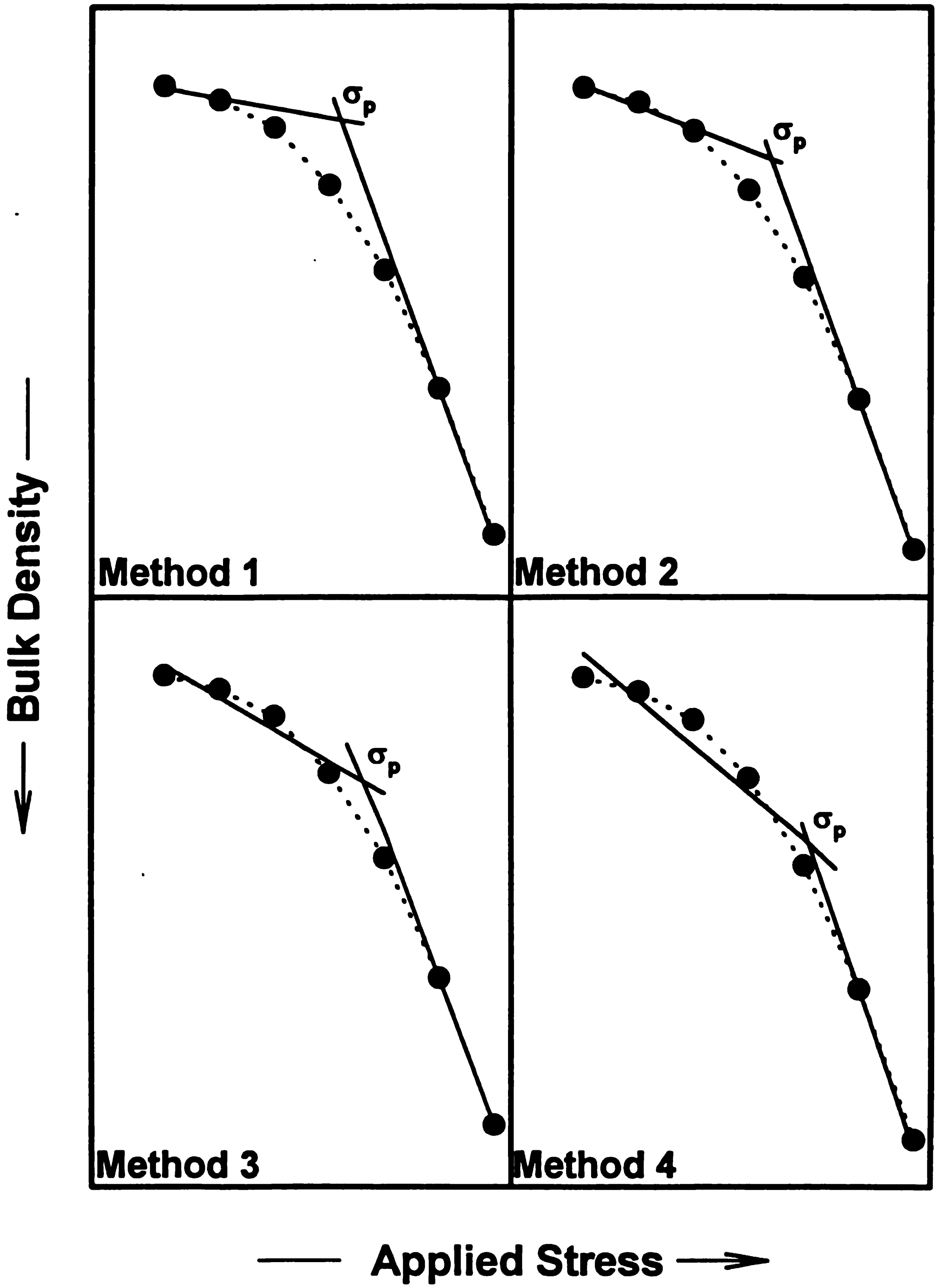

Figure 2. Illustration of methods 1 through 4 for determination of the preconsolidation pressure (σ_p) for soil compression curves.

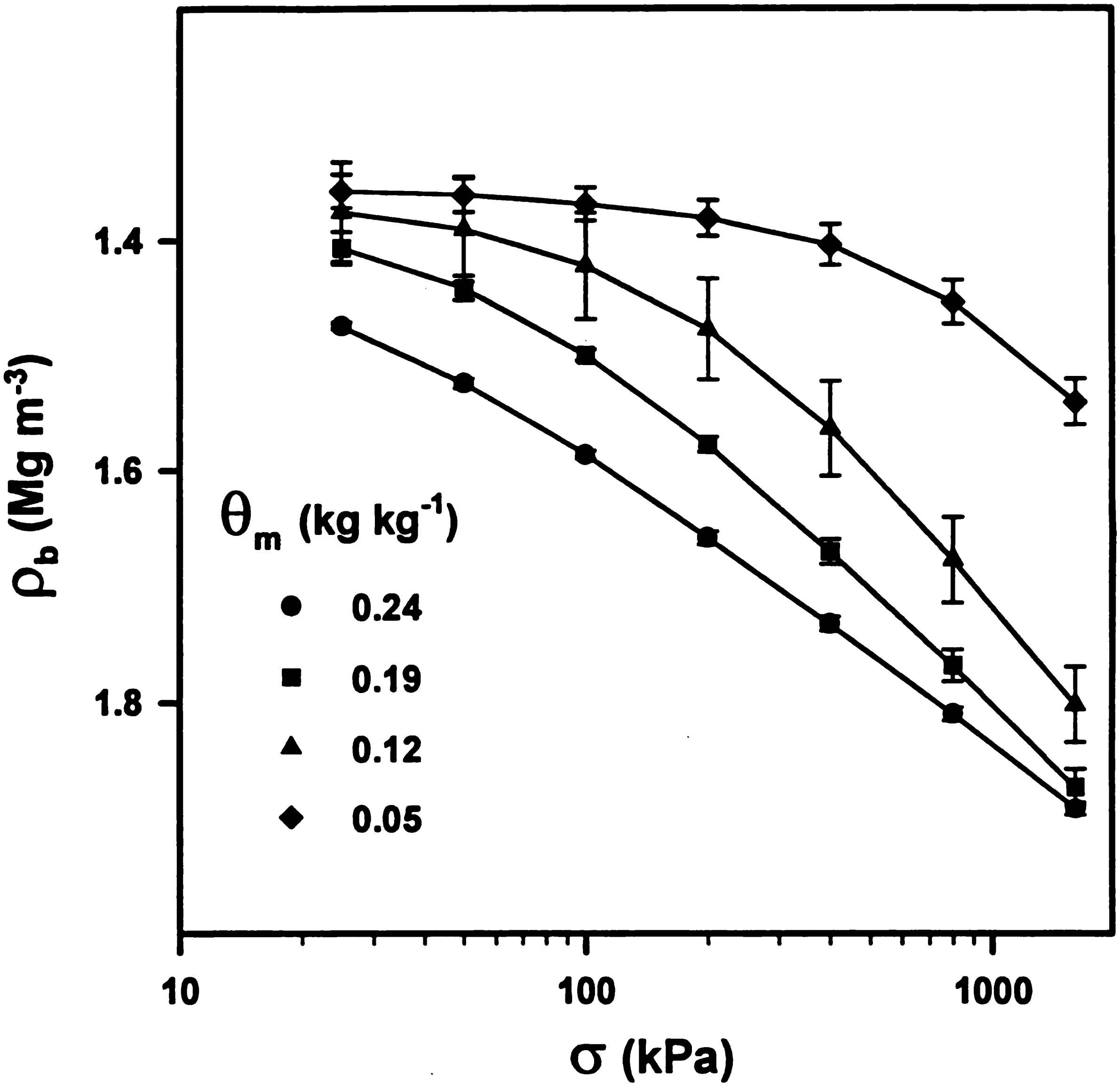

Figure 3. The effect of water content on the soil compression curves for a Capac loam soil.

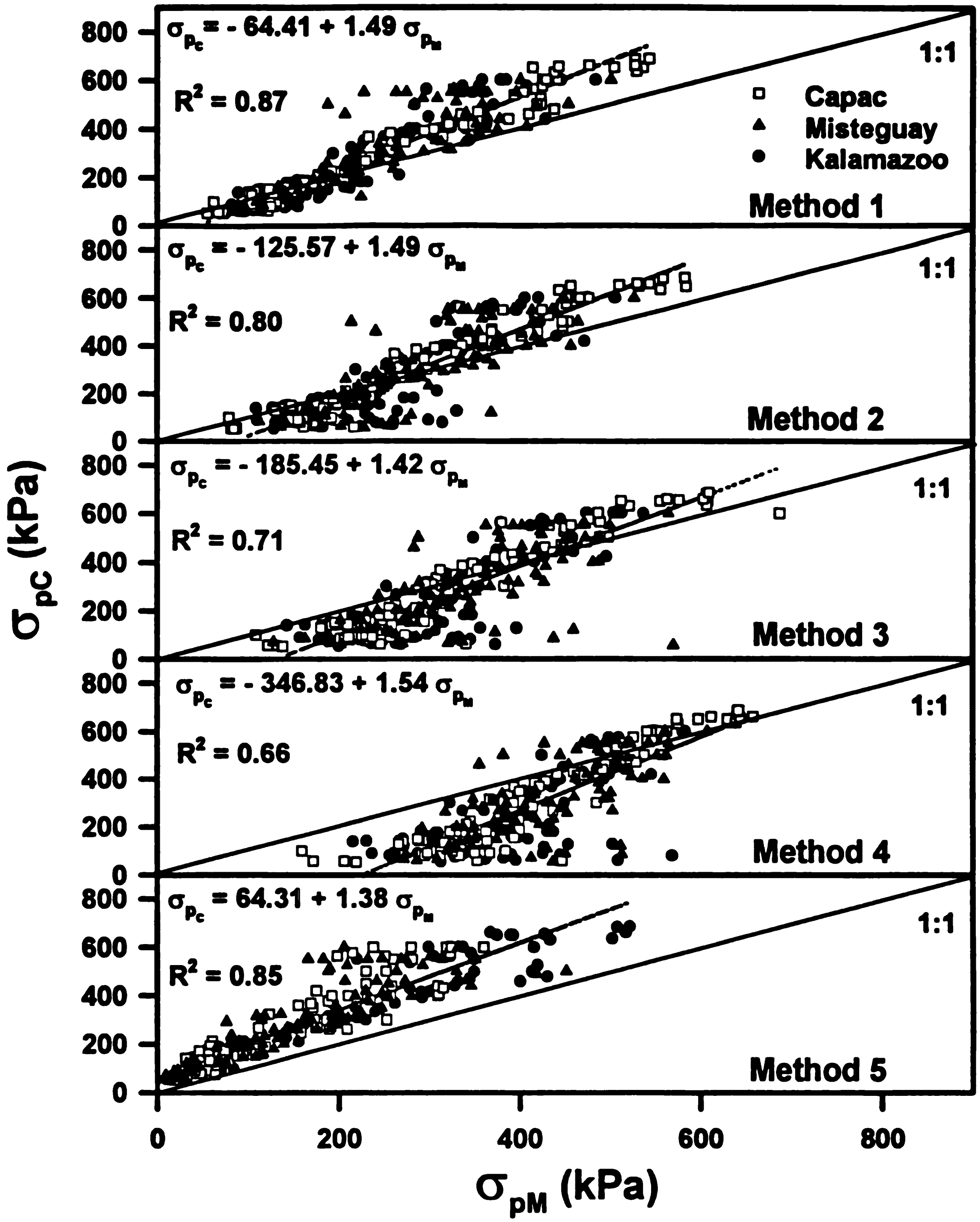

Figure 4. Regression of preconsolidation pressure determined by the Casagrande (1936) procedure (σ_{pC}) on preconsolidation pressure estimated by methods 1 through 5 (σ_{pM}) for 288 compression curves from three soil series in Michigan.

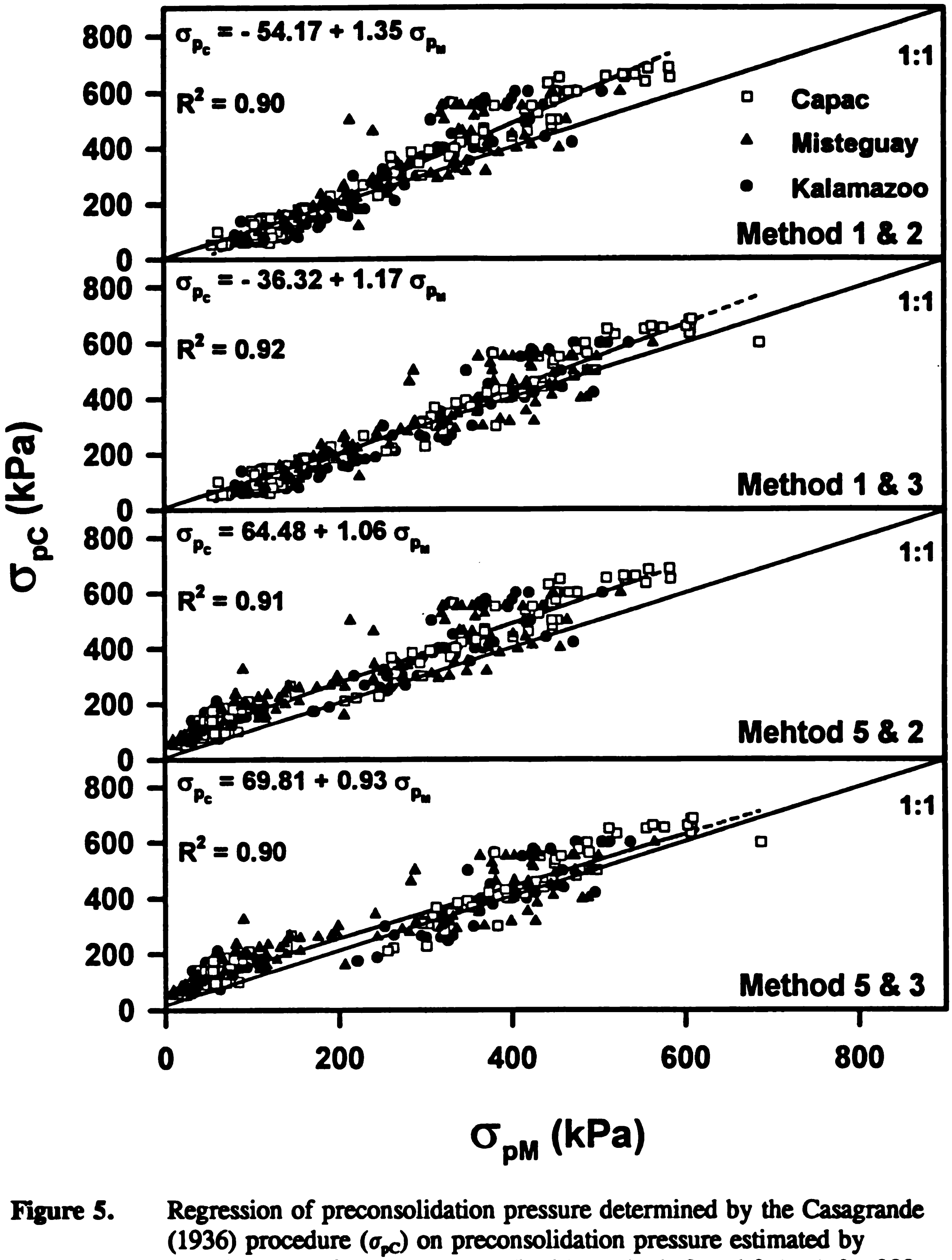

Figure 5. Regression of preconsolidation pressure determined by the Casagrande (1936) procedure (σ_{pC}) on preconsolidation pressure estimated by combinations of methods 1 and 5 with methods 2 and 3 (σ_{pM}) for 288 compression curves from three soil series in Michigan.

LOAD (kPa)	LOG LOAD	BULK DENS (Mgm^{-3})	B.Dvcc (Mgm^{-3})	B.Dreg (Mgm^{-3})
25	1.3979	1.5531	1.2632	1.5462
50	1.6990	1.5624	1.3623	1.5681
100	2.0000	1.5809	1.4614	1.5900
200	2.3010	1.6199	1.5605	1.6119
400	2.6021	1.6779	1.6596	1.6338
800	2.9031	1.7587	1.7587	1.6557
1600	3.2041	1.8578	1.8578	

** METHOD 1

m_{sc} = 0.0309
x = 2.3698

σ_p = 234
ρ_b = 1.58

** METHOD 3

m_{vcc} = 0.3292
x = 2.5015

σ_p = 317
ρ_b = 1.63

Regression Output:

		B.D$_{scc}$ (Mgm^{-3})
Constant	1.4446	
Std Err of Y Est	0.0107	1.5531
R Squared	0.9135	1.5624
No. of Observations	4	1.5717
Degrees of Freedom	2	1.5810
		1.5903
X Coefficient (s)	0.0727	1.5996
Std Err of Coef.	0.0158	

Figure 6. Reproduction of the computer screen of the spreadsheet for determination of the preconsolidation pressure for soil compression curves.

SUMMARY AND CONCLUSIONS

This study assessed the effect of stress history on the compression behavior of three Michigan soils in response to changes in soil properties induced by tillage and wheel traffic; proposed a two component model of soil compressibility that accounts for stress history, and presented a spreadsheet procedure for estimation of the preconsolidation pressure.

Changes in soil properties induced by tillage and wheel traffic affected the compressive behavior of these three soils. Soil moisture regulated the shape of the compression curve, while initial bulk density regulated its position. The initial bulk density of the Misteguay silty clay, and subsequently the compressive behavior, was greatly affected by soil water content, and required a normalization of the compression curves to fit the generalized relationship of shifts in soil compression curves with changes in soil water content. In general, no-tillage shifted the compression curves, increased σ_p in the Capac and Kalamazoo soils but not in the Misteguay, and had little effect on m in any of the soils. No-tillage also corresponded to higher field measured unconfined strength than CT in the Capac soil. Wheel traffic shifted the position of the compression curves, due to their influence on initial conditions, increased σ_p, and decreased m. These shifts would support the notion of improved trafficability on no-tilled and trafficked soils. No-tillage had some effect, but wheel traffic did more to decrease the susceptibility of these soils to further compaction by decreasing m and increasing σ_p. Specifically, wheel traffic in no-tillage (NTT) had a higher σ_p in the Capac and Kalamazoo soil, although CTT was higher in the Misteguay soil. The perception of increased trafficability of soils in no-tillage, as reported by farmers, relates not so much to tillage-induced differences in soil physical properties but is primarily due to wheel traffic effects and the fact that controlled traffic is likely in long-term NT. The other source of improved trafficability would be associated with improved drainage if this were the case in soils under long-term no-tillage management. Soils that dry faster would support higher loads earlier. Therefore, farmers should not only consider the adoption of controlled traffic patterns to reduce overall soil compaction, but should focus mainly on the enhanced resistance due to decrease in water content.

The proposed soil compaction model accounts for stress history in terms of σ_p as a function of θ_m. The stress history model predicted reasonable values of σ_p and σ_c from the literature and was a good predictor of critical strength for root elongation. Because σ_p was closely related to field measured US, it was possible to construct soil compression curves from field measurements of US, ρ_b, and θ_m with knowledge of laboratory measured soil compression curves from which values of σ_p, m, and possibly σ_c can be obtained. This model has immediate application in estimating soil workability or trafficability for a range of soils and soil management conditions using currently available soil management models.

For unsaturated soil conditions, the preconsolidation pressure can be estimated by using a spreadsheet procedure which uses a combination of method 1 for moisture conditions at matric potential higher than or equal to - 100 kPa, and method 3 for moisture conditions at matric potential lower than - 100 kPa. Preconsolidation pressures estimated with this procedure corresponded to standard graphical methods and literature values. This spreadsheet procedure, provide a fast and reliable estimation of the preconsolidation pressure. In addition, when used in the analysis of data for a research project involving σ_p, the use of a consistent, repeatable procedure rather than a graphical procedure will eliminate one source of variability, such as subjective judgment associated with classical graphical procedures.

Future research should be conducted to link the model developed in this study with currently available soil management models in order to generate trafficability / workability maps using available computer mapping programs. These maps will be a useful tool for farmers uses in order to avoid soil compaction.

APPENDIX 1: **Cells of the suggested spreadsheet procedure for estimation of the preconsolidation pressure from soil compression curves.**

```
A1: ^LOAD
B1: ^LOG LOAD
C1: [W11] ^BULK DENS
D1: [W9] ^B.D retav
E1: [W9] ^B.D reg
F1: [W16] '** METHOD 1
F2: [W16] "Csc =
G2: (F4) (C4-C3)/(B4-B3)
A3: 25
B3: (F4) @LOG(A3)
C3: (F4) [W11] 1.5531
D3: (F4) [W9] (G$10*(B3-B$8)+C$8)
E3: (F4) [W9] (D$12+C$18*B3)
F3: [W16] "x =
G3: (F4) (G2*(-B4)+C4-C9-G10*
     (-B9))/(G10-G2)
A4: 50
B4: (F4) @LOG(A4)
C4: (F4) [W11] 1.5624
D4: (F4) [W9] (G$10*(B4-B$8)+C$8)
E4: (F4) [W9] (D$12+C$18*B4)
A5: 100
B5: (F4) @LOG(A5)
C5: (F4) [W11] 1.5809
D5: (F4) [W9] (G$10*(B5-B$8)+C$8)
E5: (F4) [W9] (D$12+C$18*B5)
F5: [W16] 'Prec press reta=
G5: (F0) 10^G$3
A6: 200
B6: (F4) @LOG(A6)
C6: (F4) [W11] 1.6199
D6: (F4) [W9] (G$10*(B6-B$8)+C$8)
E6: (F4) [W9] (D$12+C$18*B6)
F6: [W16] 'Bulk Dens reta =
G6: (F2) (G2*(@LOG(G$5)-B4)+C4)
A7: 400
B7: (F4) @LOG(A7)
C7: (F4) [W11] 1.6779
D7: (F4) [W9] (G$10*(B7-B$8)+C$8)
E7: (F4) [W9] (D$12+C$18*B7)
A8: 800
B8: (F4) @LOG(A8)
C8: (F4) [W11] 1.7587
D8: (F4) [W9] (G$10*(B8-B$8)+C$8)
E8: (F4) [W9] (D$12+C$18*B8)
A9: 1600
B9: (F4) @LOG(A9)
C9: (F4) [W11] 1.8578
D9: (F4) [W9] (G$10*(B9-B$8)+C$8)
F9: [W16] '** METHOD 3
F10: [W16] "Cvcc =
G10: (F4) (C9-C8)/(B9-B8)
B11: 'Regression Output:
E11: [W9] 'B.Dscc
F11: [W16] "X =
G11: (F4)
(D$12+G$10*B$9-C$9)/(G$10-C$18)
A12: 'Constant
D12: (F4) [W9] 1.4445859880058
F12: [W16] "Log Pre pressu =
G12: (F4) @LOG(G$14)
A13: 'Std Err of Y Est
D13: (F4) [W9] 0.010651455299629
E13: (F4) [W9] (G$2*(B3-B$4)+C$4)
A14: 'R Squared
D14: (F4) [W9] 0.91348565970866
E14: (F4) [W9] (G$2*(B4-B$4)+C$4)
F14: [W16] 'Prec. Pressure =
G14: (F0) 10^G$11
A15: 'No. of Observations
D15: [W9] 4
E15: (F4) [W9] (G$2*(B5-B$4)+C$4)
F15: [W16] 'Bulk Density   =
G15: (F2) (D$12+C$18*G$12)
A16: 'Degrees of Freedom
D16: [W9] 2
E16: (F4) [W9] (G$2*(B6-B$4)+C$4)
E17: (F4) [W9] (G$2*(B7-B$4)+C$4)
A18: 'X Coefficient(s)
C18: (F4) [W11] 0.072717005997085
E18: (F4) [W9] (G$2*(B8-B$4)+C$4)
```

APPENDIX 2: Computer screen and cells of the free flow spreadsheet for computation of the compression test.

This spreadsheet performs the computation of the compression test and redraw the graphic that can be viewed by the user in the graphics subdirectory ("view"). To perform the computations the user needs only to alter the columns "STRESS" and "DIAL READINGS".

SAMPLE No 2 R2 MSU NT-T-DEPTH 1 - 6 kPa
BDi= 1.38 g cm-3 Hs= 1.36 cm
DP= 2.65 g cm-3 Hi= 2.6 cm
Ini Moist = 0.25 kg kg-1 Ws= 113.81 g
Area = 31.67 cm-2 ei= 0.9118

STRESS (KPa)	DIAL REA (cm)	Δ H (cm)	Δ e	VOID RATIO	HEIGHT (cm)	VOLUME (cm^3)	BD (Mg m^{-3})	POROSITY (%)	REDUCTION (%)
0	0.0000			0.9118	2.6000	82.3420	1.3822	47.8429	
25	0.0564	0.0564	0.0415	0.8703	2.5436	80.5558	1.4128	46.6864	2.4173
50	0.1290	0.0726	0.0534	0.8169	2.4710	78.2566	1.4543	45.1200	5.6913
100	0.2108	0.0818	0.0601	0.7568	2.3892	75.6660	1.5041	43.2411	9.6186
200	0.3104	0.0996	0.0732	0.6836	2.2896	72.5116	1.5695	40.7720	14.7794
400	0.4140	0.1036	0.0762	0.6074	2.1860	69.2306	1.6439	37.9651	20.6465
800	0.5144	0.1004	0.0738	0.5336	2.0856	66.0510	1.7231	34.9787	26.8884
1600	0.6114	0.0970	0.0713	0.4622	1.9886	62.9790	1.8071	31.8071	33.5176

Spreadsheet cells.
A1: ^SAMPLE
B1: 2
C1: ^R2
D1: 'MSU
E1: ^NT-T-DEPTH
1- 6 kPa
A2: "BDi=
B2: 1.38
C2: 'g cm-3
D2: "Hs=
E2: 1.36
F2: 'cm
A3: "D P=
B3: 2.65
C3: 'g cm-3
D3: "Hi=
E3: 2.6
F3: 'cm
A4: 'Moist i=
B4: (F2) 0.2496
C4: 'kg kg-1
D4: "Ws=
E4: 113.81
F4: 'g
A5: 'Area =
B5: 31.67
C5: 'cm-2
D5: "Ei=
E5: 0.9118
A7: ^LOAD
B7: ^DIAL REA
C7: ^DELTA H
D7: ^DELTA E
E7: ^VOID
F7: ^HEIGHT
G7: ^VOLUME
H7: ^BD
I7: ^POROSITY
J7: [W11]
^REDUCTION
A8: ' (KPa)
B8: ^ (cm)
C8: ^ (cm)
E8: ^RATIO
F8: ^ (cm)
G8: ^ (cm)
H8: ^ (g/cm3)
I8: ^ (%)
J8: [W11] ^ (%)
B9: '
A10: (F0) 0
B10: (F4) 0
E10: (F4) +E$5
F10: (F4) +E$3
G10: (F4) +F10*B$5
H10: (F4) +E$4/G10
I10: (F4) (1-H10/B$3)*100
A11: (F0) 25
B11: (F4) 0.0564
C11: (F4) (B11-B10)
D11: (F4) +C11/E$2
E11: (F4) +E10-D11
F11: (F4) +F10-C11
G11: (F4) +F11*B$5
H11: (F4) +E$4/G11
I11: (F4) (1-H11/B$3)*100
J11: (F4) [W11]
(100-(I11/I$10)*100)
A12: (F0) 50
B12: (F4) 0.129
C12: (F4) (B12-B11)
D12: (F4) +C12/E$2
E12: (F4) +E11-D12
F12: (F4) +F11-C12
G12: (F4) +F12*B$5
H12: (F4) +E$4/G12
I12: (F4) (1-H12/B$3)*100
J12: (F4) [W11]
(100-(I12/I$10)*100)
A13: (F0) 100
B13: (F4) 0.2108
C13: (F4) (B13-B12)
D13: (F4) +C13/E$2
E13: (F4) +E12-D13
F13: (F4) +F12-C13
G13: (F4) +F13*B$5
H13: (F4) +E$4/G13
I13: (F4) (1-H13/B$3)*100
J13: (F4) [W11]
(100-(I13/I$10)*100)
A14: (F0) 200
B14: (F4) 0.3104
C14: (F4) (B14-B13)
D14: (F4) +C14/E$2
E14: (F4) +E13-D14
F14: (F4) +F13-C14
G14: (F4) +F14*B$5
H14: (F4) +E$4/G14
I14: (F4) (1-H14/B$3)*100
J14: (F4) [W11]
(100-(I14/I$10)*100)
A15: (F0) 400
B15: (F4) 0.414
C15: (F4) (B15-B14)
D15: (F4) +C15/E$2
E15: (F4) +E14-D15
F15: (F4) +F14-C15
G15: (F4) +F15*B$5
H15: (F4) +E$4/G15
I15: (F4) (1-H15/B$3)*100
J15: (F4) [W11]
(100-(I15/I$10)*100)
A16: (F0) 800
B16: (F4) 0.5144
C16: (F4) (B16-B15)
D16: (F4) +C16/E$2
E16: (F4) +E15-D16
F16: (F4) +F15-C16
G16: (F4) +F16*B$5
H16: (F4) +E$4/G16
I16: (F4) (1-H16/B$3)*100
J16: (F4) [W11]
(100-(I16/I$10)*100)
A17: (F0) 1600
B17: 0.6114
C17: (F4) (B17-B16)
D17: (F4) +C17/E$2
E17: (F4) +E16-D17
F17: (F4) +F16-C17

G17: (F4) +F17*B$5
H17: (F4) +E$4/G17
I17: (F4) (1-H17/B$3)*100
J17: (F4) [W11]
(100-(I17/I$10)*100)